



LUIZ HENRIQUE FASOLIN

**“Self-assembly systems to obtain products with different applications: microemulsions, liquid crystalline and microemulsion-based gels”**

**“Sistemas auto-organizáveis na obtenção de produtos com diferentes aplicações: microemulsões, cristais líquidos e géis a base de microemulsões”**

CAMPINAS  
2013





**Universidade Estadual de Campinas  
Faculdade de Engenharia de Alimentos**

LUIZ HENRIQUE FASOLIN

**“Self-assembly systems to obtain products with different applications:  
microemulsions, liquid crystalline and microemulsion-based gels”**

**Orientadora: Profa. Dra. Rosiane Lopes da Cunha**

**“Sistemas auto-organizáveis na obtenção de produtos com diferentes aplicações:  
microemulsões, cristais líquidos e géis a base de microemulsões”**

Tese de doutorado apresentada ao Programa de Pós-Graduação em Engenharia de Alimentos da Faculdade de Engenharia de Alimentos da Universidade Estadual de Campinas para obtenção do título de Doutor em Engenharia de Alimentos

**ESTE EXEMPLAR CORRESPONDE À VERSÃO FINAL  
DA TESE DEFENDIDA PELO ALUNO LUIZ HENRIQUE  
FASOLIN E ORIENTADO PELA PROFA. DRA.  
ROSIANE LOPES DA CUNHA**

---

Profa. Dra. Rosiane Lopes da Cunha

**CAMPINAS  
2013**

FICHA CATALOGRÁFICA ELABORADA POR  
CLAUDIA AP. ROMANO DE SOUZA – CRB8/5816 - BIBLIOTECA DA FACULDADE DE  
ENGENHARIA DE ALIMENTOS – UNICAMP

F263s Fasolin, Luiz Henrique  
Sistemas auto-organizáveis na obtenção de produtos  
com diferentes aplicações: microemulsões, cristais  
líquidos e géis a base de microemulsões / Luiz Henrique  
Fasolin. -- Campinas, SP: [s.n.], 2013.

Orientador: Rosiane Lopes da Cunha.  
Tese (doutorado) - Universidade Estadual de  
Campinas, Faculdade de Engenharia de Alimentos.

1. Microemulsão. 2. Líquido cristalino. 3. Co-surfactante. 4. Géis de microemulsão. 5. Gelana. I. Cunha, Rosiane Lopes. II. Universidade Estadual de Campinas. Faculdade de Engenharia de Alimentos. III. Título.

Informações para Biblioteca Digital

Título em inglês: Self-assembly systems to obtain products with different applications: microemulsion, liquid crystalline and microemulsion-based gels

Palavras-chave em inglês:

Microemulsion

Liquid crystalline

Cosurfactant

Microemulsion-based gels

Gellan

Área de concentração: Engenharia de Alimentos

Titulação: Doutor em Engenharia de Alimentos

Banca examinadora:

Rosiane Lopes da Cunha [Orientador]

Ângelo Luiz Fazani Cavallieri

Carlos Raimundo Ferreira Grosso

Fernanda Yumi Ushikubo

Miguel Ângelo Parente Ribeiro Cerqueira

Data da defesa: 28-05-2013

Programa de Pós Graduação: Engenharia de Alimentos

## **BANCA EXAMINADORA**

---

***Profa. Dra. Rosiane Lopes da Cunha***

(Orientadora) – Depto. de Engenharia de Alimentos/FEA/UNICAMP

---

***Prof. Dr. Ângelo Luiz Fazani Cavallieri***

(Membro Titular) – Depto. de Tecnologia de Alimentos/UFG

---

***Prof. Dr. Carlos Raimundo Ferreira Grosso***

(Membro Titular) – Depto. de Engenharia de Alimentos/FEA/UNICAMP

---

***Dra. Fernanda Yumi Ushikubo***

(Membro Titular) – Depto. de Engenharia de Alimentos/FEA/UNICAMP

---

***Dr. Miguel Ângelo Parente Ribeiro Cerqueira***

(Membro Titular) – Depto. de Engenharia Biológica/Universidade do Minho/Portugal

---

***Dra. Fabiana de Assis Perrechil***

(Membro Titular) – Depto. de Engenharia de Alimentos/FEA/UNICAMP

---

***Profa. Dra. Jane Sélia dos Reis Coimbra***

(Membro Titular) – Depto. de Tecnologia de Alimentos/UFV

---

***Profa. Dra. Maria Helena Andrade Santana***

(Membro Suplente) – Depto. de Engenharia de Materiais e Bioprocessos/FEQ/UNICAMP



*“Aqueles que se sentem satisfeitos  
sentam-se e nada fazem. Os insatisfeitos são  
os únicos benfeiteiros do mundo.”*

*(Walter S. Landor)*



## **AGRADECIMENTOS**

*À Faculdade de Engenharia de Alimentos da UNICAMP, seus professores e funcionários pela oportunidade de realização desse trabalho*

*Ao CNPq pela bolsa de mestrado concedida e pelo auxílio financeiro.*

*À Capes e a FAPESP pelo auxílio financeiro.*

*À Profa. Dra. Rosiane Lopes da Cunha. Obrigado pela orientação, apoio, amizade e principalmente pelas discussões que me ajudaram a crescer e levaram à realização deste trabalho.*

*Aos membros da banca examinadora pelas correções que contribuíram para a melhoria deste trabalho.*

*Ao Laboratório Nacional de Luz Síncrotron pela possibilidade de realizar as análises de SAXS nas suas instalações*

*A Cargill pela doação do óleo de girassol alto oléico.*

*À minha família, em especial meus pais Luiz e Telma e meu irmão João Guilherme por estarem sempre ao meu lado incondicionalmente.*

*Aos amigos da FEA, principalmente os que me acompanham desde o mestrado: Priscilla, Simone, Bebel.*

*A Rejane e Carol pela ajuda no desenvolvimento desse trabalho, tanto na parte prática como nas discussões dos resultados.*

*Aos demais colegas de laboratório, obrigado pela convivência diária, amizade, paciência e não menos importante ajuda nas discussões de resultados.*

*Aos moradores da república nesse período em que me aguentaram, Lidia, Diego, Irede, Marina, Ana e Grazi.*

*A Zildene e Patrícia, pela ajuda no laboratório.*

*A todos que de alguma forma contribuíram direta ou indiretamente para a elaboração deste trabalho.*

*Muito obrigado a todos*

x

## **SUMÁRIO**

<b>RESUMO GERAL .....</b>	<b>XXIX</b>
<b>ABSTRACT .....</b>	<b>XXXIII</b>
<b>CAPÍTULO 1– INTRODUÇÃO E OBJETIVOS .....</b>	<b>1</b>
1. INTRODUÇÃO .....	3
2. OBJETIVOS .....	5
2.1. <i>Objetivos específicos</i> .....	6
3. ORGANIZAÇÃO DA TESE EM CAPÍTULOS .....	6
4. REFERÊNCIAS BIBLIOGRÁFICAS .....	8
<b>CAPÍTULO 2 – REVISÃO BIBLIOGRÁFICA.....</b>	<b>13</b>
1. SISTEMAS DE EMULSIFICAÇÃO ESPONTÂNEA.....	15
2. INGREDIENTES DE MICROEMULSÕES PARA ALIMENTOS .....	23
2.1. <i>Surfactantes</i> .....	23
2.2. <i>Co-surfactantes</i> .....	25
2.3. <i>Óleos</i> .....	27
3. GÉIS A PARTIR DE MICROEMULSÕES.....	29
4. GELANA.....	32
5. REFERÊNCIAS BIBLIOGRÁFICAS .....	35
<b>CAPÍTULO 3 – EFFECT OF ETHANOL AND OIL UNSATURATION IN SELF-ASSEMBLY SYSTEMS .....</b>	<b>49</b>
ABSTRACT .....	51
1. INTRODUCTION .....	52
2. MATERIAL AND METHODS .....	54
2.1. <i>Material</i> .....	54
2.2. <i>Phase behavior and diagrams construction</i> .....	54
2.3. <i>Phase diagrams characterization</i> .....	55
2.4. <i>Microemulsions and liquid crystalline characterization</i> .....	56
2.4.1. <i>Droplets size distribution</i> .....	56



2.4.2. Small angle X-Ray Scattering (SAXS).....	57
2.4.3. Rheological measurements .....	57
2.3.4.1. Steady-shear rheology .....	57
2.4.3.2. Dynamic shear rheology.....	58
3. RESULTS .....	58
3.1. <i>Construction of phase diagrams</i> .....	58
3.1.1. Visual observation and polarized light microscopy.....	58
3.1.2. Electrical conductivity .....	61
3.2. <i>Phase diagram analysis</i> .....	62
3.2.1. Droplets size distribution.....	64
3.2.2. Rheological measurements .....	66
3.2.2.1. Steady-state rheology.....	66
3.2.2.2. Dynamic rheology.....	69
3.2.3. SAXS measurements .....	70
4. DISCUSSION .....	73
5. CONCLUSION.....	76
6. ACKNOWLEDGEMENTS.....	77
7. REFERENCES .....	77
<b>CAPÍTULO 4 – ORGANIC ACIDS AS COSURFACTANT IN SELF-ASSEMBLY SYSTEMS.....</b>	<b>81</b>
ABSTRACT .....	83
1. INTRODUCTION .....	84
2. MATERIAL AND METHODS .....	86
2.1. <i>Material</i> .....	86
2.2. <i>Phase behavior and diagrams construction</i> .....	86
2.3. <i>Phase diagrams characterization</i> .....	87
2.4. <i>Microemulsions and liquid crystalline characterization</i> .....	88
2.4.1. Small angle X-Ray Scattering (SAXS).....	88



---

## Sumário

2.4.2. Rheological measurements .....	90
3. RESULTS .....	90
3.1. Phase diagrams.....	90
3.2. Small-angle scattering (SAXS) measurements.....	93
3.3. Rheological measurements.....	99
4. DISCUSSION .....	102
5. CONCLUSION.....	105
6. ACKNOWLEDGEMENTS.....	106
7. REFERENCES .....	107
<b>CAPÍTULO 5 – POLYSACCHARIDE INTERACTION IN SELF-ASSEMBLY SYSTEMS.....</b>	<b>111</b>
ABSTRACT .....	113
1. INTRODUCTION .....	114
2. MATERIAL AND METHODS .....	116
2.1. Material.....	116
2.2. Gel preparation.....	116
2.3. Zeta potential.....	117
2.4. Electrical conductivity measurements .....	117
2.5. Mechanical properties .....	117
2.6. Rheological measurements.....	119
2.7. Scanning electron microscopy (SEM) .....	120
2.8. Statistical analysis .....	120
3. RESULTS AND DISCUSSION .....	120
3.1. Zeta potential.....	120
3.2. Conductivity measurements.....	121
3.3. Scanning electron microscopy .....	122
3.4. Oscillatory measurements.....	123
3.5. Mechanical properties .....	126



---

*Sumário*

4. DISCUSSION .....	129
5. CONCLUSION.....	133
6. ACKNOWLEDGEMENTS.....	134
7. REFERENCES .....	134
<b>CAPÍTULO 6 – MICROEMULSION-BASED GELS .....</b>	<b>139</b>
ABSTRACT .....	141
1. INTRODUCTION .....	142
2. MATERIAL AND METHODS .....	144
2.1. <i>Material</i> .....	144
2.2. <i>Gel preparation</i> .....	144
2.3. <i>Mechanical properties</i> .....	146
2.4. <i>Rheological measurements</i> .....	147
2.5. <i>Scanning electron microscopy (SEM)</i> .....	148
2.6. <i>Statistical analysis</i> .....	148
3. RESULTS AND DISCUSSION .....	148
3.1. <i>Microemulsion-based gels</i> .....	148
3.2. <i>Effect of cosurfactant</i> .....	154
4. CONCLUSIONS .....	158
5. ACKNOWLEDGEMENTS.....	159
6. REFERENCES .....	160
<b>CAPÍTULO 7– CONCLUSÕES GERAIS.....</b>	<b>165</b>



## ÍNDICE DE TABELAS

### Capítulo 2

Tabela 1. Alguns surfactantes de grau alimentício e seus valores de BHL.....	24
Tabela 2. Composição em ácidos graxos de óleos vegetais.....	28

### Capítulo 3

Table 1. Composition of the formulations used to construct phase diagrams .....	55
Table 2. Real composition of the systems corresponding to lines 8 and 9 of phase diagram .....	60
Table 3. Characteristic parameters for phase diagrams formulated with water/Tween80/ethanol/sunflower oil or HOSO with different oil:ethanol ratios .....	64
Table 4. Rheological properties of different systems of Line 9 formulated with water/Tween80/ethanol/sunflower oil or HOSO with different oil:ethanol ratios. ....	68
Table 5. Structural parameters evaluated by SAXS for dilution Line 9 of phase diagrams formulated with water/Tween80/ethanol/sunflower oil or HOSO with different oil:ethanol ratios.....	72

### Capítulo 4

Table 1. Composition of the formulations used to construct phase diagrams .....	87
Table 2. Characteristic parameters for phase diagrams formulated with water/Tween80/cosurfactant/sunflower oil or HOSO using propionic or acetic acid as cosurfactant	93
Table 3. Structural parameters evaluated by SAXS for systems formulated with water/Tween80/sunflower oil using propionic or acetic acid as cosurfactant .....	95
Table 4. Structural parameters evaluated by SAXS for systems formulated with water/Tween80/HOSO/cosurfactant using propionic or acetic acid as cosurfactant .....	98
Table 5. Rheological properties of different systems formulated with water/Tween80/cosurfactant/sunflower oil or HOSO using propionic or acetic acid as cosurfactant .....	101



**Capítulo 5**

Table 1. Gel or transition temperatures for systems with 3.0% (w/w) gellan gum at natural pH (5.0) or pH 3.0 with different Tween80 concentration..... 126

Table 2. BST parameters of gels of 3.0% (w/w) gellan gum at natural pH and pH 3.0 with different Tween80 concentrations. .... 129

**Capítulo 6**

Table 1. Composition of the systems. .... 146

Table 2. Temperature transition of some systems with 3.0% (w/w) gellan gum in systems formulated with water + HOSO + Tween80 without acetic acid. .... 151

Table 3. Temperature transition for systems with 3.0% (w/w) gellan gum in systems formulated with water + HOSO + Tween80 +acetic acid. .... 156



## ÍNDICE DE FIGURAS

### Capítulo 2

Figura 1. Diagrama esquemático da energia livre de sistemas emulsionados e microemulsionados em comparação com o estado de separação de fases. ....	17
Figura 2. Sistema de classificação de Winsor. Fonte: FLANAGAN et al. (2006). ....	19
Figura 3. Esquema representativo da microestrutura das microemulsões (A) microemulsão O/A, (B) microemulsão bicontínua e (C) microemulsão A/O. Fonte: MEHTA et al. (2008). ....	19
Figura 4. Representação esquemática das diferentes estruturas formadas pela auto-associação dos surfactantes. Adaptado de HOLMBERG et al. (2002). ....	21
Figura 5. Diagrama de fases esquemático de um sistema ternário composto por água, óleo e surfactante, identificando as regiões formadoras de microemulsões O/A, A/O ou BC (bicontínua) (Adaptado de ZHONG et al., 2009)....	22
Figura 6. Estrutura química do polisorbato 80, ou Tween 80. ....	25
Figura 7. Estrutura dos géis a base de microemulsão proposta por ATKINSON et al., 1991 (Adaptado de KANTARIA et al., 1999).....	31
Figura 8. Unidade tetramérica que compõem a goma gelana desacilada (TANG et al., 1996). ....	33
Figura 9. Representação esquemática do processo de transição conformacional da gelana (MIYOSHI et al., 1996).....	34

### Capítulo 3

Figure 1. Visual appearance of Lines 8 and 9 (80% and 90% of initial surfactant, respectively) of systems formulated with water/Tween80/ethanol/sunflower oil or HOSO with different oil:ethanol ratios. The arrows show the phase separation (Winsor I system) and numbers refers to water mass fraction (% w/w). (2TP) Two transparent phases; (EM) macroemulsion; ( $L_1$ and $L_2$ ) microemulsions; (LC) liquid crystalline and (gel) liquid crystalline with gel-like structure. ....	59
Figure 2. Electrical conductivity of Lines 8 and 9 of microemulsions formulated with water/Tween80/ethanol/sunflower oil or HOSO with different oil:ethanol ratios. (+) Line 8; (*) Line 9. A) S1E2; B) H1E2; C) S2E1; D) H2E1. $\Phi_c$ is the percolation threshold or critical water content; $\kappa_b$ is the conductivity at water fraction $\Phi_b$ , and $\kappa_m$ is the maximal conductivity at water fraction $\Phi_m$ . ....	61
Figure 3. Phase diagrams formulated with water/Tween80/ethanol/sunflower oil or HOSO with different oil:ethanol ratios. (EM) Macroemulsion; (2TP) Two transparent phases; (LC) Liquid crystalline phase, ( $L_2$ ) Microemulsion W/O and ( $L_1$ ) Microemulsion O/W. ....	63



## Índice de Figuras

Figure 4. Particles size distribution along dilution line 9. (♦)S1E2; (□)H1E2; (▲)S2E1; (×)H2E1. 65

Figure 5. Flow curves of different systems of the Line 9 formulated with water/Tween80/ethanol/sunflower oil or HOSO with different oil:ethanol ratios. (♦)S1E2; (□)H1E2; (▲)S2E1; (×)H2E1. A) System 9040 and 9050 step 1 and B) System 9040 and 9050 step 3..... 67

Figure 6. Storage modulus as a function of frequency for samples with gel-like behavior in Line 9. Systems formulated with water/Tween80/ethanol/sunflower oil or HOSO with 2:1 oil:ethanol ratio. A) S1E2; B) S2E1; C) H1E2; D) H2E1. (♦) 9030; (▲) 9040; (■) 9045; (●) 9050 (\*) 9060. .... 69

Figure 7. SAXS patterns of the dilution Line 9 formulated with water/Tween80/ethanol/sunflower oil or HOSO with different oil:ethanol ratios. A)S1E2; B)S2E1; C)H1E2; D)H2E1. .... 71

## **Capítulo 4**

Figure 1. Phase diagrams formulated with water/Tween80/cosurfactant/sunflower oil or HOSO using propionic or acetic acid as cosurfactant. (LC) Liquid crystalline, ( $L_2$ ) W/O microemulsion and ( $L_1$ ) O/W microemulsion. .... 92

Figure 2. SAXS patterns for systems formulated with water/Tween80/sunflower oil/cosurfactant using propionic or acetic acid as cosurfactant ..... 96

Figure 3. SAXS patterns for systems formulated with water/Tween80/HOSO/cosurfactant using propionic or acetic acid as cosurfactant. .... 99

## **Capítulo 5**

Figure 1. Zeta potential profile of gellan gum at different pH values..... 121

Figure 2. Electrical conductivity ( $\kappa$ ) of Tween80/water systems at 80°C. (■) pH 3.0, and (□) pH 5.0. .... 122

Figure 3. SEM micrographs of 3.0% (w/w) gellan gum gels. (A) Natural pH (5.0) and no addition of Tween80; (B) Natural pH and 10% of Tween80 and (C) pH 3.0 and 10% of Tween80. Magnification 1,000  $\times$ . .... 123

Figure 4. Thermal scanning rheograms of gels with 3.0% (w/w) gellan gum at natural pH (5.0) and pH 3.0 containing different concentrations of Tween80. (A) 0%; (B) 10%; (C) 20%; (D), 30%; (E), 40%, (F) 50% and (G) 60%. (♦,◊) pH 3.0 and (●,○) pH 5.0 (natural). Full and empty symbols refers to G' and G'', respectively..... 125

Figure 5. Typical uniaxial compression curves for 3.0% (w/w) gellan gum gels. (A) Gel with rupture point and (B) squeezing gel..... 127



Figure 6. Mechanical properties of gels of 3.0% (w/w) gellan gum at natural pH and pH 3.0 at different Tween80 concentrations. (A) Maximum stress ( $\sigma$ ) and (B) Strain ( $\epsilon$ ). White bars refer to gels with rupture point and gray bars to squeeze gels. Means with different letters show statistically significant differences ( $p<0.05$ ): Capital letters (between pH) and small letter (Tween 80 concentration). NG – non-self supporting gels..... 128

## **Capítulo 6**

Figure 1. Phase diagrams composed by water + Tween80 + HOSO. (A) With acid acetic addition and (B) without acid acetid. \*Formulations with gellan addition. 1TP = one transparent phase, 2TP = two transparent phase and LC = liquid crystalline phase..... 145

Figure 2. Thermal scanning rheograms of gels with 3.0% (w/w) gellan gum in systems formulated with water + HOSO + Tween80. (A) 40% water; (B) 50% water; (C) 60% water and (D) 70% water. Full symbols ( $G'$ ), empty symbols ( $G''$ )..... 150

Figure 3. SEM micrographs of 3.0% (w/w) gellan gum gels formulated with water + HOSO + Tween80. (A and B) 4040, (C and D) 5040 and (E and F) 6070. (A, C and E) 1000 $\times$  magnification and (B, D and F) 2000 $\times$  magnification. .... 152

Figure 4. Mechanical properties of gels with 3.0% (w/w) gellan gum in systems composed by water + HOSO + Tween80 without acetic acid addition. (A) Maximum stress ( $\sigma_{Max}$ ) and (B) strain ( $\epsilon_{Max}$ ). Means with different letters show statistically significant differences ( $p<0.05$ ): Capital letters on the z axis (surfactant concentration) and small letter on the x axis (water concentration). ..... 153

Figure 5. Thermal scanning rheograms of gels with 3.0% (w/w) gellan gum in systems formulated with water + HOSO + Tween80 + acetic acid. (A) 40% of water; (B) 50% of water; (C) 60% of water and (D) 70% of water. Full symbols ( $G'$ ), empty symbols ( $G''$ )..... 155

Figure 6. SEM micrographs of 3.0% (w/w) gellan gum gels formulated with water + HOSO + Tween80 + acetic acid (System 7070). (A) 1000 $\times$  magnification and (B) 2000 $\times$  magnification. .... 157

Figure 7. Mechanical properties of gels with 3.0% (w/w) gellan gum in systems composed by water + HOSO + Tween80 + acetic acid. (A) Maximum ( $\sigma_{Max}$ ) and (B) Strain ( $\epsilon_{Max}$ ). Means with different letters show statistically significant differences ( $p<0.05$ ): Capital letters on the z axis (surfactant concentration) and small letter on the x axis (water concentration). NG means non-self supporting gels. .... 158



## **Tese de doutorado**

**AUTOR: Luiz Henrique Fasolin**

**TÍTULO: Sistemas auto-organizáveis na obtenção de produtos com diferentes aplicações: microemulsões, cristais líquidos e géis a base de microemulsões**

**ORIENTADORA: Profa. Dra. Rosiane Lopes da Cunha**

**Dept. Engenharia de Alimentos – FEA – Unicamp**

---

## **RESUMO GERAL**

Os sistemas auto-organizáveis como meio para obtenção de produtos com diferentes características têm sido estudados como uma alternativa aos métodos tradicionais de produção de emulsões e gelificação. Todavia, a formação de produtos com ingredientes biocompatíveis ainda é pouco explorada, devido à complexidade e a toxicidade de alguns dos ingredientes geralmente utilizados. Nesse contexto, o objetivo geral desse trabalho foi produzir sistemas com diferentes características a partir do estudo do diagrama de fases de sistemas compostos por água, óleo vegetal, surfactante e co-surfactante biocompatíveis, além de um biopolímero gelificante. Na primeira parte deste estudo, a influência da concentração do co-surfactante (etanol) e da insaturação do óleo (óleo de girassol comum ou óleo de girassol alto oléico, HOSO) foi investigada. Os resultados mostraram que, dependendo da composição do meio, foram obtidas diferentes estruturas (microemulsões ou líquidos cristalinos) com distintos comportamentos reológicos. A formação dessas estruturas foi influenciada pela insaturação do óleo e pela concentração de etanol. Na segunda etapa, a substituição do etanol por ácidos orgânicos (acético e propiônico) foi estudada, bem como sua influência no comportamento reológico-estrutural dos sistemas. Nesse caso, a estruturação dos sistemas foi dependente da combinação entre os ingredientes. O óleo de girassol solubilizou maior quantidade de ácido propiônico devido sua maior hidrofobicidade, enquanto o HOSO

XXX

apresentou mais afinidade com o ácido acético. Essa diferença de afinidades levou a mudanças no mecanismo de difusão do co-surfactante, bem como sua susceptibilidade à partição. A fim de estudar a viabilidade da adição da goma gelana nas microemulsões para obtenção de sistemas gelificados, uma terceira etapa foi realizada com o intuito de avaliar a interação desse polissacarídeo com o surfactante. Foram observados dois comportamentos predominantes, dependendo da concentração dos componentes. Em baixas concentrações de surfactante, a rede de gelana prevaleceu formando géis fortes com claro ponto de ruptura. Com o aumento da concentração, o surfactante começou a se auto-organizar em estruturas mais complexas até que em altas concentrações sua estrutura se tornou predominante com formação de géis fracos. Na última etapa do trabalho, a goma gelana foi adicionada em alguns sistemas do diagrama de fases formulados com HOSO com ou sem ácido acético. Os géis formulados sem ácido acético foram homogêneos e dependentes da razão água/surfactante. A maior quantidade de água levou a géis mais resistentes devido à formação de uma rede de gelana mais densa. Por outro lado, maiores concentrações de surfactante levaram a géis mais fracos e ao aparecimento de uma temperatura de transição relacionada à estruturação do surfactante. A adição de ácido levou à desestabilização da estrutura cristalina, impedindo a estruturação do surfactante. Além disso, ao invés de géis homogêneos, foram formados géis particulados ou microgéis, que foram auto-sustentáveis apenas em altas concentrações de água. Por fim, este trabalho mostrou que sistemas auto-organizados são de particular utilidade na obtenção de produtos com diferentes características tecnológicas, cujas propriedades podem ser moduladas de acordo com a aplicação.

**Palavras-chave:** microemulsão, líquido cristalino, géis de microemulsão, co-surfactante, gelana



## **Ph. D. Thesis**

**AUTHOR: Luiz Henrique Fasolin**

**TITLE: Self-assembly systems to obtain products with different applications:  
microemulsions, liquid crystalline and microemulsion-based gels**

**SUPERVISOR: Profa. Dra. Rosiane Lopes da Cunha**

**Depto. Engenharia de Alimentos – FEA – Unicamp**

---

## **ABSTRACT**

Self-assembly systems as a way to obtaining products with different characteristics have been studied as an alternative to traditional emulsification and gelation methods. However, the use of biocompatible ingredients in these systems was scarcely explored due to the complexity or toxicity of the most common ingredients. Thus, the aim of this work was to produce systems with different technological characteristics from the study of phase diagrams composed by water, edible oil, surfactant and biocompatible cosurfactants, as well as a gelling biopolymer. In the first part of this work, the influence of the cosurfactant (ethanol) concentration and oil unsaturation (sunflower oil or high oleic sunflower oil, HOSO) was investigated from the phase-diagrams construction. Results showed that depending on the systems composition different structures could be obtained (microemulsion or liquid crystalline) with different rheological behavior. Moreover, the formation of these structures was influenced by the oil unsaturation and ethanol concentration. In the second step, the replacement of ethanol by organic acids (acetic and propionic) was evaluated, as well as their influence on the rheological-structural behavior. In this case, the systems self-assemble was dependent on the ingredients combination. Sunflower oil solubilized a great amount of propionic acid due to its higher hydrophobicity, whereas HOSO presented more affinity with acetic acid. These affinity differences between oil and cosurfactant changed the diffusion mechanism of the acid through the



surfactant and oil tails as well as its susceptibility to the partition phenomenon. In order to study the feasibility of gellan gum addition in the microemulsion to obtain gelled systems, a third step was carried out to evaluate the interactions between this polysaccharide and the surfactant. It was observed two prevailing behavior depending on the components concentration. At low surfactant concentration the gellan network prevailed and formed hard gels were formed with clear rupture point. With the surfactant content increase, its moieties started to self-assembly in highly organized structures until that, at high concentration, these structures became predominant with the formation of weak or soft gels. In the last part of this work gellan gum was added to some systems of the phase diagram formulated with HOSO with or without acetic acid. The gels formulated without acetic acid were homogeneous gels and dependent on the water/surfactant ratio. The higher water content led to harder gels due to the formation of a denser gellan network. On the other hand, higher surfactant concentration led to weaker gels and a transition temperature related to the surfactant structuration was observed. The acid acetic addition led to the liquid crystalline destabilization, hindering the surfactant structuration. Moreover, instead of bulky gels, particulate gels or microgels were formed, which were self-supporting only at high water concentration. Finally, this work showed that self-assembly systems are particularly useful to obtain products with different technological characteristics, whose properties can be modulated according to the application.

**Keywords:** microemulsion, liquid crystalline, microemulsion-based gels cosurfactant, gellan gum



**– CAPÍTULO 1–**  
***Introdução e Objetivo***



## **1. INTRODUÇÃO**

A produção de sistemas com diversificadas propriedades físico-químicas e de textura é de interesse de diferentes segmentos industriais, como farmacêutico, cosmético, médico e alimentício. Sistemas que tem chamado atenção devido a sua versatilidade de atuação e interação com diferentes compostos são aqueles formados através da auto-organização dos componentes da mistura ou emulsificação espontânea, também chamados de microemulsões e cristais líquidos. Esses sistemas são atraentes principalmente por aumentar a eficiência de reações, permitirem extrações seletivas e por sua habilidade em solubilizar grandes quantidades de ingredientes hidrofílicos e lipofílicos devido à presença das fases aquosa e oleosa (DE CAMPO et al., 2004; ENGSTROM; LARSSON, 1999).

As microemulsões são formadas espontaneamente e são macroscopicamente homogêneas, pois o tamanho de suas gotas está no domínio coloidal. Dessa forma, as microemulsões são sistemas isotrópicos, transparentes e termodinamicamente estáveis, compostos basicamente pela mistura de água, óleo e surfactante (FLANAGAN; SINGH, 2006; ZHANG et al., 2010). No entanto, para a formação das microemulsões é necessária geralmente a utilização de co-surfactantes para aumentar a flexibilidade da interface (LV et al., 2005). Todavia, dependendo da concentração dos ingredientes pode ocorrer a auto-organização das moléculas de surfactante em estruturas mais complexas, podendo levar a uma grande variedade de morfologias com diferentes configurações moleculares. Essas estruturas deixam então de ser caracterizadas como microemulsão e são denominadas de líquido cristalino, podendo apresentar conformação lamelar, cúbica ou hexagonal (BINKS et al., 2010). Os ingredientes utilizados e a composição do sistema têm

extrema importância na auto-organização das microemulsões e na sua funcionalidade. Microemulsões feitas com ingredientes seguros e que possam ser utilizadas nas indústrias farmacêutica e alimentícia são difíceis de produzir devido à complexidade dos ingredientes usados. Os óleos utilizados na produção de microemulsões são geralmente de cadeia curta ou média, pois os óleos de cadeia longa, como é o caso dos triacilgliceróis comestíveis, apresentam alto volume molecular e baixa solubilidade (FLANAGAN; SINGH, 2006; GAONKAR; BAGWE, 2002). Por outro lado, a maior parte dos surfactantes e co-surfactantes apresenta certo grau de toxicidade ou podem ser utilizados apenas em baixíssimas concentrações (FENG et al., 2009; FLANAGAN; SINGH, 2006; PATEL et al., 2006). Existem alguns trabalhos sobre microemulsões alimentícias (FENG et al., 2009; FLANAGAN et al., 2006; PATEL et al., 2006; RAO; MCCLEMENTS, 2011; ROZNER et al., 2010; YAGHMUR et al., 2004) mas estes sempre apresentam ao menos um ingrediente que não é alimentício, ou usam óleos de cadeia curta ou média. A possibilidade da utilização de óleos comestíveis como fase oleosa na produção de microemulsões tem sido pouco estudada apesar de serem interessantes para a indústria de alimentos e do fato desses óleos apresentarem alta disponibilidade e serem de fontes renováveis.

Além da utilização de microemulsionados e/ou cristais líquidos obtidos pela auto-organização de surfactantes, diferentes características podem ser alcançadas com a interação desses sistemas com compostos adicionais. A adição de polímeros têm sido de considerável interesse principalmente no que diz respeito à modificação de textura, a partir da formação de géis. A indústria farmacêutica já explora esses géis a base de microemulsões há algum tempo, principalmente com a adição de gelatina como agente gelificante para veiculação de bioativos (BAROT et al., 2012; CHEN et al., 2007;

KANTARIA et al., 1999; LOPEZ et al., 2004). Todavia, nos últimos anos o uso de polissacarídeos gelificantes em microemulsões também começou a ser explorado, apesar de poucos tipos de polissacarídeos terem sido estudados nestes sistemas (GONG et al., 2012; KOOP et al., 2012; VALENTA; SCHULTZ, 2004). A gelana é um polissacarídeo extracelular produzido pela bactéria *Sphingomonas elodea* que possui alto poder gelificante inclusive em baixas concentrações. Os géis obtidos são rígidos, translúcidos e resistentes a baixos valores de pH, diferentemente de outros polissacarídeos amplamente utilizados na indústria de alimentos, como agarose e carragenas (MORITAKA et al., 1995; PICONE; CUNHA, 2011; YAMAMOTO; CUNHA, 2007). A formação de géis de microemulsões com adição de gelana poderia favorecer a proteção de qualquer composto adicionado devido ao aumento da estabilidade dos sistemas. Além disso, esses géis permitem sua utilização como sistemas de liberação controlada através da forma oral ou tópica (CHEN et al., 2007; D'CRUZ; UCKUN, 2001; KANTARIA et al., 1999; ZHAO et al., 2007) com veiculação de bioativos hidrofílicos e hidrofóbicos.

## **2. OBJETIVOS**

Este trabalho teve como objetivo geral produzir sistemas com diferentes características físico-químicas e mecânico/estruturais a partir do estudo de diagrama de fases de sistemas compostos por água, óleo vegetal, surfactante e co-surfactante biocompatíveis, além de um biopolímero gelificante, para aplicação em diferentes segmentos industriais.

## **2.1. Objetivos específicos**

Os objetivos específicos deste trabalho foram:

- Avaliar o efeito da predominância de uma ou duas insaturações no óleo sobre a produção de microemulsões e líquido cristalino;
- Avaliar o efeito do etanol ou ácidos orgânicos de cadeia curta como co-surfactantes na produção de microemulsões e líquido cristalino;
- Avaliar a interação entre o surfactante polissorbato 80 e a goma gelana na produção de sistemas gelificados em diferentes valores de pH.
- Estudar as propriedades de géis formados a partir de microemulsão ou líquido cristalino utilizando gelana como agente gelificante.
- Avaliar o efeito da presença de co-surfactante na produção de géis de microemulsão.

## **3. ORGANIZAÇÃO DA TESE EM CAPÍTULOS**

A apresentação deste trabalho foi organizada em sete capítulos como descrita a seguir:

### ***Capítulo 1: Introdução e objetivos***

### ***Capítulo 2: Revisão bibliográfica***

Neste capítulo são abordados aspectos teóricos dos sistemas estudados, bem como uma revisão bibliográfica relatando a literatura recente e mais relevante sobre o tema deste trabalho.

***Capítulo 3: Microemulsions and liquid crystalline formulated with triacylglycerols:  
Effect of ethanol and oil unsaturation***

Esse capítulo teve o intuito de utilizar apenas ingredientes biocompatíveis e avaliar a influência do co-surfactante e insaturação do óleo na formação de microemulsões e cristais líquidos. Diagramas de fase pseudo-ternários foram construídos tendo água, polissorbato 80 (Tween 80) como surfactante, etanol como co-surfactante e óleo de girassol comum ou alto oleico (HOSO) como fase oleosa. As estruturas formadas foram avaliadas em relação à estrutura, tamanho de gotas e comportamento reológico. Os resultados foram publicados na Colloids and Surfaces A: Physicochemical and Engineering Aspects (2012), v.415, p.31-40.

***Capítulo 4: Organic acids partition on production of microemulsions and liquid crystalline formulated with triacylglycerols***

Após avaliar o efeito do etanol como co-surfactante na produção de microemulsões e cristais líquidos no Capítulo 3, a substituição do etanol por ácidos orgânicos foi avaliada. Dessa forma, a utilização dos sistemas formados poderia ser ampliada devido às restrições de aplicações de sistemas com conteúdo alcoólico. Foram avaliados os ácidos acético e propiônico e sua influência nas estruturas formadas nos diagramas de fase, visando análises reológicas e estruturais.

***Capítulo 5: Gellan-polysorbate interaction in concentrated polysaccharide systems***

Antes de avaliar a viabilidade da adição de goma gelana nos sistemas obtidos no Capítulo 4, a interação do surfactante com esse biopolímero foi estudada. A influência da concentração de Tween 80 nas propriedades reológicas, mecânicas e na estrutura dos

géis formados foi estudada. Além disso, foi avaliada a influência da acidificação dos sistemas com o intuito de obter informações sobre o comportamento dos géis quanto à adição de ácido acético como co-surfactante.

***Capítulo 6: Physical properties of gellan microemulsion based gels***

Após estudar a interação entre gelana e Tween 80 no Capítulo 5, este polissacarídeo foi adicionado em alguns sistemas do diagrama de fases obtido no Capítulo 4, composto por água, polissorbato 80, ácido acético e HOSO. Além disso, sistemas sem co-surfactante também foram estudados. Os géis obtidos com os dois diagramas foram avaliados em relação às suas propriedades reológicas, mecânicas e estruturais.

***Capítulo 7. Conclusões gerais***

**4. REFERÊNCIAS BIBLIOGRÁFICAS**

BAROT, B. S.; PAREJIYA, P. B.; PATEL, H. K.; MEHTA, D. M.; SHELAT, P. K. Microemulsion-based antifungal gel delivery to nail for the treatment of onychomycosis: formulation, optimization, and efficacy studies. **Drug Delivery and Translational Research**, v. 2, n. 6, p.463-476. 2012.

BINKS, B. P.; FLETCHER, P. D. I.; TIAN, L. Influence of nanoparticle addition to Winsor surfactant microemulsion systems. **Colloids and Surfaces A-Physicochemical and Engineering Aspects**, v. 363, n. 1-3, p.8-15. 2010.

CHEN, H.; MOU, D.; DU, D.; CHANG, X.; ZHU, D.; LIU, J.; XU, H.; YANG, X. Hydrogel-thickened microemulsion for topical administration of drug molecule at an extremely low concentration. **International Journal of Pharmaceutics**, v. 341, n. 1-2, p.78-84. 2007.

D'CRUZ, O. J.; UCKUN, F. M. Gel-microemulsions as vaginal spermicides and intravaginal drug delivery vehicles. **Contraception**, v. 64, n. 2, p.113-123. 2001.

DE CAMPO, L.; YAGHMUR, A.; GARTI, N.; LESER, M. E.; FOLMER, B.; GLATTER, O. Five-component food-grade microemulsions: structural characterization by SANS. **Journal of Colloid and Interface Science**, v. 274, n. 1, p.251-267. 2004.

ENGSTROM, S.; LARSSON, K. Microemulsion in foods. In: Kumar, P., Mittal, K. L. **Handbook of microemulsion science and technology**, New York: Dekker, 789-796, 1999.

FENG, J. L.; WANG, Z. W.; ZHANG, J.; WANG, Z. N.; LIU, F. Study on food-grade vitamin E microemulsions based on nonionic emulsifiers. **Colloids and Surfaces A- Physicochemical and Engineering Aspects**, v. 339, n. 1-3, p.1-6. 2009.

FLANAGAN, J.; KORTEGAARD, K.; PINDER, D. N.; RADES, T.; SINGH, H. Solubilisation of soybean oil in microemulsions using various surfactants. **Food Hydrocolloids**, v. 20, n. 2-3, Mar-May, p.253-260. 2006.

FLANAGAN, J.; SINGH, H. Microemulsions: A potential delivery system for bioactives in food. **Critical Reviews in Food Science and Nutrition**, v. 46, n. 3, p.221-237. 2006.

GAONKAR, A.; BAGWE, R.P. Microemulsions in Foods. In: Shah, D.O. e Mittal, K.L. **Adsorption and Aggregation of Surfactants in Solution**, New york:CRC Press, 407-430, 2002.

GONG, Y.; LIU, Q. L.; ZHU, A. M.; ZHANG, Q. G. One-pot synthesis of poly(N-isopropylacrylamide)/chitosan composite microspheres via microemulsion. **Carbohydrate Polymers**, v. 90, n. 1, p.690-705. 2012.

KANTARIA, S.; REES, G. D.; LAWRENCE, M. J. Gelatin-stabilised microemulsion-based organogels: rheology and application in iontophoretic transdermal drug delivery. **Journal of Controlled Release**, v. 60, n. 2-3, p.355-365. 1999.

KOOP, H. S.; DA-LOZZO, E. J.; DE FREITAS, R. A.; FRANCO, C. R. C.; MITCHELL, D. A.; SILVEIRA, J. L. M. Rheological Characterization of a Xanthan-Galactomannan Hydrogel Loaded with Lipophilic Substances. **Journal of Pharmaceutical Sciences**, v. 101, n. 7, p.2457-2467. 2012.

LOPEZ, F.; VENDITTI, F.; AMBROSONE, L.; COLAFEMMINA, G.; CEGLIE, A.; PALAZZO, G. Gelatin microemulsion-based gels with the cationic surfactant cetyltrimethylammonium bromide: A self-diffusion and conductivity study. **Langmuir**, v. 20, n. 22, p.9449-9452. 2004.

LV, F. F.; ZHENG, L. Q.; TUNG, C. H. Phase behavior of the microemulsions and the stability of the chloramphenicol in the microemulsion-based ocular drug delivery system. **International Journal of Pharmaceutics**, v. 301, n. 1-2, p.237-246. 2005.

MORITAKA, H.; NISHINARI, K.; TAKI, M.; FUKUBA, H. Effects of Ph, Potassium-Chloride, and Sodium-Chloride on the Thermal and Rheological Properties of Gellan Gum Gels. **Journal of Agricultural and Food Chemistry**, v. 43, n. 6, p.1685-1699. 1995.

PATEL, N.; SCHMID, U.; LAWRENCE, M. J. Phospholipid-based microemulsions suitable for use in foods. **Journal of Agricultural and Food Chemistry**, v. 54, n. 20, p.7817-7824. 2006.

PICONE, C. S. F.; CUNHA, R. L. Influence of pH on formation and properties of gellan gels. **Carbohydrate Polymers**, v. 84, n. 1, p.662-668. 2011.

RAO, J. J.; MCCLEMENTS, D. J. Food-grade microemulsions, nanoemulsions and emulsions: Fabrication from sucrose monopalmitate & lemon oil. **Food Hydrocolloids**, v. 25, n. 6, p.1413-1423. 2011.

ROZNER, S.; SHALEV, D. E.; SHAMES, A. I.; OTTAVIANI, M. F.; ASERIN, A.; GARTI, N. Do food microemulsions and dietary mixed micelles interact? **Colloids and Surfaces B-Biointerfaces**, v. 77, n. 1, p.22-30. 2010.

VALENTA, C.; SCHULTZ, K. Influence of carrageenan on the rheology and skin permeation of microemulsion formulations. **Journal of Controlled Release**, v. 95, n. 2, p.257-265. 2004.

YAGHMUR, A.; DE CAMPO, L.; ASERIN, A.; GARTI, N.; GLATTER, O. Structural characterization of five-component food grade oil-in-water nonionic microemulsions. **Physical Chemistry Chemical Physics**, v. 6, n. 7, p.1524-1533. 2004.

YAMAMOTO, F.; CUNHA, R. L. Acid gelation of gellan: Effect of final pH and heat treatment conditions. **Carbohydrate Polymers**, v. 68, n. 3, p.517-527. 2007.

ZHANG, H.; XU, Y. Q.; WU, L. J.; ZHENG, X. D.; ZHU, S. M.; FENG, F. Q.; SHEN, L. R. Anti-yeast activity of a food-grade dilution-stable microemulsion. **Applied Microbiology and Biotechnology**, v. 87, n. 3, p.1101-1108. 2010.

ZHAO, X. Y.; XU, J.; ZHENG, L. Q.; LI, X. W. Preparation of temperature-sensitive microemulsion-based gels formed from a triblock copolymer. **Colloids and Surfaces a-Physicochemical and Engineering Aspects**, v. 307, n. 1-3, p.100-107. 2007.

**– CAPÍTULO 2 –**  
***REVISÃO BIBLIOGRÁFICA***



## **1. SISTEMAS DE EMULSIFICAÇÃO ESPONTÂNEA**

Sistemas compostos pela mistura de dois líquidos imiscíveis (usualmente óleo e água) são tradicionalmente conhecidos como emulsões. A preparação de emulsões é um processo que utiliza elevada quantidade de energia mecânica, que é necessária para misturar os componentes, fazendo que um dos líquidos fique disperso no outro na forma de pequenas gotas geralmente de tamanho micrométrico (JAFARI et al., 2008; MCCLEMENTS, 2005). Todavia, todas as emulsões são termodinamicamente instáveis e tendem a se romper com o tempo, resultando em duas fases líquidas separadas. No entanto, a estabilidade cinética desse tipo de sistema pode ser alcançada de outras maneiras, possibilitando o desenvolvimento de produtos que apresentem propriedades desejáveis por um período de tempo suficientemente longo. Desta maneira, para produzir emulsões cineticamente estáveis é necessária a adição de dois tipos de ingredientes: emulsificantes e estabilizantes (DICKINSON, 2003). Além disso, dependendo das condições de processo, homogeneização e ingredientes utilizados, esses sistemas podem compreender gotas de tamanho variando até a escala nanométrica. Essas emulsões são chamadas de nanoemulsões, miniemulsões ou macroemulsões (BELENKI et al., 2013; KABALNOV et al., 1996; MCCLEMENTS, 2011).

As microemulsões por sua vez, são soluções isotrópicas, transparentes e com partículas de tamanho nanométrico (<100 nm). Além disso, ao contrário das emulsões, são sistemas termodinamicamente estáveis, o que significa que são formados espontaneamente pela auto-organização das partes hidrofílicas e hidrofóbicas das moléculas de surfactante na interface óleo-água (FLANAGAN et al., 2006; GAONKAR; BAGWE, 2002). Em todo sistema composto por surfactante, óleo e/ou água, as moléculas

anfifílicas se localizam na interface entre o domínio dos dois líquidos. A associação das moléculas anfifílicas é um fenômeno termodinamicamente favorável que busca a otimização da solvatação da molécula e a redução da energia livre do sistema (LAWRENCE; REES, 2000). Diferentemente das emulsões que requerem baixa concentração de surfactante (até 2%) para alcançar a estabilidade cinética, a concentração desse composto necessária para a formação das microemulsões é em torno de 20% ou mais (RAKSHIT; MOULIK, 2008). Em condições adequadas de processo, os surfactantes levam a uma mudança de curvatura (positiva para sistemas óleo em água O/A e negativa para sistemas água em óleo A/O) na interface óleo-água e à transição de fases, formando gotas dispersas em um meio contínuo. Esta mudança pode ocorrer através do ajuste da composição do sistema a temperatura constante (método de emulsificação espontânea) ou através da mudança de temperatura, a composição constante (método de temperatura de inversão de fases) (SAGALOWICZ; LESER, 2010). Para que ocorra a formação das microemulsões é necessário que a energia livre de Gibbs seja negativa (Equação 1).

$$\Delta G_f = \Delta H - T \cdot \Delta S_f + \gamma \cdot \Delta A \quad (1)$$

onde  $\Delta G_f$  é a energia livre de formação,  $\Delta H$  a variação de entalpia,  $T$  a temperatura,  $\Delta S_f$  a variação da entropia de formação,  $\gamma$  a tensão interfacial e  $\Delta A$  a variação na área interfacial.

A variação da entalpia quando água e óleos imiscíveis são misturados pode ser considerada insignificante. Já quando as fases aquosa e oleosa são misturadas na presença de surfactante, este se difunde na interface óleo-água e as gotas se formam,

aumentando a entropia do sistema ( $T \Delta S_f >> 0$ ). No entanto, durante a formação das gotas nas emulsões ou microemulsões, a variação da área interfacial  $\Delta A$  é muito grande, já que ocorre a formação de gotas de tamanho reduzido. Isso poderia levar a valores de  $\Delta G_f$  positivos, pois a tensão interfacial é positiva e o sistema não se formaria espontaneamente, como no caso das emulsões. Assim, para fazer com que  $\Delta G_f$  se torne negativo, a tensão interfacial tem que ser reduzida a um valor muito baixo, o que pode ser alcançado com a adição de surfactantes (RAKSHIT; MOULIK, 2008). A Figura 1 compara a influência da energia livre de Gibbs na formação das microemulsões e na separação de fases das emulsões. É possível perceber que, como a energia livre de formação é negativa ( $\Delta G_f < 0$ ), o processo de emulsificação torna-se espontâneo e o sistema resultante é termodinamicamente favorável (LAWRENCE; REES, 2000; RAKSHIT; MOULIK, 2008).

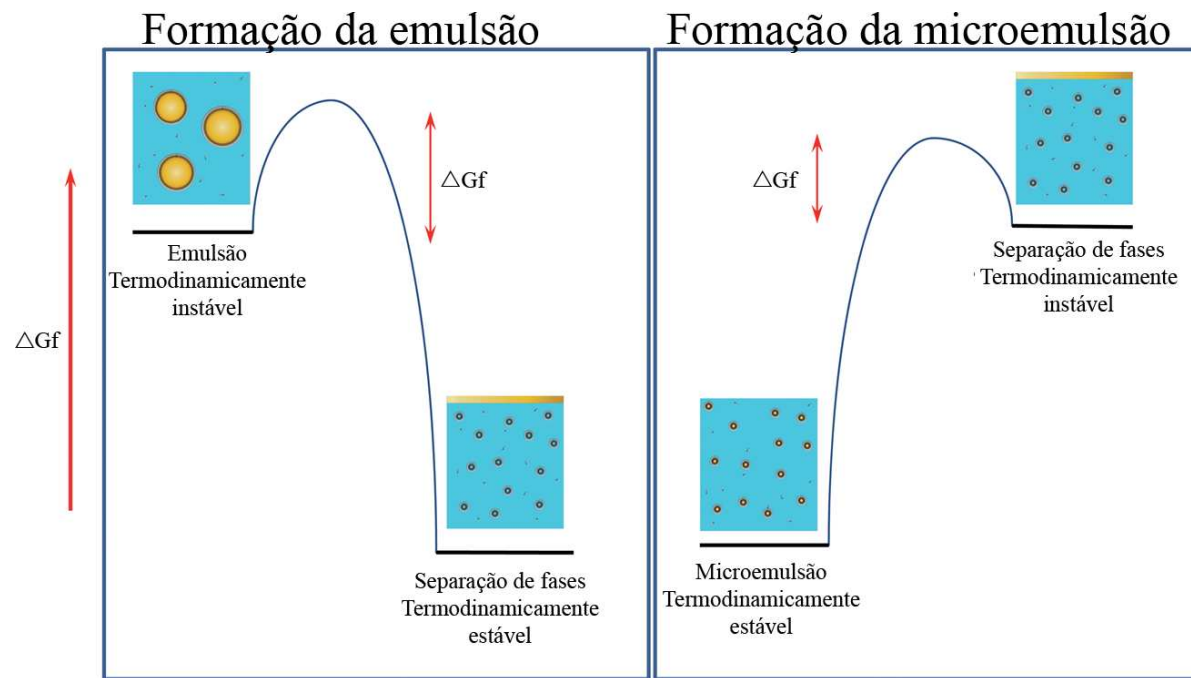


**Figura 1. Diagrama esquemático da energia livre de sistemas emulsionados e microemulsionados em comparação com o estado de separação de fases.**

O preparo de microemulsões a partir do método de emulsificação espontânea se baseia na mistura de componentes (óleo, água, surfactante e co-surfactante) em concentração específica a temperatura constante até a formação de um sistema isotropicamente translúcido (ANTON; VANDAMME, 2009; RAKSHIT; MOULIK, 2008). Os ingredientes podem ser misturados de maneiras diferentes: adicionando água a uma mistura de óleo e surfactante, diluindo uma mistura de óleo e surfactante em água; diluindo uma mistura de água e surfactante em óleo; ou misturando todos os componentes ao mesmo tempo para uma dada formulação final. A ordem de adição dos ingredientes influencia na formação das microemulsões de alguns sistemas, sendo que a titulação de uma solução aquosa em uma mistura prévia de óleo e surfactante/co-surfactante tem se mostrado mais adequada (FLANAGAN et al., 2006).

Além das microemulsões monofásicas, o sistema óleo, água, surfactante e co-surfactante pode apresentar-se como um sistema multifásico, convenientemente descrito pela classificação de Winsor (Figura 2) (WINSOR, 1948). O sistema Winsor I consiste em uma microemulsão O/A em equilíbrio com uma fase superior com excesso de óleo. O sistema Winsor II representa uma microemulsão A/O em equilíbrio com uma fase inferior com excesso de água. Quando volumes iguais de óleo e água estão presentes, uma estrutura bicontínua é formada, e uma fase superior de óleo e uma fase inferior de água podem existir (FLANAGAN et al., 2006), sendo este sistema classificado como Winsor III. Finalmente, o sistema Winsor IV define macroscopicamente o sistema simples de microemulsão O/A ou A/O.

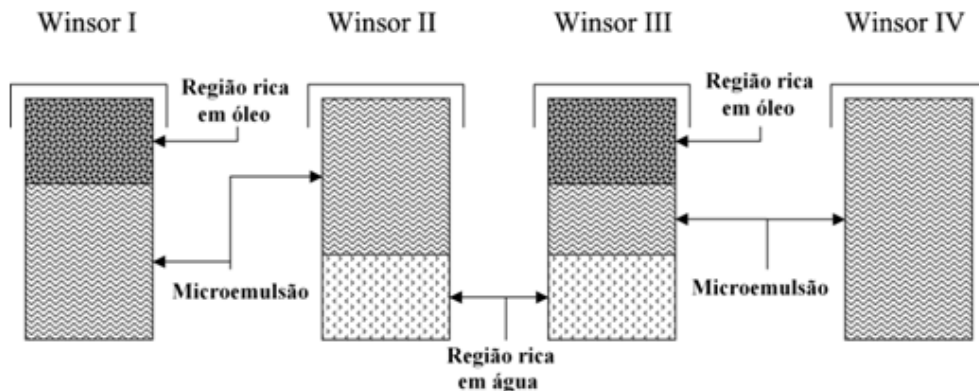


**Figura 2. Sistema de classificação de Winsor.** Fonte: FLANAGAN et al. (2006).

Microemulsões O/A são constituídas por micelas contendo óleo em sua parte central (Figura 3A) e são formadas quando uma baixa concentração de fase oleosa está presente. Já as microemulsões A/O são produzidas quando pequenas concentrações de fase aquosa estão presentes, formando micelas reversas (Figura 3C). A microemulsão bicontínua existe quando quantidades similares das fases aquosa e oleosa estão presentes. O óleo e a água coexistem como uma fase contínua na presença de uma interface estabilizada por um filme de surfactante contínuo e flutuante cuja curvatura é zero (Figura 3B) (LAWRENCE; REES, 2000).

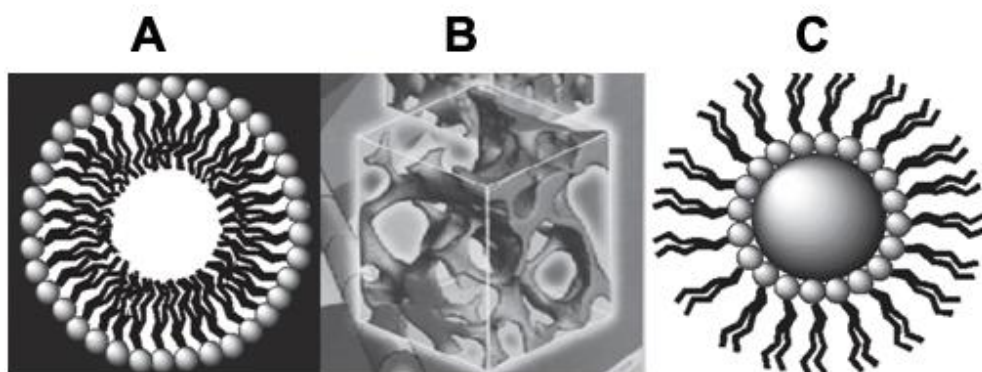


**Figura 3. Esquema representativo da microestrutura das microemulsões (A) microemulsão O/A, (B) microemulsão bicontínua e (C) microemulsão A/O.** Fonte: MEHTA et al. (2008).

Quando o surfactante se encontra em concentrações muito baixas, eles ficam dispersos de forma discreta no meio contínuo. Acima de uma concentração específica, conhecida como concentração micelar crítica (CMC), além da forma micelar (Figura 3A e 3C), os surfactantes se auto-organizam formando estruturas ordenadas caracterizadas por regiões hidrofóbicas e hidrofílicas alternadas. Estes sistemas podem originar estruturas altamente organizadas quando incorporados de quantidades relevantes de surfactantes, sendo classificados como líquidos cristalinos ou algumas vezes também chamados de mesofase (FORMARIZ et al., 2006; LAWRENCE; REES, 2000). Essas estruturas podem conter vários padrões de agregação e morfologia (microestrutura). Métodos como *nuclear magnetic resonance* – NMR, *dynamic light scattering* (DLS), *small-angle neutron scattering* (SANS), *small angle x-ray scattering* (SAXS), reologia, condutividade elétrica, têm sido utilizados para tentar elucidar e entender a formação das diferentes microestruturas das microemulsões (MOULIK; PAUL, 1998; RAKSHIT; MOULIK, 2008)

O aumento inicial da concentração de surfactante ou tensoativo transforma a estrutura esférica micelar típica em uma estrutura micelar mais alongada ou micela inchada (Figura 4A). Um aumento ainda maior na concentração pode causar a orientação e o empacotamento rígido da micela alongada em formações hexagonais (Figura 4B). Dependendo do tensoativo utilizado, um aumento adicional da concentração resulta em uma estrutura lamelar (Figura 4C). Já a fase cúbica (Figura 4D), que ocorre entre as condições de estrutura hexagonal e lamelar, é uma estrutura contínua complexa, apresentando curvaturas positivas e negativas na interface (ATTWOOD; FLORENCE, 2003; LAWRENCE, 1994). A habilidade de formar cada tipo de estrutura é consequência da estrutura do surfactante (tamanho da cauda hidrofóbica e volume da cabeça

hidrofílica), que facilita a organização da suas moléculas em determinados arranjos. Ao contrário das microemulsões, que apresentam transparência e viscosidade muito baixa, essas estruturas são anisotrópicas e também podem apresentar características elásticas de sólidos, já que são caracterizadas por sistemas ordenados. A fase lamelar apresenta-se como um líquido viscoso, a fase hexagonal tem viscosidade semelhante a um gel e por sua vez, a viscosidade da fase cúbica é extremamente elevada (HYDE, 2001; LAWRENCE, 1994).

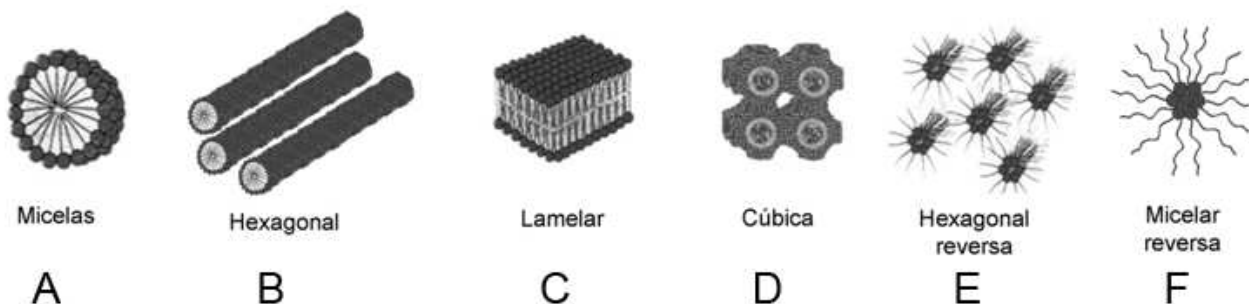


**Figura 4. Representação esquemática das diferentes estruturas formadas pela auto-associação dos surfactantes. Adaptado de HOLMBERG et al. (2002).**

Com o intuito de compreender os diferentes sistemas e definir a extensão e a natureza das regiões de formação de microemulsões, diagramas de fases são construídos (Figura 5). Sistemas simples compostos por água, óleo e surfactante são avaliados em diagramas de fases ternários, onde cada vértice representa 100 % de um componente particular. Quando as microemulsões são compostas por mais substâncias, como co-surfactante e bioativos dissolvidos, diagramas de fases pseudo-ternários são utilizados, tendo um ou mais vértices do diagrama representados por uma mistura binária, como surfactante/co-surfactante, água/bioativo ou óleo/bioativo (AIKENS; FRIBERG, 2008; LAWRENCE; REES, 2000).

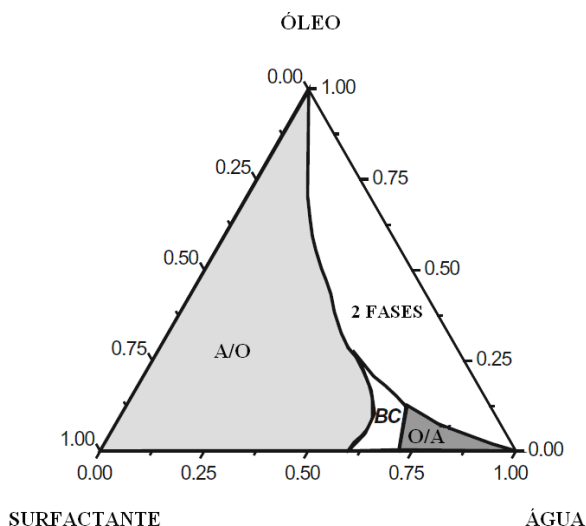


**Figura 5. Diagrama de fases esquemático de um sistema ternário composto por água, óleo e surfactante, identificando as regiões formadoras de microemulsões O/A, A/O ou BC (bicontínua) (Adaptado de ZHONG et al., 2009).**

Existem numerosas aplicações para as microemulsões e líquidos cristalinos em diversas áreas, incluindo farmacêutica, cosmética, recuperação de óleos, e como agente veiculador de substâncias hidrofílicas ou hidrofóbicas (DE CAMPO et al., 2004; ENGSTROM; LARSSON, 1999; SJOBLOM et al., 1996). Contudo, sua aplicação em alimentos é limitada, uma vez que a maioria dos surfactantes e co-surfactantes utilizados na produção das microemulsões não são permitidos, ou só podem ser utilizados em baixas concentrações. Outro problema é o tipo de óleo utilizado na preparação das microemulsões. Os óleos comestíveis são geralmente triacilgliceróis de cadeia longa como óleo de soja, e são difíceis de serem solubilizados (FLANAGAN et al., 2006; GAONKAR; BAGWE, 2002), não sendo adequados para a formação das microemulsões. Em geral são utilizados óleos essenciais de cadeia curta como óleo de limão (FANUN, 2010b; RAO; MCCLEMENTS, 2011), tolueno (BINKS et al., 2010) ou misturas de triglycerídeos de cadeia média (ANTON; VANDAMME, 2009).

## **2. INGREDIENTES DE MICROEMULSÕES PARA ALIMENTOS**

As propriedades das substâncias que compõem a microemulsão (água, óleo, surfactante e co-surfactante) influenciam diretamente no comportamento das fases, assim como na capacidade de solubilização de outro composto adicionado (YAGHMUR et al., 2002). A estrutura e propriedades da fase lipídica apresentam variação principalmente devido ao tamanho da cadeia e número de insaturações, uma vez que os óleos utilizados na indústria de alimentos são triacilgliceróis. A temperatura também não pode variar muito para favorecer a produção das microemulsões, pois os alimentos ou bebidas precisam geralmente ser estáveis na temperatura de armazenamento. Com isso o que se torna importante é a natureza e a concentração do surfactante e co-surfactante utilizados (GAONKAR; BAGWE, 2002).

### ***2.1. Surfactantes***

A estrutura do surfactante determina se, no equilíbrio, a interface terá uma curvatura positiva ou negativa e dessa forma se serão formadas microemulsões com água ou óleo como meio contínuo (O/A ou A/O, respectivamente) ou mesofases. É sabido que surfactantes com uma “cabeça” hidrofílica maior e “cauda” menor formam micelas de microemulsões O/A. Por sua vez, os surfactantes com pequenas “cabeças” e longas “caudas” tendem a formar micelas reversas ou microemulsões A/O (GAONKAR; BAGWE, 2002).

Os surfactantes podem ser classificados quanto ao balanço hidrofílico-lipofílico (BHL) de acordo com sua estrutura molecular. Os surfactantes mais hidrofóbicos apresentam um baixo valor de BHL, sendo mais solúveis em óleo, enquanto que os compostos com elevado valor de BHL possuem um caráter hidrofílico mais pronunciado,

sendo solúveis em água. Como regra geral, surfactantes com valores de BHL de 3 - 6 são apropriados para a estabilização de emulsões A/O, enquanto que aqueles com valores de 8 – 18 atuam como emulsificantes de emulsões O/A (ARAUJO, 2001). Os surfactantes são também classificados de acordo com a natureza de sua porção polar, podendo ser catiônicos, aniônicos, não iônicos ou zwiteriônicos (também denominados como anfóteros ou anfolíticos). Com poucas exceções, os surfactantes alimentares são na maioria não-iônicos. Alguns surfactantes e seus respectivos valores de BHL estão apresentados na Tabela 1.

**Tabela 1. Alguns surfactantes de grau alimentício e seus valores de BHL**

<b>Tipo de Surfactante</b>	<b>Exemplos</b>	<b>BHL</b>
Aniônicos		
Éster de ácido láctico	Estearyl 2-lactil lactato de sódio (Esterlac E)	21,0
Zwiteriônicos		
Fosfolipídios	Lecitina	~ 9
Não-iônico		
Alcoóis alifáticos	Hexadecanol	1,0
Monoglicerídios	Monoestearato de glicerol	3,8
Ester de monoglicerídios	Monopalmitato de lactoil	8,0
Span 80	Monooleato de sorbitana	4,3
Span 60	Monoestearato de sorbitana	4,7
Span 40	Monopalmitato de sorbitana	6,7
Span 20	Monolaurato de sorbitana	8,6
Tween 80	Monooleato de polioxietileno de sorbitana	15,0
Tween 60	Monoestearato de polioxietileno de sorbitana	14,9
Tween 40	Monopalmitato de polioxietileno de sorbitana	15,6
Tween 20	Monolaurato de polioxietileno de sorbitana	16,7

(Fonte: ARAUJO (2001) e WALSTRA (2002))

Os surfactantes aniônicos contêm geralmente um dos quatro grupos polares solúveis carboxilato, sulfonato, sulfato ou fosfato, apresentando dessa forma, altos valores de BHL. Os surfactantes catiônicos são muito utilizados em agentes de limpeza e cosméticos em geral, sendo compostos por um ou vários grupos amônio terciários ou quaternários. Já os zwiteriônicos são constituídos por dois grupos carregados, um positivo e outro negativamente (KIRK et al., 1996). Por sua vez, os surfactantes não-iônicos são os mais comumente utilizados e abrangem uma alta faixa de valores de BHL. Entre esses surfactantes encontram-se os polissorbatos, que são amplamente utilizados na indústria alimentícia. São derivados de sorbitanas (grupo hidrofílico) esterificadas com ácidos graxos (grupo hidrofóbico), com um total de 20 subunidades de óxido de etileno por molécula (JIAO, 2008; KERWIN, 2008). Os diferentes polissorbatos variam no comprimento da cadeia de polioxietileno, tipo de ácido graxo e grau de esterificação. O polissorbato 80 ou Tween 80 (Figura 6) é uma mistura de ésteres de polioxietileno obtidos da mistura parcial de ésteres de ácido oléico com anidridos de sorbitol e compostos relacionados.

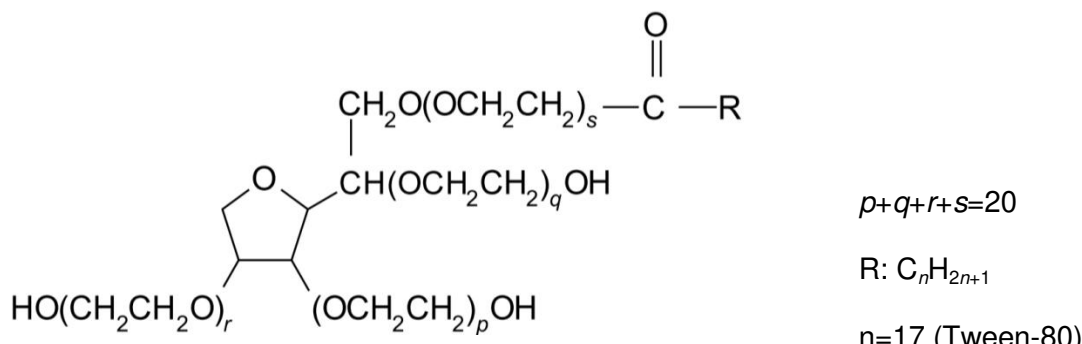


**Figura 6. Estrutura química do polisorbato 80, ou Tween 80.**

## **2.2. Co-surfactantes**

Os co-surfactantes são moléculas anfifílicas que se estendem na interface óleo-água juntamente com os surfactantes, agindo também como emulsificantes (MILLER;

NEOGI, 2007). As moléculas de co-surfactante são suficientemente polares para se localizarem entre as caudas dos surfactantes, aumentando o volume da região hidrofóbica, a flexibilidade da interface e a fluidez da microemulsão (FLANAGAN; SINGH, 2006; YAGHMUR et al., 2002). Dessa forma, o uso de co-surfactantes aumenta a região de formação de microemulsão no diagrama de fases e suas funções em uma microemulsão são:

- Ajustar o balanço hidrofílico-lipofílico (BHL) e a curvatura espontânea da interface através do controle da distribuição do surfactante;
- Destruir o cristal líquido ou estruturas tipo gel;
- Diminuir a sensibilidade às variações de composição do sistema (FLANAGAN; SINGH, 2006; GAONKAR; BAGWE, 2002; YAGHMUR et al., 2002)

Os co-surfactantes mais utilizados são alcoóis e glicóis, de massa molecular baixa ou média, que apresentam uma cadeia contendo entre dois a dez carbonos. O etanol é um co-surfactante permitido em alguns alimentos (FENG et al., 2009; PATEL et al., 2006), mas sua eficiência é inferior aos alcoóis de grau não alimentício, comumente utilizados na formação de microemulsões (butanol, propanol pentanol e hexanol). Apesar disso, alguns estudos relataram a formação de microemulsões contendo 10 a 20 % de etanol, com potencial uso em bebidas alcoólicas (FLANAGAN; SINGH, 2006).

Recentemente tem sido estudada a possibilidade do uso de ácidos orgânicos como co-surfactantes, o que viabilizaria o consumo de microemulsões com restrições ao uso de álcool (CID-SAMAMED et al., 2008; LI et al., 2010; SPERNATH et al., 2006; ZHANG et al., 2009; ZHANG et al., 2010). A adição de ácidos orgânicos de cadeia curta (ácido acético, cítrico, propiônico) levariam ao aumento da região da microemulsão, uma

vez que agiriam como co-solvente e co-surfactante (SPERNATH et al., 2006; ZHANG et al., 2009). Além disso, o comportamento dos diferentes ácidos orgânicos nas microemulsões também depende da configuração e tamanho da cadeia de sua molécula, da mesma forma que os alcoóis.

### **2.3. Óleos**

Dependendo da natureza do óleo, em particular do tamanho da cadeia de hidrocarboneto, o óleo pode penetrar em diferentes extensões no filme de surfactante que envolve a gota. Óleos vegetais de cadeia longa são compostos por uma longa cadeia de ácidos graxos, são semi-polares e muito volumosos para penetrarem facilmente no filme interfacial e viabilizar a curvatura ótima de formação da microemulsão (FLANAGAN et al., 2006). Por este motivo, hidrocarbonetos saturados de cadeia curta ( $C_nH_{2n+2}$ ) de grau não alimentício, como o hexano, formam microemulsões com maior facilidade (YAGHMUR et al., 2002). Óleos essenciais também possuem massa molar pequena, sendo caracterizados por uma mistura complexa de hidrocarbonetos (geralmente cílicos e insaturados), alcoóis e compostos carbonílicos (ARAUJO, 2001). Desta maneira, óleos de cadeia média, como Miglyol (PATEL et al., 2006), e óleos essenciais, como o limoneno (AMAR et al., 2003; YAGHMUR et al., 2002) e óleo de menta (FANUN, 2010a; ZHONG et al., 2009), têm sido utilizados no preparo de microemulsões de grau alimentício.

Apesar destas dificuldades, há um grande interesse em se produzir microemulsões com óleos vegetais tradicionais, como o óleo de soja, milho ou girassol já que eles estão disponíveis em elevada quantidade e a um preço acessível. Contudo, óleos com diferentes estruturas apresentam diferentes propriedades. O aumento do grau de insaturação pode levar ao aumento da hidrofobicidade do óleo e à diminuição da energia

de interação entre o surfactante e o triacilglicerol. Esse comportamento pode ser devido ao arranjo mais desorganizado da cadeia de triacilglicerol, pela maior mobilidade causada pela presença da maior quantidade de insaturações (PHAN et al., 2010). A composição em ácidos graxos de alguns destes óleos está apresentada na Tabela 2.

**Tabela 2. Composição em ácidos graxos de óleos vegetais.**

Ácido Graxo (% m/m)	Óleos					
	Girassol					
	Girassol <sup>1</sup>	Alto oléico <sup>2</sup>	Oliva <sup>3</sup>	Soja <sup>4</sup>	Milho <sup>5</sup>	Algodão <sup>6</sup>
C6:0	-	-	-	-	-	-
C8:0	-	-	-	-	-	-
C10:0	-	-	-	-	-	-
C12:0	-	-	-	-	-	-
C14:0	-	-	-	0,09	-	0,32
C16:0	7,20	3,8	12,40	11,18	13,8	15,53
C16:1	-	-	-	0,09	0,19	0,12
C17:0	-	-	-	-	-	-
C18:0	3,00	4,5	2,80	4,13	2,20	3,40
C18:1	23,00	83,0	77,80	25,62	34,45	21,23
C18:2	66,00	9,55	7,00	51,28	47,39	54,07
C18:3	0,5	-	-	6,12	0,83	4,59
C20:0	-	-	-	0,45	0,48	0,36
C20:1	-	-	-	0,31	0,34	-
C20:4	0,30	-	-	-	0,17	-
C22:0	-	-	-	0,54	0,19	0,38

FONTE: <sup>1</sup>MOHSEN-NIA; KHODAYARI (2008), <sup>2</sup>DELPLANQUE (2000), <sup>3</sup>GONZALEZ et al. (1997), <sup>4</sup>LANZA et al. (2009), <sup>5</sup>DA SILVA et al. (2010), <sup>6</sup>RODRIGUES et al. (2005)

O óleo de girassol (*Helianthus annuus* L.) é um dos mais importantes óleos vegetais, devido a sua alta qualidade nutricional, sendo utilizado na culinária como óleo de salada, para fritura e na produção de margarina (ZLATANOV et al., 2009). Geralmente no óleo de girassol tradicional, até 90% dos ácidos graxos são insaturados (oléico C18:1, 16%-19% e linolênico C:18:2, 68%-72%), enquanto os ácidos graxos saturados somam cerca de 10% (SKORIC et al., 2008). Além disso, esse óleo é rico em tocoferóis ( $\alpha$ -tocoferol como componente majoritário), que são antioxidantes naturais, prevenindo a auto-oxidação dos lipídeos a temperatura ambiente. Com o intuito de melhorar o uso do óleo de girassol na culinária, novas variedades vêm sendo selecionadas, onde o ácido graxo principal é representado pelo ácido oléico, que pode apresentar quase 90% de ácido oléico em sua composição (Tabela 2). O interesse crescente no óleo de girassol alto oléico (HOSO – do inglês *high oleic sunflower oil*) é devido aos benefícios nutricionais do efeito da alta quantidade de óleos monoinsaturados e baixo conteúdo de ácidos graxos saturados (DELPLANQUE, 2000). Os HOSO são considerados como uma alternativa para os óleos hidrogenados ou parcialmente hidrogenados que são utilizados em muitos produtos alimentícios e em aplicações industriais onde a alta estabilidade frente à oxidação é necessária (NIEMELA et al., 1996; ZLATANOV et al., 2009).

### **3. GÉIS A PARTIR DE MICROEMULSÕES**

Além dos componentes que formam as microemulsões e cristais líquidos (água, surfactante, óleo e co-surfactante), outros materiais podem ser veiculados ou solubilizados nesses sistemas. Particularmente, a solubilização de macromoléculas (proteínas e polissacarídeos) têm sido de considerável interesse principalmente no que

diz respeito à modificação de textura para veiculação de bioativos pela indústria farmacêutica (BAROT et al., 2012; CHEN et al., 2007; FANUN, 2012; JOSEF et al., 2010; WANG et al., 2008). A utilização desses biopolímeros permite a gelificação do sistema e dependendo da fase predominante podem ser classificados como hidrogéis ou organogéis e são chamados na literatura respectivamente de MBH ou MBG (do inglês *microemulsion-based hidrogels* ou *microemulsion-based gels*). A formação de MBGs a partir de microemulsões A/O foi primeiramente descrita em 1986 (HAERING; LUISI, 1986; QUELLET; EICKE, 1986) utilizando a gelatina como agente gelificante. Esse tipo de estrutura foi estudado e caracterizado em relação a sua microestrutura (ATKINSON et al., 1991; LUISI et al., 1990) e propriedades físico-químicas (ATKINSON et al., 1991; JENTA et al., 1997). Embora não haja um consenso entre as estruturas propostas para as MBG, essas diferenças podem ser atribuídas às diferentes formulações empregadas em cada estudo. Todavia, todos os modelos disponíveis estão de acordo que existe no interior do sistema uma rede polimérica (gelatina) interligada no interior da fase hidrofóbica contínua, que é estabilizada por uma camada de surfactante. O modelo esquemático proposto por ATKINSON et al. (1991) afirma que a rede de biopolímero proposta coexiste com uma população de gotas de microemulsão convencional (Figura 7).

A grande parte dos trabalhos foca no uso da gelatina como agente gelificante (ALIOTTA et al., 1996; ATKINSON et al., 1991; KANTARIA et al., 1999; LOPEZ et al., 2004; QUELLET; EICKE, 1986; ZHAO et al., 2006), todavia, nos últimos anos a tendência da utilização de outros compostos macromoleculares tem sido visada com o intuito de gelificar não somente a fase hidrofílica como também a hidrofóbica e até mesmo a produção de géis híbridos. Os biopolímeros mais utilizados para a gelificação desses sistemas são carragena, xantana e quitosana (GONG et al., 2012; KAWANO et al., 2010;

KOOP et al., 2012; VALENTA; SCHULTZ, 2004). Contudo, há ausência de estudos que levem ao entendimento da estrutura física dos géis de microemulsão, embora as propriedades desses sistemas indiquem que a fase oleosa possa estar alojada no interior da rede de gel tridimensional ou nas microemulsões transformadas em estruturas altamente ordenadas (cristais líquidos) (GULSEN; CHAUHAN, 2005; LAPASIN et al., 2001; PELTOLA et al., 2003)

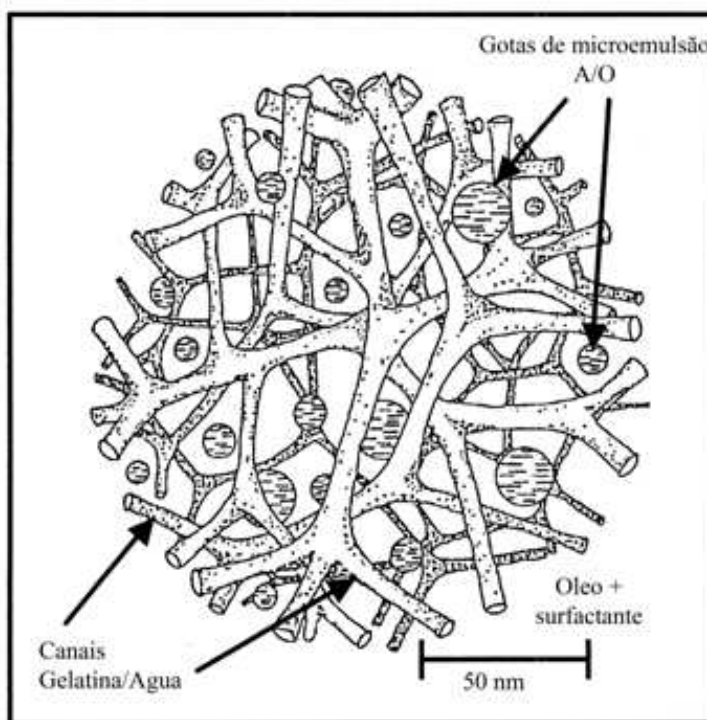


**Figura 7. Estrutura dos géis a base de microemulsão proposta por ATKINSON et al., 1991 (Adaptado de KANTARIA et al., 1999).**

Comparados aos hidrogéis comuns, os MBG ou MBH apresentam diversas vantagens principalmente em relação à sua maior estabilidade, uma vez que são preparados a partir de microemulsões, que são sistemas termodinamicamente estáveis (ZHAO et al., 2007). Além disso, os compostos orgânicos presentes no sistema podem

oferecer resistência à contaminação microbiana quando comparados à fase aquosa pura (COOK et al., 1993). Além disso, esses géis apresentam alta viscosidade o que aumenta seu tempo de residência, permitindo sua utilização como sistemas de liberação controlada (CHEN et al., 2007; D'CRUZ; UCKUN, 2001; ZHAO et al., 2007). Outras propriedades que tornam os géis a partir de microemulsões atrativos é a possibilidade de veicular bioativos hidrofílicos e hidrofóbicos, além de apresentarem alta condutividade elétrica (SAKATA et al., 2012), ao contrário da maioria dos organogéis apresentando, dessa forma, potencial aplicação ou transdérmica (KANTARIA et al., 1999; KANTARIA et al., 2003).

#### **4. GELANA**

A gelana é um polissacarídeo aniónico extracelular produzido pela bactéria *Sphingomonas elodea*. O produto direto da fermentação consiste de repetidas unidades de um tetrassacarídeo contendo um glicerato por unidade repetida e um acetato a cada duas unidades. Essa forma altamente acilada produz géis fracos devido à presença dos grupos glicerato que causam impedimento estérico no momento da agregação das hélices para formar a rede tridimensional. O tratamento com álcalis resulta na gelana desacilada, que é normalmente comercializada e possui um elevado poder gelificante. A gelana em sua forma desacilada é composta por uma sequência complexa de unidades de tetrassacarídeo (Figura 8) que se repetem:  $\beta$ -D-glicose,  $\beta$ -D-ácido glicurônico,  $\beta$ -D-glicose e  $\alpha$ -L-ramnose. Cada unidade tetramérica repetida possui um grupo carboxílico lateral (MILAS; RINAUDO, 1996; SANDERSON, 1990).

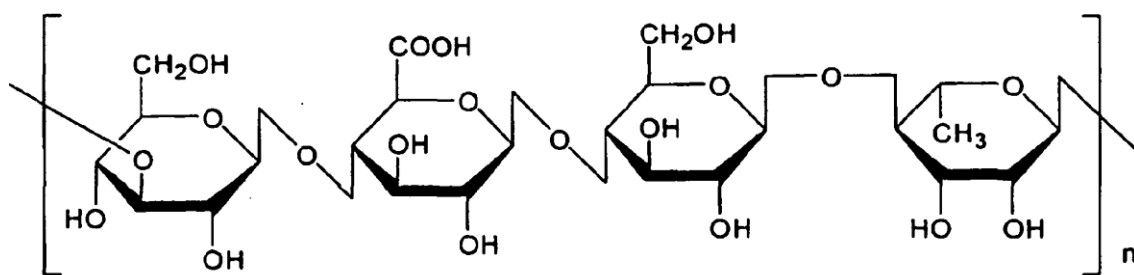


**Figura 8. Unidade tetramérica que compõem a goma gelana desacilada (TANG et al., 1996).**

A gelana possui alto poder gelificante inclusive em baixas concentrações. Os géis obtidos são rígidos, translúcidos e resistentes a baixos valores de pH, diferente de outros polissacarídeos amplamente utilizados na indústria de alimentos, como agarose e carragenas (MORITAKA et al., 1995; PICONE; CUNHA, 2011; YAMAMOTO; CUNHA, 2007). O mecanismo de gelificação da gelana é considerado como um processo em duas etapas, sendo a primeira a formação de duplas-hélices ordenadas (transição conformacional), seguida pela interação entre as hélices (transição sol – gel). Em solução aquosa, a gelana apresenta repulsão eletrostática intra e intermolecular entre seus grupos carboxílicos laterais, o que impede a formação e agregação das hélices para a formação do gel. O modelo mais comumente aceito para explicar o mecanismo de gelificação desse biopolímero é o de domínios, o qual sugere que a altas temperaturas, a gelana se apresenta em estado desordenado e enovelada. Assim, resfriando-se a solução em condições não gelificantes, os novelos se convertem reversivelmente em duplas-hélices e a associação dessas hélices por forças de van der Waals leva à gelificação macroscópica (transição sol-gel), como pode ser observado na Figura 9 (RODRIGUEZ-HERNANDEZ et al., 2003).

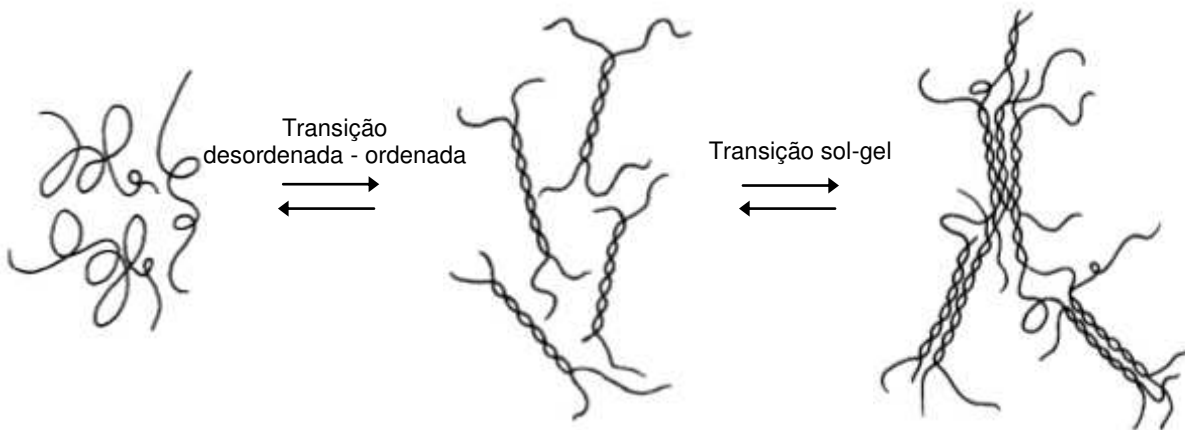


**Figura 9.** Representação esquemática do processo de transição contromacional da gelana (MIYOSHI et al., 1996).

A transição conformacional ocorre com o aumento da temperatura da solução e depende da concentração de polímero e da composição da solução. Além disso, a interação entre as duplas-hélices depende da presença de cátions na solução que promovem a formação de zonas de junção, possibilitando a formação da rede. As propriedades mecânicas dos géis resultantes dependem da concentração da gelana e dos cátions em solução (IKEDA et al., 2004; KASAPIS et al., 1999; OGAWA et al., 2006; RODRIGUEZ-HERNANDEZ et al., 2003).

O pH natural de uma solução típica de gelana contendo íons cálcio em concentrações de 1,5 a 60 mM está em torno de 5,0 (SANDERSON, 1990). A redução de pH de dispersões de gelana até valores próximos a 4 resulta no aumento da força dos géis, independentemente do tipo de acidificação empregada (MORITAKA et al., 1995; YAMAMOTO; CUNHA, 2007). Nestas condições, a repulsão eletrostática entre as moléculas é reduzida e a formação de zonas de junção é favorecida. No entanto, quando o pH é reduzido para valores próximos a 2, dois comportamentos distintos são relatados na literatura dependendo da forma de acidificação do meio. A acidificação direta com

sistema com HCl até pH 2 levou à produção de sistemas com aspecto turvo e separação de fases, que possivelmente estariam relacionados à hidrólise ácida das moléculas (MORITAKA et al., 1995). Já YAMAMOTO; CUNHA (2007) estudaram a acidificação indireta de soluções de gelana a partir da adição de glucona- $\delta$ -lactona GDL e obtiveram elevados valores de tensão de ruptura em sistemas formados em pH 2. Aparentemente, a acidificação indireta não provoca hidrólise das moléculas de gelana mesmo a baixos valores de pH. O decréscimo do pH também reduz a mobilidade das cadeias de gelana, facilitando a agregação e gelificação. Sabe-se que a redução do pH gera dissociação dos grupos carboxílicos laterais das moléculas de gelana, tornando-a um polieletróltio menos aniónico. A redução da repulsão eletrostática intermolecular favorece a formação de duplas-hélices pela associação de duas moléculas, com a presença de pontes de hidrogênio entre o ácido glucurônico de uma cadeia e a glicose e a ramnose de outra cadeia. Além disso, íons  $H^+$  se ligam à superfície das hélices individuais e diminuem sua densidade de carga, reduzindo a barreira eletrostática para a agregação das hélices e possibilitando a formação de “zonas de junção”. Interações secundárias, incluindo pontes de hidrogênio, ligam as cadeias às zonas de junção, o que resulta na gelificação macroscópica (transição sol – gel) (IKEDA et al., 2004; KASAPIS et al., 1999; OGAWA et al., 2006; RODRIGUEZ-HERNANDEZ et al., 2003).

## 5. REFERÊNCIAS BIBLIOGRÁFICAS

AIKENS, P; FRIBERG, S. A Phase Diagram Approach to Microemulsions. In: **Microemulsions** Boca raton: CRC Press, 2008.

ALIOTTA, F.; ARCOLEO, V.; LAMANNA, G.; LIVERI, V. T. Structural and dynamical investigation of gelatin containing water-in-oil microemulsions. **Colloid and Polymer Science**, v. 274, n. 10, p.989-994. 1996.

AMAR, I.; ASERIN, A.; GARTI, N. Solubilization Patterns of Lutein and Lutein Esters in Food Grade Nonionic Microemulsions. **Journal of Agricultural and Food Chemistry**, v. 51, n. 16, p.4775-4781. 2003.

ANTON, N.; VANDAMME, T. F. The universality of low-energy nano-emulsification. **International Journal of Pharmaceutics**, v. 377, n. 1-2, p.142-147. 2009.

ARAUJO, J.M.A. Química de alimentos: Teoria e prática. 2. Viçosa: UFV, 2001.

ATKINSON, P. J.; ROBINSON, B. H.; HOWE, A. M.; HEENAN, R. K. Structure and Stability of Microemulsion-Based Organo-Gels. **Journal of the Chemical Society-Faraday Transactions**, v. 87, n. 20, p.3389-3397. 1991.

ATTWOOD, D.; FLORENCE, A.T. **Princípios Físico-Químicos em Farmácia Vol. 4**. São Paulo: EDUSP, 2003.

BAROT, B.; PAREJIYA, P.; PATEL, H.; MEHTA, D.; SHELAT, P. K. Microemulsion-based antifungal gel delivery to nail for the treatment of onychomycosis: formulation, optimization, and efficacy studies. **Drug Delivery and Translational Research**, v. 2, n. 6, p.463-476. 2012.

BELENKI, C.; WINKELMANN, M.; NIEGER, M.; GERLINGER, W.; SACHWEH, B.; SCHUCHMANN, H. P.; MULLER, T.; BRÄSE, S. Cleavable surfactants to tune the stability

of W/O miniemulsions. **Journal of Colloid and Interface Science**, v. 393, p.203-209. 2013.

BINKS, B. P.; FLETCHER, P. D. I.; TIAN, L. Influence of nanoparticle addition to Winsor surfactant microemulsion systems. **Colloids and Surfaces A-Physicochemical and Engineering Aspects**, v. 363, n. 1-3, p.8-15. 2010.

CHEN, H. B.; MOU, D. S.; DU, D. R.; CHANG, X. L.; ZHU, D. D.; LIU, J.; XU, H. B.; YANG, X. L. Hydrogel-thickened microemulsion for topical administration of drug molecule at an extremely low concentration. **International Journal of Pharmaceutics**, v. 341, n. 1-2, p.78-84. 2007.

CID-SAMAMED, A.; GARCIA-RIO, L.; FERNANDEZ-GANDARA, D.; MEJUTO, J. C.; MORALES, J.; PEREZ-LORENZO, M. Influence of n-alkyl acids on the percolative phenomena in AOT-based microemulsions. **Journal of Colloid and Interface Science**, v. 318, n. 2, p.525-539. 2008.

COOK, A. D.; SAGERS, R. D.; PITI, W. G. Bacterial Adhesion to Poly(Hema)-Based Hydrogels. **Journal of Biomedical Materials Research**, v. 27, n. 1, p.119-126. 1993.

D'CRUZ, O. J.; UCKUN, F. M. Gel-microemulsions as vaginal spermicides and intravaginal drug delivery vehicles. **Contraception**, v. 64, n. 2, p.113-123. 2001.

DA SILVA, C. A. S.; SANAIOTTI, G.; LANZA, M.; FOLLEGATTI-ROMERO, L. A.; MEIRELLES, A. J. A.; BATISTA, E. A. C. Mutual Solubility for Systems Composed of Vegetable Oil plus Ethanol plus Water at Different Temperatures. **Journal of Chemical and Engineering Data**, v. 55, n. 1, p.440-447. 2010.

DE CAMPO, L.; YAGHMUR, A.; GARTI, N.; LESER, M. E.; FOLMER, B.; GLATTER, O. Five-component food-grade microemulsions: structural characterization by SANS. **Journal of Colloid and Interface Science**, v. 274, n. 1, p.251-267. 2004.

DELPLANQUE, B. The nutritional value of sunflower oils: linoleic sunflower seeds and seeds with high oleic content. **Oci-Oleagineux Corps Gras Lipides**, v. 7, n. 6, p.467-472. 2000.

DICKINSON, E. Hydrocolloids at interfaces and the influence on the properties of dispersed systems. **Food Hydrocolloids**, v. 17, n. 1, p.25-39. 2003.

ENGSTROM, S.; LARSSON, K. Microemulsion in foods. In: Kumar, P. e Mittal, K. L. **Handbook of microemulsion science and technology** New York: Dekker, 789-796, 1999.

FANUN, M. Formulation and characterization of microemulsions based on mixed nonionic surfactants and peppermint oil. **Journal of Colloid and Interface Science**, v. 343, n. 2, p.496-503. 2010a.

FANUN, M. Properties of microemulsions with mixed nonionic surfactants and citrus oil. **Colloids and Surfaces A-Physicochemical and Engineering Aspects**, v. 369, n. 1-3, p.246-252. 2010b.

FANUN, M. Microemulsions as delivery systems. **Current Opinion in Colloid & Interface Science**, v. 17, n. 5, p.306-313. 2012.

FENG, J. L.; WANG, Z. W.; ZHANG, J.; WANG, Z. N.; LIU, F. Study on food-grade vitamin E microemulsions based on nonionic emulsifiers. **Colloids and Surfaces A: Physicochemical and Engineering Aspects**, v. 339, n. 1–3, p.1-6. 2009.

FLANAGAN, J.; KORTEGAARD, K.; PINDER, D. N.; RADES, T.; SINGH, H. Solubilisation of soybean oil in microemulsions using various surfactants. **Food Hydrocolloids**, v. 20, n. 2-3, p.253-260. 2006.

FLANAGAN, J.; SINGH, H. Microemulsions: A potential delivery system for bioactives in food. **Critical Reviews in Food Science and Nutrition**, v. 46, n. 3, p.221-37. 2006.

FORMARIZ, T. R.; SARMENTO, V. H. V.; SILVA-JUNIOR, A. A.; SCARPA, M. V.; SANTILLI, C. V.; OLIVEIRA, A. G. Doxorubicin biocompatible O/W microemulsion stabilized by mixed surfactant containing soya phosphatidylcholine. **Colloids and Surfaces B-Biointerfaces**, v. 51, n. 1, p.54-61. 2006.

GAONKAR, A.; BAGWE, R.P. Microemulsions in Foods. In: Shah, D.O. e Mittal, K.L. **Adsorption and Aggregation of Surfactants in Solution**, New York:CRC Press, 407-30, 2002.

GONG, Y.; LIU, Q. L.; ZHU, A. M.; ZHANG, Q. G. One-pot synthesis of poly(N-isopropylacrylamide)/chitosan composite microspheres via microemulsion. **Carbohydrate Polymers**, v. 90, n. 1, p.690-705. 2012.

GONZALEZ, C.; RESA, J. M.; RUIZ, A.; GUTIERREZ, J. I. Excess molar volumes of mixtures of hexane plus natural oils from 298.15 to 313.15 K. **Journal of Chemical and Engineering Data**, v. 42, n. 2, p.339-341. 1997.

GULSEN, D.; CHAUHAN, A. Dispersion of microemulsion drops in HEMA hydrogel: a potential ophthalmic drug delivery vehicle. **International Journal of Pharmaceutics**, v. 292, n. 1-2, p.95-117. 2005.

HAERING, G.; LUISI, P. L. Hydrocarbon Gels from Water-in-Oil Microemulsions. **Journal of Physical Chemistry**, v. 90, n. 22, p.5892-5905. 1986.

HOLMBERG, K.; JÖNSSON, B.; KRONBERG, B.; LINDMAN, B. **Surfactants and Polymers in Aqueous Solution**. Chichester: John Wiley & Sons, 2002.

HYDE, S.T. Identification of lyotropic liquid crystalline mesophases. In: Holmberg, G.K. **Handbook of Applied Surface and Colloid Chemistry** New York: John Wiley & Sons, 299-332, 2001.

IKEDA, S.; NITTA, Y.; TEMSIRIPONG, T.; PONGSAWATMANIT, R.; NISHINARI, K. Atomic force microscopy studies on cation-induced network formation of gellan. **Food Hydrocolloids**, v. 18, n. 5, p.727-735. 2004.

JAFARI, S. M.; ASSADPOOR, E.; HE, Y. H.; BHANDARI, B. Re-coalescence of emulsion droplets during high-energy emulsification. **Food Hydrocolloids**, v. 22, n. 7, Oct, p.1191-202. 2008.

JENTA, T. R. J.; BATT, G.; REES, G. D.; ROBINSON, B. H. Biocatalysis using gelatin microemulsion-based organogels containing immobilized Chromobacterium viscosum lipase. **Biotechnology and Bioengineering**, v. 53, n. 2, p.121-131. 1997.

JIAO, J. Polyoxyethylated nonionic surfactants and their applications in topical ocular drug delivery. **Advanced Drug Delivery Reviews**, v. 60, n. 15, p.1663-1673. 2008.

JOSEF, E.; ZILBERMAN, M.; BIANCO-PELED, H. Composite alginate hydrogels: An innovative approach for the controlled release of hydrophobic drugs. **Acta Biomaterialia**, v. 6, n. 12, p.4642-9. 2010.

KABALNOV, A.; TARARA, T.; ARLAUSKAS, R.; WEERS, J. Phospholipids as emulsion stabilizers .2. Phase behavior versus emulsion stability. **Journal of Colloid and Interface Science**, v. 184, n. 1, Dec 1, p.227-35. 1996.

KANTARIA, S.; REES, G. D.; LAWRENCE, M. J. Gelatin-stabilised microemulsion-based organogels: rheology and application in iontophoretic transdermal drug delivery. **Journal of Controlled Release**, v. 60, n. 2-3, p.355-365. 1999.

KANTARIA, S.; REES, G. D.; LAWRENCE, M. J. Formulation of electrically conducting microemulsion-based organogels. **International Journal of Pharmaceutics**, v. 250, n. 1, p.65-83. 2003.

KASAPIS, S.; GIANNOULI, P.; HEMBER, M. W. N.; EVAGELIOU, V.; POULARD, C.; TORT-BOURGEOIS, B.; SWORN, G. Structural aspects and phase behaviour in deacylated and high acyl gellan systems. **Carbohydrate Polymers**, v. 38, n. 2, p.145-154. 1999.

KAWANO, S.; KOBAYASHI, D.; TAGUCHI, S.; KUNITAKE, M.; NISHIMI, T. Construction of Continuous Porous Organogels, Hydrogels, and Bicontinuous Organo/Hydro Hybrid Gels from Bicontinuous Microemulsions. **Macromolecules**, v. 43, n. 1, p.473-479. 2010.

KERWIN, B. A. Polysorbates 20 and 80 used in the formulation of protein biotherapeutics: Structure and degradation pathways. **Journal of Pharmaceutical Sciences**, v. 97, n. 8, p.2924-2935. 2008.

KIRK, R. E.; OTHMER, D. F.; HOWE-GRANT, M. . **Kirk-Othmer encyclopedia of chemical technology**. 4. New York: Wiley, 1996.

KOOP, H. S.; DA-LOZZO, E. J.; DE FREITAS, R. A.; FRANCO, C. R. C.; MITCHELL, D. A.; SILVEIRA, J. L. M. Rheological Characterization of a Xanthan-Galactomannan Hydrogel Loaded with Lipophilic Substances. **Journal of Pharmaceutical Sciences**, v. 101, n. 7, p.2457-2467. 2012.

LANZA, M.; SANAIOTTI, G.; BATISTA, E. A. C.; POPPI, R. J.; MEIRELLES, A. J. A. Liquid-Liquid Equilibrium Data for Systems Containing Vegetable Oils, Anhydrous Ethanol, and Hexane at (313.15, 318.15, and 328.15) K. **Journal of Chemical and Engineering Data**, v. 54, n. 6, p.1850-1859. 2009.

LAPASIN, R.; GRASSI, M.; COCEANI, N. Effects of polymer addition on the rheology of o/w microemulsions. **Rheologica Acta**, v. 40, n. 2, p.185-192. 2001.

LAWRENCE, M. J. Surfactant Systems - Their Use in Drug-Delivery. **Chemical Society Reviews**, v. 23, n. 6, p.417-424. 1994.

LAWRENCE, M. J.; REES, G. D. Microemulsion-based media as novel drug delivery systems. **Advanced Drug Delivery Reviews**, v. 45, n. 1, p.89-121. 2000.

LI, X. Q.; CHAI, J. L.; SHANG, S. C.; LI, H. L.; LU, J. J.; YANG, B.; WU, Y. T. Phase Behavior of Alcohol-Free Microemulsion Systems Containing Butyric Acid as a

Cosurfactant. **Journal of Chemical and Engineering Data**, v. 55, n. 9, p.3224-3228. 2010.

LOPEZ, F.; VENDITTI, F.; AMBROSONE, L.; COLAFEMMINA, G.; CEGLIE, A.; PALAZZO, G. Gelatin microemulsion-based gels with the cationic surfactant cetyltrimethylammonium bromide: A self-diffusion and conductivity study. **Langmuir**, v. 20, n. 22, p.9449-9452. 2004.

LUISI, P. L.; SCARTAZZINI, R.; HAERING, G.; SCHURTERENBERGER, P. Organogels from Water-in-Oil Microemulsions. **Colloid and Polymer Science**, v. 268, n. 4, p.356-374. 1990.

MCCLEMENTS, D. J. Edible nanoemulsions: fabrication, properties, and functional performance. **Soft Matter**, v. 7, n. 6, p.2297-2316. 2011.

MCCLEMENTS, D.J. **Food Emulsions: Principles, Practice, And Techniques**. 2nd. Washington: CRC Press, 2005.

MEHTA, S.; KAUR, K.; KAUR, G.; BHASIN, K. Percolating Phenomenon in Microemulsions. In: Fanun, M. **Microemulsions**, Boca Raton: CRC Press, 59-78, 2008.

MILAS, M.; RINAUDO, M. The gellan sol-gel transition. **Carbohydrate Polymers**, v. 30, n. 2-3, p.177-184. 1996.

MILLER, C.A.; NEOGI, P. Interfacial Phenomena: Equilibrium and Dynamic Effects, Second Edition, New York: Taylor & Francis, 2007.

MIYOSHI, E.; TAKAYA, T.; NISHINARI, K. Rheological and thermal studies of gel-sol transition in gellan gum aqueous solutions. **Carbohydrate Polymers**, v. 30, n. 2-3, p.109-119. 1996.

MOHSEN-NIA, M.; KHODAYARI, A. De-acidification of sunflower oil by solvent extraction: (Liquid plus liquid) equilibrium data at  $T = (303.15$  and  $313.15)$  K. **Journal of Chemical Thermodynamics**, v. 40, n. 8, p.1325-1329. 2008.

MORITAKA, H.; NISHINARI, K.; TAKI, M.; FUKUBA, H. Effects of Ph, Potassium-Chloride, and Sodium-Chloride on the Thermal and Rheological Properties of Gellan Gum Gels. **Journal of Agricultural and Food Chemistry**, v. 43, n. 6, p.1685-9. 1995.

MOULIK, S. P.; PAUL, B. K. Structure, dynamics and transport properties of microemulsions. **Advances in Colloid and Interface Science**, v. 78, n. 2, p.99-195. 1998.

NIEMELA, J. R. K.; WESTER, I.; LAHTINEN, R. M. Industrial frying trials with high oleic sunflower oil. **Grasas Y Aceites**, v. 47, n. 1-2, p.1-4. 1996.

OGAWA, E.; TAKAHASHI, R.; YAJIMA, H.; NISHINARI, K. Effects of molar mass on the coil to helix transition of sodium-type gellan gums in aqueous solutions. **Food Hydrocolloids**, v. 20, n. 2-3, p.378-385. 2006.

PATEL, N.; SCHMID, U.; LAWRENCE, M. J. Phospholipid-based microemulsions suitable for use in foods. **Journal of Agricultural and Food Chemistry**, v. 54, n. 20, p.7817-7824. 2006.

PELTOLA, S.; SAARINEN-SAVOLAINEN, R.; KIESVAARA, J.; SUHONEN, T. M.; URTTI, A. Microemulsions for topical delivery of estradiol. **International Journal of Pharmaceutics**, v. 254, n. 2, p.99-107. 2003.

PHAN, T. T.; HARWELL, J. H.; SABATINI, D. A. Effects of Triglyceride Molecular Structure on Optimum Formulation of Surfactant-Oil-Water Systems. **Journal of Surfactants and Detergents**, v. 13, n. 2, p.189-194. 2010.

PICONE, C. S. F.; CUNHA, R. L. Influence of pH on formation and properties of gellan gels. **Carbohydrate Polymers**, v. 84, n. 1, p.662-668. 2011.

QUELLET, C.; EICKE, H. F. Mutual Gelation of Gelatin and Water-in-Oil Microemulsions. **Chimia**, v. 40, n. 7-8, p.233-238. 1986.

RAKSHIT, A.K.; MOULIK, S.P. Physicochemistry of W/O Microemulsions. In: Fanun, M. **Microemulsions**, Boca Raton: CRC Press, 2008.

RAO, J. J.; MCCLEMENTS, D. J. Food-grade microemulsions, nanoemulsions and emulsions: Fabrication from sucrose monopalmitate & lemon oil. **Food Hydrocolloids**, v. 25, n. 6, p.1413-1423. 2011.

RODRIGUES, C. E. C.; REIPERT, E. C. D.; DE SOUZA, A. F.; PESSOA, P. A.; MEIRELLES, A. J. A. Equilibrium data for systems composed by cottonseed oil plus commercial linoleic acid plus ethanol plus water plus tocopherols at 298.2K. **Fluid Phase Equilibria**, v. 238, n. 2, p.193-203. 2005.

---

Capítulo 2

RODRIGUEZ-HERNANDEZ, A. I.; DURAND, S.; GARNIER, C.; TECANTE, A.; DOUBLIER, J. L. Rheology-structure properties of gellan systems: evidence of network formation at low gellan concentrations. **Food Hydrocolloids**, v. 17, n. 5, p.621-628. 2003.

SAGALOWICZ, L.; LESER, M. E. Delivery systems for liquid food products. **Current Opinion in Colloid & Interface Science**, v. 15, n. 1-2, Apr, p.61-72. 2010.

SAKATA, K.; MAKITA, Y.; UEMURA, S.; NISHIMI, T.; KUNITAKE, M. Electrochemical elucidation of structural changes in physical organo bicontinuous microemulsion gel systems. **Chemical Communications**, v. 48, n. 90, p.11124-6. 2012.

SANDERSON, G.R. Gellan Gum. In: Harris, P. **Food Gels**, New York: Elsevier Applied Science, 201-31, 1990.

SJOBLOM, J.; LINDBERG, R.; FRIBERG, S. E. Microemulsions - Phase equilibria characterization, structures, applications and chemical reactions. **Advances in Colloid and Interface Science**, v. 65, n., p.125-287. 1996.

SKORIC, D.; JOCIC, S.; SAKAC, Z.; LECIC, N. Genetic possibilities for altering sunflower oil quality to obtain novel oils. **Canadian Journal of Physiology and Pharmacology**, v. 86, n. 4, p.215-221. 2008.

SPERNATH, A.; ASERIN, A.; GARTI, N. Fully dilutable microemulsions embedded with phospholipids and stabilized by short-chain organic acids and polyols. **Journal of Colloid and Interface Science**, v. 299, n. 2, p.900-909. 2006.

TANG, J. M.; TUNG, M. A.; ZENG, Y. Y. Compression strength and deformation of gellan gels formed with mono- and divalent cations. **Carbohydrate Polymers**, v. 29, n. 1, p.11-16. 1996.

VALENTA, C.; SCHULTZ, K. Influence of carrageenan on the rheology and skin permeation of microemulsion formulations. **Journal of Controlled Release**, v. 95, n. 2, p.257-265. 2004.

WALSTRA, P. **Physical Chemistry of Foods**, New York: Marcel Dekker, 2002.

WANG, C. M.; GONG, Y. H.; LIN, Y. M.; SHEN, J. B.; WANG, D. A. A novel gellan gel-based microcarrier for anchorage-dependent cell delivery. **Acta Biomaterialia**, v. 4, n. 5, p.1226-1234. 2008.

WINSOR, P. A. Hydrotropy, Solubilisation and Related Emulsification Processes .8. Effect of Constitution on Amphiphilic Properties. **Transactions of the Faraday Society**, v. 44, n. 7, p.463-471. 1948.

YAGHMUR, A.; ASERIN, A.; GARTI, N. Phase behavior of microemulsions based on food-grade nonionic surfactants: effect of polyols and short-chains alcohols. **Colloids and Surfaces A-Physicochemical and Engineering Aspects**, v. 209, n. 1, p.71-81. 2002.

YAMAMOTO, F.; CUNHA, R. L. Acid gelation of gellan: Effect of final pH and heat treatment conditions. **Carbohydrate Polymers**, v. 68, n. 3, p.517-527. 2007.

ZHANG, H.; SHEN, Y.; WENG, P. F.; ZHAO, G. Q.; FENG, F. Q.; ZHENG, X. D. Antimicrobial activity of a food-grade fully dilutable microemulsion against Escherichia coli

and *Staphylococcus aureus*. **International Journal of Food Microbiology**, v. 135, n. 3, p.211-215. 2009.

ZHANG, H.; XU, Y. Q.; WU, L. J.; ZHENG, X. D.; ZHU, S. M.; FENG, F. Q.; SHEN, L. R. Anti-yeast activity of a food-grade dilution-stable microemulsion. **Applied Microbiology and Biotechnology**, v. 87, n. 3, p.1101-1108. 2010.

ZHAO, X. Y.; CAO, Q.; ZHENG, L. Q.; ZHANG, G. Y. Rheological properties and microstructures of gelatin-containing microemulsion-based organogels. **Colloids and Surfaces a-Physicochemical and Engineering Aspects**, v. 281, n. 1-3, p.67-73. 2006.

ZHAO, X. Y.; XU, J.; ZHENG, L. Q.; LI, X. W. Preparation of temperature-sensitive microemulsion-based gels formed from a triblock copolymer. **Colloids and Surfaces a-Physicochemical and Engineering Aspects**, v. 307, n. 1-3, p.100-107. 2007.

ZHONG, F.; YU, M.; LUO, C. R.; SHOEMAKER, C.; LI, Y.; XIA, S. Q.; MA, J. G. Formation and characterisation of mint oil/S and CS/water microemulsions. **Food Chemistry**, v. 115, n. 2, p.539-544. 2009.

ZLATANOV, M. D.; ANGELOVA-ROMOVA, M. J.; ANTOVA, G. A.; DIMITROVA, R. D.; MOMCHILOVA, S. M.; NIKOLOVA-DAMYANOVA, B. M. Variations in Fatty Acids, Phospholipids and Sterols During the Seed Development of a High Oleic Sunflower Variety. **Journal of the American Oil Chemists Society**, v. 86, n. 9, p.867-875. 2009.

**– CAPÍTULO 3 –**

***Effect of ethanol and oil unsaturation in  
self-assembly systems***



**MICROEMULSIONS AND LIQUID CRYSTALLINE FORMULATED WITH  
TRIACYLGLYCEROLS: EFFECT OF ETHANOL AND OIL UNSATURATION**

L.H. Fasolin, R.C. Santana, R.L. Cunha\*

*In: Colloids and Surfaces A (2012), v.415, p.31-40*

Department of Food Engineering, Faculty of Food Engineering, University of Campinas – UNICAMP, 13083-862, Campinas, SP, Brazil

\*Corresponding author. Tel: +55-19-35214047; Fax: +55-19-35214027;  
email: rosiane@fea.unicamp.br

**ABSTRACT**

Pseudo-ternary phase diagrams were constructed in order to evaluate the effect of the prevailing oil unsaturation and cosurfactant concentration on the phase behavior of systems prepared with sunflower oil or high oleic sunflower oil (HOSO), water, Tween 80 and ethanol. All phase diagrams showed small areas of one single translucent phase with production of water-in-oil ( $L_2$ ) and oil-in-water ( $L_1$ ) microemulsions. A higher cosurfactant concentration increased microemulsion area and allowed solubilize more water using lower surfactant content. Moreover, small angle X-ray scattering (SAXS) measurements showed that depending of the composition the surfactant self-assembly led to lamellar ( $L\alpha$ ) or hexagonal ( $H_1$ ) structures. Microemulsions showed Newtonian behavior, while  $L\alpha$  and  $H_1$  showed shear-thinning behavior, viscoelasticity and thixotropy. This more complex rheological behavior was accentuated at lower cosurfactant concentration and with the less unsaturated oil, showing that both oil unsaturation and ethanol content exerted

influence on systems properties. However, the higher ethanol concentration masked the effect of oil unsaturation.

*Keywords:* *microemulsions, liquid crystalline, phase diagram, rheology, cosurfactant, oil unsaturation*

## 1. INTRODUCTION

Microemulsions are spontaneously formed and macroscopically homogeneous due their droplets size, which are in colloidal domain. Therefore, microemulsions are isotropic, transparent and thermodynamically stable mixtures usually composed by oil, water and surfactant [1,2]. An interfacial tension near zero or a more flexible interface is required to form a microemulsion, which is generally achieved with the additional use of cosurfactants [3]. Nevertheless, depending on the concentration of these ingredients, a surfactant self-assembly can occur assuming a large variety of morphologies, such as lamellar, cubic or hexagonal phases [4] and these systems are denominated as liquid crystal. The microemulsions and liquid crystal characterization can be performed with a large variety of methods as nuclear magnetic resonance (NMR), dynamic light scattering (DLS), small-angle neutron scattering (SANS), small-angle X-ray scattering (SAXS), polarized light, conductivity and viscosity measurements [5,6]. In addition to viscosity, other rheological measurements could be used to identify and characterize the microemulsions, helping to define the phase diagram boundaries. Steady-state and oscillatory measurements are useful to identify the structure dependence with the shear and time-dependent viscoelastic properties, respectively.

The characteristics of microemulsions have attracted considerable attention, mainly because of their ability to solubilize large amount of lipophilic or hydrophilic additives, to enhance reactions efficiency and to allow chemical reactions as preparation of inorganic particles or polymerization of organic monomers [7,8,9]. However, the ingredients and the system composition are extremely important on the microemulsion formation and its functionality. Polyoxyethylene sorbitan esters (Tweens) are probably the most widely used surfactants, showing the polyoxyethylene head groups attached to a sorbitan ring, which increases the hydrophilicity of the sorbitan fatty esters [10]. Regarding the cosurfactants, alcohols are the most used in microemulsion formulations. Among the alcohols, ethanol is known with less toxicity [11,12]. Besides, the apolar phases most used on biocompatible systems are medium-chain triglycerides and cyclic oils (as citrus and mint oil), which have a more apolar structure and a lower molecular weight than long-chain triglycerides (vegetable oils), being easily solubilized [13,14]. However, the possibility of using vegetable oils as the oil phase has been scarcely investigated despite of their importance and been in accordance with the principles of the green chemistry since they are obtained from renewable sources produced in large scale [13,15].

Oils with different chemical structures can show different physical properties. The increase of the degree of unsaturation can increase the triglyceride oil hydrophobicity and the interaction energy between surfactant and triglyceride molecules might decrease. This behavior is probably due to the more crooked spatial arrangement of the triglyceride hydrocarbon chain caused by the double bonds [14]. Traditional sunflower oil (*Helianthus annuus* L.) is one of the most important vegetable oil that consists in about 90% of unsaturated fatty acids, which are mainly oleic (C18:1, 16–19%) and linoleic (C18:2, 68–72%) [16]. In order to upgrade the use of sunflower oil, new varieties have been selected,

where the main fatty acid is represented by oleic acid and the oil is denominated high oleic sunflower oil (HOSO) [17]. Thus, the aim of this work was to construct phase diagrams using sunflower oil or HOSO, water, Tween 80 as surfactant and ethanol as cosurfactant, evaluating the effect of the prevailing oil unsaturation and the cosurfactant concentration on the formation of microemulsions or liquid crystalline zones. These systems were rheologically characterized to evaluate the efficiency of this technique on identifying the phase diagrams limits in addition to other measurements as SAXS and the traditionally used polarized light microscopy, electrical conductivity and droplets size distribution.

## **2. MATERIAL AND METHODS**

### ***2.1. Material***

Sunflower oil and HOSO were kindly donated by Cargill (Mairinque, Brazil) and were used without additional purification. The surfactant polyoxyethylene sorbitan monooleate (Tween 80) was purchased from Sigma–Aldrich Co. (EUA) and ethanol 99.5% was obtained from Ecibra Co. (Brazil).

### ***2.2. Phase behavior and diagrams construction***

The four-component systems were described using pseudo-ternary diagrams produced by spontaneous emulsification method at room temperature (25 °C). The influence of the prevailing oil unsaturation was performed using sunflower oil or HOSO and the cosurfactant effect was evaluated using different oil:cosurfactant ratios (1:2 and 2:1). Four phase diagrams were constructed and named as shown in Table 1.

An initial mixture of surfactant, cosurfactant and oil was prepared under magnetically stirring at different ratios of surfactant:oil + cosurfactant (10:90; 20:80; 30:70; 40:60; 50:50; 60:40; 70:30; 80:20 and 90:10) [18]. Then, deionized water was titrated under constant stirring with volume increments of 10% (w/w) forming water dilution Lines 1 up to 9. Line 1 corresponds to the initial mixture of surfactant 10% and oil + cosurfactant 90%, and Line 9 to the mixture of surfactant 90% and oil + cosurfactant 10%. Each system was named according to its formulation: firstly, in accordance to the initial surfactant concentration and then, with the water content. For example, a system on the Line 9 (surfactant 90%), diluted with water 40% was denominated as 9040. Each formulation was kept during 15 min under stirring and then they were stored at 25 °C for at least one week before to the construction of phase diagrams.

**Table 1. Composition of the formulations used to construct phase diagrams**

<b>Systems nomenclature</b>	<b>Surfactant</b>	<b>Oil</b>	<b>Cosurfactant</b>	<b>Oil:cosurfactant ratio</b>
S1E2	Tween 80	Sunflower	Ethanol	1:2
H1E2	Tween 80	HOSO	Ethanol	1:2
S2E1	Tween 80	Sunflower	Ethanol	2:1
H2E1	Tween 80	HOSO	Ethanol	2:1

### **2.3. Phase diagrams characterization**

After the phase diagrams construction, they were delimitated in different regions. The formulations that presented turbidity and/or phase separation with one milked-like phase were classified as macroemulsions or emulsions (EM). Translucid systems with phase separation were named as two transparent phases (2TP) and represented Winsor I

and/or Winsor II systems [1]. At last, the translucent one phase region was characterized as microemulsion O/W ( $L_1$ ), W/O ( $L_2$ ) or liquid crystalline phase (LC) from polarized light microscopy and electrical conductivity. Firstly, the polarized light microscopy was performed to identify the liquid crystalline zone and conductivity measurements were carried out in order to identify the continuous phase of the microemulsions ( $L_1$  or  $L_2$ ). For light polarized microscopy, a drop of sample was placed between a cover slip and a glass slide to be examined under polarized light. An optical microscope Olympus BX51TF (Olympus, Japan) equipped with a digital camera was used to analyze the samples at room temperature. The isotropic or anisotropic behavior of the samples could be observed and pictures were taken at a magnification of 20 $\times$ . The conductivity of the samples was determined at 25 °C using a bench top conductivimeter Orion 3 Star (Thermo Electron Co., USA) coupled to a conductivity cell (Orion 013016MD).

In addition, characteristic parameters of the systems were calculated, including the total LC region ( $A_{LC}$ ), the total microemulsion area ( $A_{me}$ ), the maximal amount of aqueous phase dispersed in the W/O microemulsion ( $W_m$ ) and the minimum surfactant concentration at this corresponding condition ( $S_m$ ) [19,20]. At last systems showing a single phase were subjected to SAXS, DLS and rheological measurements in order to better define and characterize the microemulsions and liquid crystalline boundaries.

## ***2.4. Microemulsions and liquid crystalline characterization***

### ***2.4.1. Droplets size distribution***

Particle size measurements were determined at 25 °C from dynamic light scattering (DLS), at 25 °C, using a ZetaSizer Nano-ZS (Malvern Instruments, UK) with a detection angle of 173°.

#### *2.4.2. Small angle X-Ray Scattering (SAXS)*

Quantitative information of the LC and microemulsions structures was obtained by means of small angle X-ray scattering (SAXS) measurements performed at room temperature using the beamline of the National Synchrotron Light Laboratory (LNLS, Campinas, Brazil). The beamline is equipped with an asymmetrically cut and bent silicon (1 1 1) monochromator that yields a monochromatic ( $\lambda = 1.54 \text{ \AA}$ ) and horizontally focused beam. A position-sensitive X-ray detector and a multichannel analyzer were used to record the SAXS intensity,  $I(q)$ , as a function of modulus of scattering vector  $q$ :  $q = (4\pi/\lambda) \sin(\theta/2)$ ,  $\theta$  being the scattering angle. Each SAXS pattern corresponds to a data collection time of 100 s.

#### *2.4.3. Rheological measurements*

The rheological measurements were performed using a rheometer Physica MCR301 (Anton Paar, Austria) at 25 °C. All measurements were done in triplicate. Measurements were performed using cone-plate geometry (50 mm, 2° angle, truncation 208 µm).

##### *2.3.4.1. Steady-shear rheology*

Flow curves were obtained by an up-down-up steps program with shear rate ranging from 0 to 100 s<sup>-1</sup>. The thixotropy was qualitatively evaluated based on the difference between the area of the curves at the transient state (curve A) and at the steady state (curve B). Newtonian viscosity  $\mu$  (Pa s) or the apparent viscosity at low shear rate ( $3 \text{ s}^{-1} - \eta_3$ ) (Pa s) were also evaluated.

#### 2.4.3.2. Dynamic shear rheology

The viscoelastic properties were evaluated by oscillatory measurements, using a frequency sweep between 0.01 and 10 Hz within the linear viscoelasticity domain.

### 3. RESULTS

#### **3.1. Construction of phase diagrams**

##### *3.1.1. Visual observation and polarized light microscopy*

Firstly, systems with different composition and ingredients concentration were visually observed to construct the pseudo-ternary phase diagrams. Figure 1 shows the visual aspect of Lines 8 and 9 (single translucent phase systems) of each phase diagram constructed and the real composition of these systems are presented in Table 2, where the high surfactant and low oil content is remarkable. Lower ethanol concentration or higher oil content (at the same water and surfactant concentrations) led to more viscous samples with some gel-like behavior and a higher number of systems with macroemulsion characteristics. In relation to prevailing oil unsaturation it was not observed significant visual differences. Systems with one transparent single phase were evaluated in relation to the birefringence. Samples showing birefringence (Figure 1) were previously classified as liquid crystalline (LC). The non-birefringent samples were classified as microemulsions.

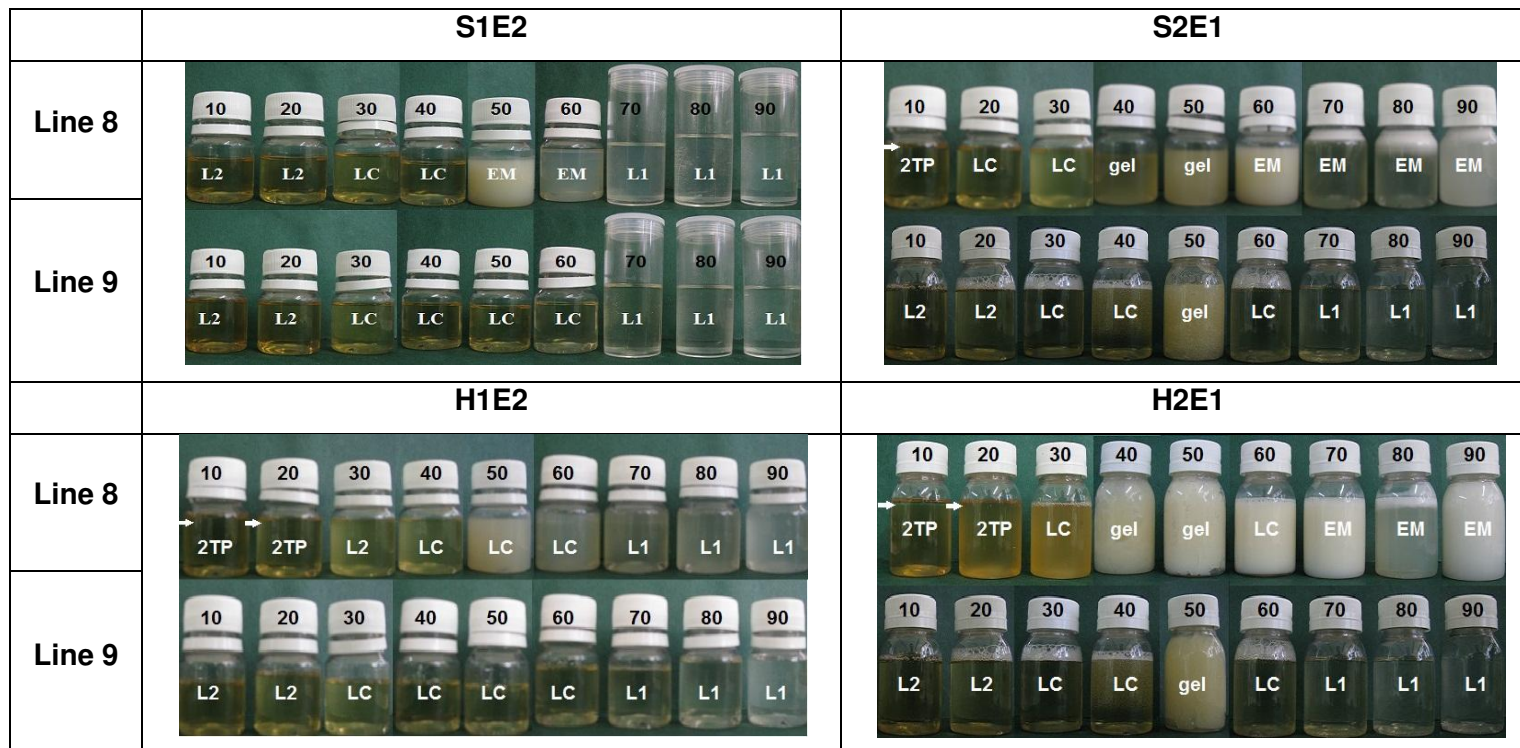


Figure 1. Visual appearance of Lines 8 and 9 (80% and 90% of initial surfactant, respectively) of systems formulated with water/Tween80/ethanol/sunflower oil or HOSO with different oil:ethanol ratios. The arrows show the phase separation (Winsor I system) and numbers refers to water mass fraction (% w/w). (2TP) Two transparent phases; (EM) macroemulsion; ( $L_1$  and  $L_2$ ) microemulsions; (LC) liquid crystalline and (gel) liquid crystalline with gel-like structure.

**Table 2. Real composition of the systems corresponding to lines 8 and 9 of phase diagram**

Systems	S1E2; H1E2				S2E1; H2E1			
	% w/w				%w/w			
	Water	Oil	Cosurfactant	Surfactant	Water	Oil	Cosurfactant	Surfactant
8	8000	0	6.67	13.33	80	0	13.33	6.67
	8010	10	6.00	12.00	72	10	12.00	6.00
	8020	20	5.33	10.67	64	20	10.67	5.33
	8030	30	4.67	9.33	56	30	9.33	4.67
	8040	40	4.00	8.00	48	40	8.00	4.00
	8050	50	3.33	6.67	40	50	6.67	3.33
	8060	60	2.67	5.33	32	60	5.33	2.67
	8070	70	2.00	4.00	24	70	4.00	2.00
	8080	80	1.33	2.67	16	80	2.67	1.33
	8090	90	0.67	1.33	8	90	1.33	0.67
9	9000	0	3.33	6.67	90	0	6.67	3.33
	9010	10	3.00	6.00	81	10	6.00	3.00
	9020	20	2.67	5.33	72	20	5.33	2.67
	9030	30	2.33	4.67	63	30	4.67	2.33
	9040	40	2.00	4.00	54	40	4.00	2.00
	9050	50	1.67	3.33	45	50	3.33	1.67
	9060	60	1.33	2.67	36	60	2.67	1.33
	9070	70	1.00	2.00	27	70	2.00	1.00
	9080	80	0.67	1.33	18	80	1.33	0.67
	9090	90	0.33	0.67	9	90	0.67	0.33

### 3.1.2. Electrical conductivity

The conductivity measurements were carried out as a function of the system composition along the dilution lines to identify the boundary between L<sub>2</sub> (W/O) and L<sub>1</sub> (O/W) microemulsions. Figure 2 shows that all systems presented a similar characteristic profile of percolative conductivity for the Lines 8 and 9. However, not all systems could be evaluated due their high viscosity or gel-like behavior and some values are not shown in Figure 2B-D.

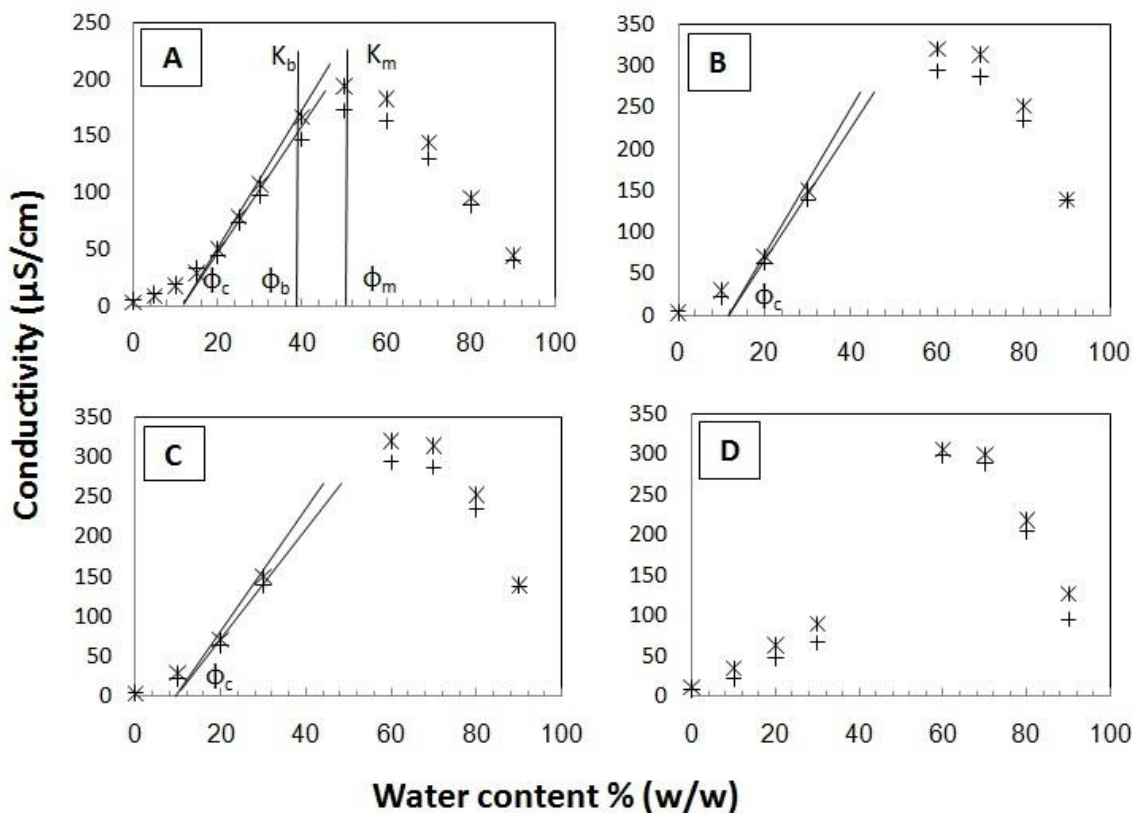


**Figure 2. Electrical conductivity of Lines 8 and 9 of microemulsions formulated with water/Tween80/ethanol/sunflower oil or HOSO with different oil:ethanol ratios. (+) Line 8; (\*) Line 9. A) S1E2; B) H1E2; C) S2E1; D) H2E1.  $\Phi_c$  is the percolation threshold or critical water content;  $\kappa_b$  is the conductivity at water fraction  $\Phi_b$ , and  $\kappa_m$  is the maximal conductivity at water fraction  $\Phi_m$ .**

The electrical conductivity ( $\kappa$ ) values were very low at the beginning of titration and increased smoothly up to a critical water content,  $\Phi_c$ , around 20% (w/w). From this value, structural changes could be observed with the linear and abrupt increase of the conductivity values up to  $\kappa_b$ , with a corresponding water fraction,  $\Phi_b$ , nearly 40% (w/w). However, in the region of moderate water content at  $\Phi_b < \Phi < \Phi_m$ , the conductivity curve exhibits an abnormal behavior: the electric conductivity  $\kappa$  increases nonlinearly up to a maximum. Then, a sudden decrease in these values occurs indicating the inversion from L<sub>2</sub> to L<sub>1</sub> microemulsions.

### **3.2. Phase diagram analysis**

The pseudo-ternary phase diagrams were constructed (Figure 3) from the visual observation, polarized light microscopy and electrical conductivity measurements. The phase diagrams clearly show more that the microemulsions and liquid crystalline zone were restricted to the lines with higher surfactant content (Lines 8 and 9). L<sub>1</sub> and L<sub>2</sub> regions were separated by a liquid-crystalline (LC) phase, which exhibited a translucent/opaque appearance and a high viscosity or gel formation. At lower surfactant concentrations and high oil:ethanol concentrations (independent on the oil:cosurfactant ratio), two transparent phases systems were observed characterizing Winsor I and II systems. In contrast, at low surfactant concentrations and high water concentrations, a milk-like emulsion (EM) with a cream phase separation (or not) was formed. The characteristic parameters of phase behavior are shown in Table 3. The cosurfactant concentration did not change the maximal solubilized water content, but the surfactant amount needed to solubilize this water was lower in systems with more ethanol. In relation to the prevailing oil unsaturation, the maximal water solubilized content did not show significant differences, but it was

possible to form microemulsions with less surfactant for the systems with common sunflower oil. From now, the size distribution and rheological measurements were carried out only for Line 9 in order to better characterize the microemulsions and liquid crystalline zones transition.

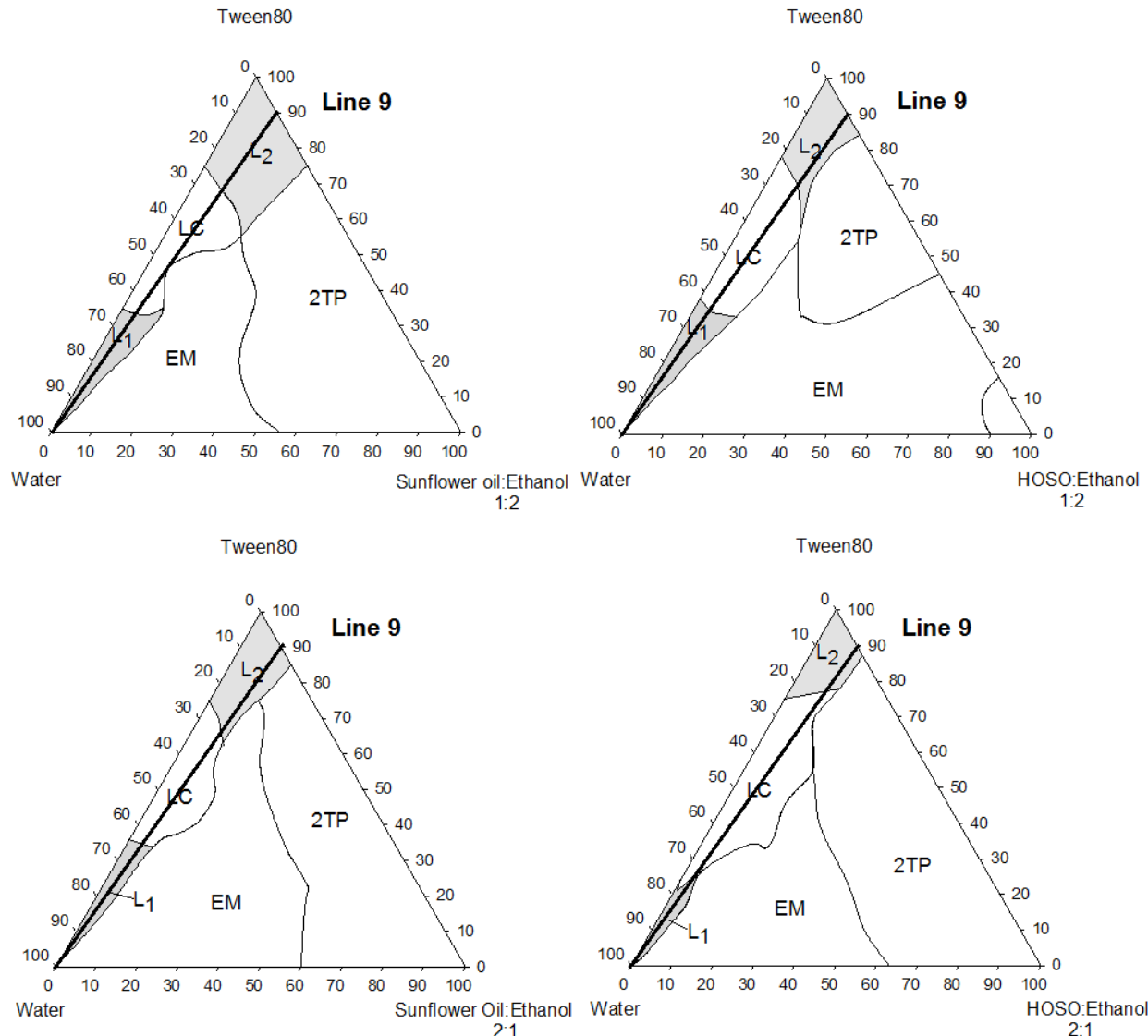


**Figure 3. Phase diagrams formulated with water/Tween80/ethanol/sunflower oil or HOSO with different oil:ethanol ratios. (EM) Macroemulsion; (2TP) Two transparent phases; (LC) Liquid crystalline phase, (L<sub>2</sub>) Microemulsion W/O and (L<sub>1</sub>) Microemulsion O/W.**

**Table 3. Characteristic parameters for phase diagrams formulated with water/Tween80/ethanol/sunflower oil or HOSO with different oil:ethanol ratios**

Parameters	Systems			
	S1E2	H1E2	S2E1	H2E1
Maximal solubilized water (Wm) (%w/w)	25	25	24	23
Minimal surfactant (Sm) (%w/w)	54	56	68	73
Microemulsion area (Ame) (%)	12.8	7.5	8.3	5.9
Crystalline liquid area (Alc) (%)	7.5	8.5	7.9	11.5

### *3.2.1. Droplets size distribution*

Figure 4 shows the droplet size distribution of the Line 9 for all phase diagrams. For L<sub>1</sub> and L<sub>2</sub> systems the mean peak did not present great differences ranging from 8 up to 15 nm. However, the higher viscosity of the systems at the range between 40% and 60% of water content did not allow to evaluate the particles size. At water concentrations higher than 60%, the mean peaks were displaced to lower values which suggest a structural transition from an LC to L<sub>1</sub> phase. However, at 70% of water content, system H2E1 presented a peak larger than 1000 nm, characterizing an LC system and showing that its LC to L<sub>1</sub> transition occurred later than other systems.

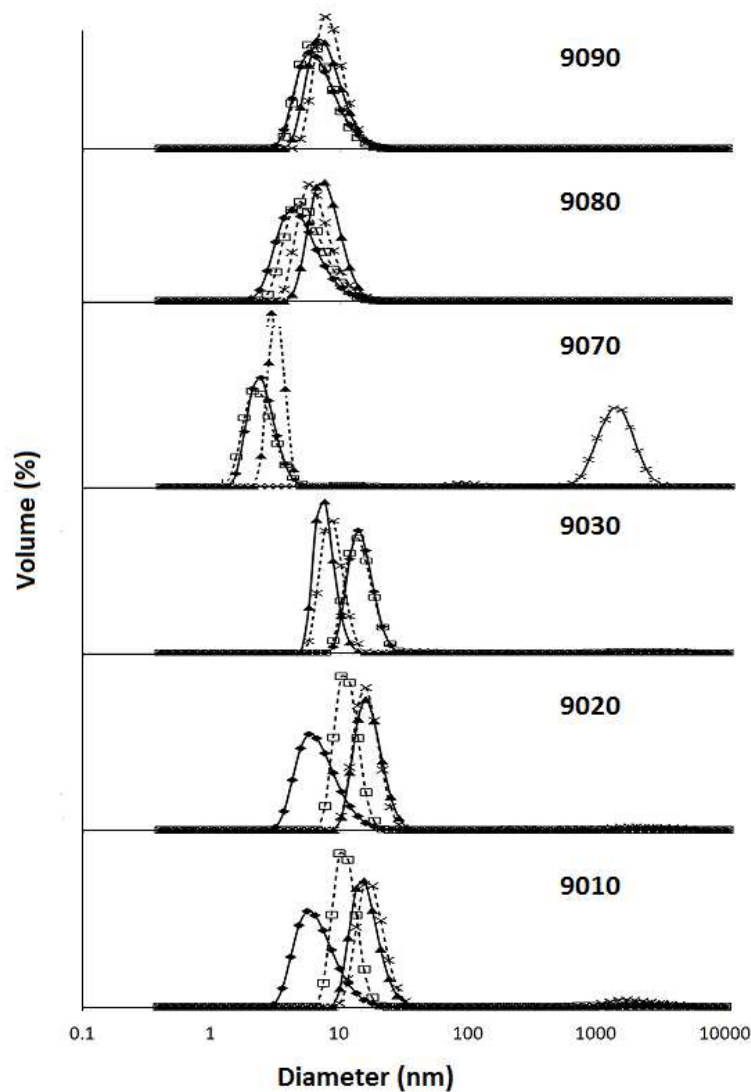


**Figure 4. Particles size distribution along dilution line 9. (◆)S1E2; (□)H1E2; (▲)S2E1; (×)H2E1.**

### *3.2.2. Rheological measurements*

#### *3.2.2.1. Steady-state rheology*

Flow curves of the different systems of the Line 9 are shown in Figure 5.

Microemulsions ( $L_1$  and  $L_2$ ) showed Newtonian behavior. Major differences were observed regarding the oil:cosurfactant ratio since S2E1 and H2E1 showed higher viscosity values than S1E2 and H1E2, respectively in  $L_2$  region and opposite behavior for  $L_1$  (Table 4). The prevailing oil unsaturation did not exert clear influence on rheological curves of microemulsions.

However, at intermediate water content (between 40% and 60%, w/w) the prevailing oil monounsaturation (HOSO) led to increased viscosity and a shear-thinning region. Some of these systems showed gel-like structures formation and values of viscosity at shear rate tending to  $3\text{ s}^{-1}$  over  $1 \times 10^6\text{ mPa s}$ . The flow index ( $n$ ) values ranged from 0.68 up to 0.96, but the smaller values were showed for the systems with lower cosurfactant content (Table 4). For the systems with less ethanol (S2E1; H2E1) and water content ranging from 30% up to 50% (w/w), the systems presented thixotropic behavior. The same behavior was observed for sample 9050 and 9040 for systems S1E2 and H1E2, respectively.

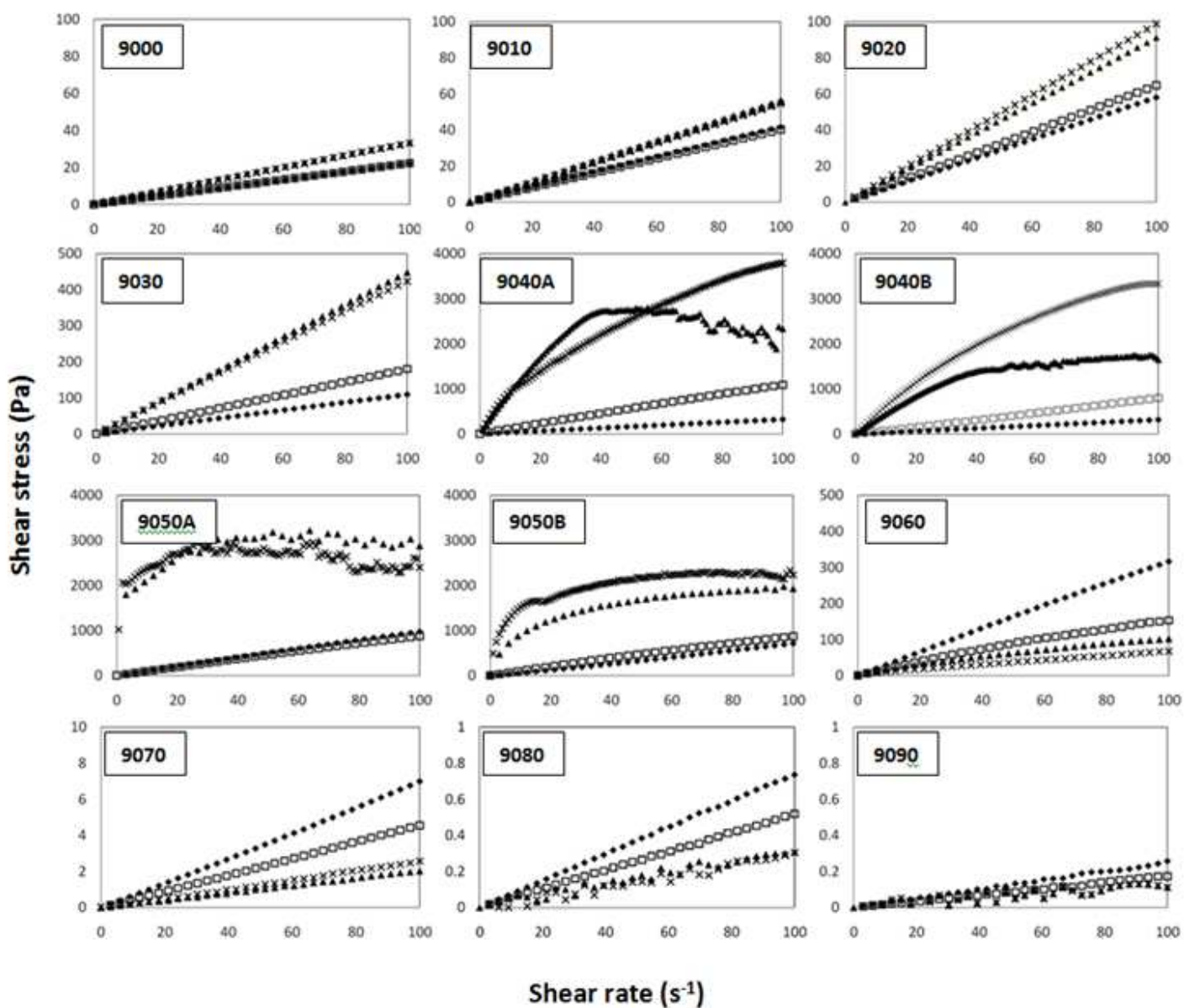


**Figure 5.** Flow curves of different systems of the Line 9 formulated with water/Tween80/ethanol/sunflower oil or HOSO with different oil:ethanol ratios. (◆)S1E2; (□)H1E2; (▲)S2E1; (×)H2E1. A) System 9040 and 9050 step 1 and B) System 9040 and 9050 step 3.

**Table 4. Rheological properties of different systems of Line 9 formulated with water/Tween80/ethanol/sunflower oil or HOSO with different oil:ethanol ratios.**

Systems	Rheological parameters																
	S1E2				H1E2				S2E1				H2E1				
	$\mu$ or $\eta_3$ (mPa.s)	k (Pa.s <sup>n</sup> )	n	R <sup>2</sup>	$\mu$ or $\eta_3$ (mPa.s)	k (Pa.s <sup>n</sup> )	n	R <sup>2</sup>	$\mu$ or $\eta_3$ (mPa.s)	k (Pa.s <sup>n</sup> )	n	R <sup>2</sup>	$\mu$ or $\eta_3$ (mPa.s)	k (Pa.s <sup>n</sup> )	n	R <sup>2</sup>	
S	9000	111	-	1	0.99	231	-	1	0.99	327	-	1	0.99	328	-	1	0.99
	9010	415	-	1	0.99	400	-	1	0.99	548	-	1	0.99	546	-	1	0.99
	9020	578	-	1	0.99	643	-	1	0.99	934	-	1	0.99	988	-	1	0.99
	9030	1085	1.01	0.96	0.99	1775	3.3	0.87	0.99	4375	6.1	0.92	0.98	5158	6.3	0.91	0.99
	9040A*	-	-	-	-	-	-	-	-	99000	-	-	-	108000	160	0.70	0.99
	9040B	3148	5.2	0.90	0.99	8040	16.7	0.82	0.99	45000	-	-	-	60100	84.56	0.83	0.99
	9050A	-	-	-	-	-	-	-	-	588000	-	-	-	1.02E6	-	-	-
	9050B	10500	13.22	0.91	0.99	9890	17.7	0.80	0.99	207000	-	-	-	374000	-	-	-
	9060	2799	3.92	0.95	0.99	1560	2.71	0.86	0.99	2350	2.88	0.78	0.99	3370	4.32	0.68	0.99
	9070	60.4	-	1	0.99	44.85	-	1	0.99	19.65	-	1	0.99	20.15	0.03	0.93	0.99
	9080	7.4	-	1	0.99	5.05	-	1	0.99	3.3	-	1	0.99	3.0	-	1	0.99
	9090	2.5	-	1	0.99	1.65	-	1	0.99	1.35	-	1	0.99	1.3	-	1	0.99

\*A-step 1, B-step 3

### 3.2.2.2. Dynamic rheology

All the systems exhibited liquid-like behavior ( $G' < G''$ ) at low and high water volume addition (<30% and >60%, w/w) (data not shown). However, a gel-like structure was observed at intermediate water content with  $G' > G''$  and some dependence of the frequency. Figure 6 shows the storage modulus for these intermediate systems (9030–9060) of dilution Line 9 of all phase diagrams. The maximum value of  $G'$  ranged between 50,000 up to 100,000 Pa, corresponding to 45% of water.

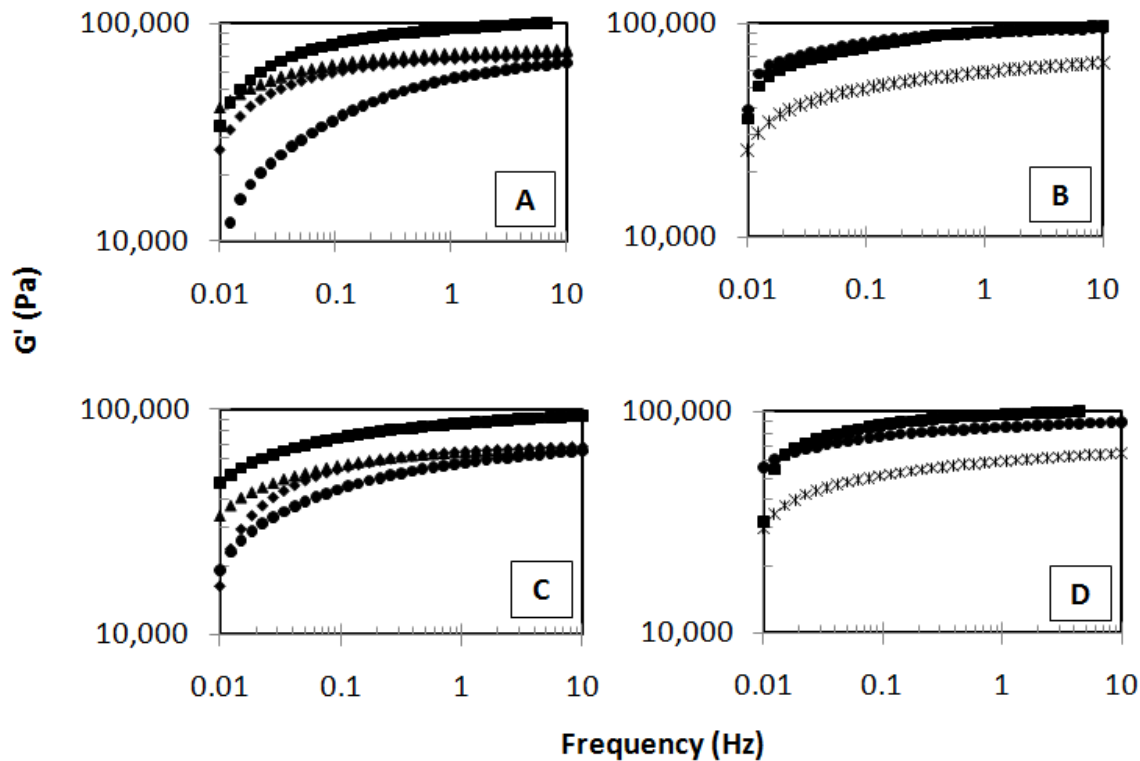


**Figure 6. Storage modulus as a function of frequency for samples with gel-like behavior in Line 9. Systems formulated with water/Tween80/ethanol/sunflower oil or HOSO with 2:1 oil:ethanol ratio. A) S1E2; B) S2E1; C) H1E2; D) H2E1. (◆) 9030; (▲) 9040; (■) 9045; (●) 9050 (\*) 9060.**

### 3.2.3. SAXS measurements

Isotropic systems with micellar agglomerates were observed for samples with the water content lower than 30% (w/w) and greater than 60% (w/w), except for H2E1 system that also presented anisotropy with 70% (w/w) of water content. The distance  $d$  between the centers of micellar structures ranged from 65 up to 76 Å for L<sub>2</sub> microemulsions, while L<sub>1</sub> showed  $d$  between 101 and 115 Å.

Figure 7 shows SAXS scattering curves of anisotropic samples of dilution Line 9. At a first sight, the oil prevailing unsaturation did not change the curves patterns, however, the cosurfactant content showed a pronounced modification on changing the surfactant self-assembly, structure type and their form parameters. All systems with 30% (w/w) of water presented a lamellar structure, which were characterized by the distance  $d$  between their planes (Table 5), determined according Equation 1.

$$d = \frac{2\pi}{q} \quad (1)$$

where  $d$  is the structure distance and  $q$  the scattering vector of SAXS measurements. Data show that with the water content increase, the distance  $d$  also increases (Table 5).

Above 40% (w/w) water content some systems started to present a normal hexagonal mesophase (H<sub>1</sub>). The parameters of these structures, ( $d$  and  $r_0$ ) were calculated with Equations 1 and 2, respectively [21].

$$r_0 = \left[ \frac{2\varphi_0}{\sqrt{3}\pi} \right]^{1/2} d \quad (2)$$

where  $r_0$  is the radius of the hexagonal structure and  $\varphi_o$  is the volumetric fraction of the hydrophobic portion.

The calculated values are shown in Table 5. The distance ( $d$ ) between the hexagonal structures increased with the water content, while the radius ( $r_0$ ) of these structures decreased.

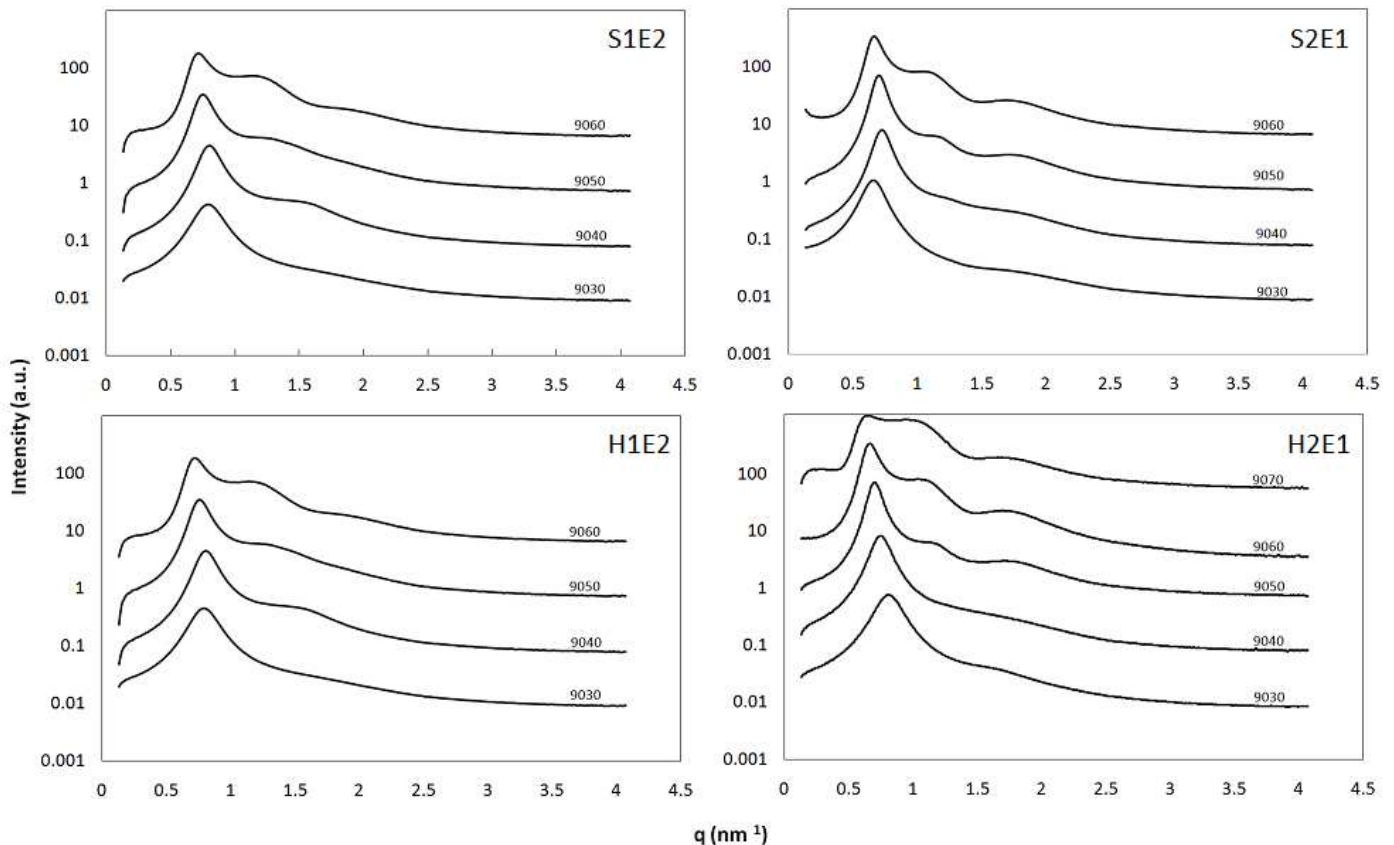


**Figure 7. SAXS patterns of the dilution Line 9 formulated with water/Tween80/ethanol/sunflower oil or HOSO with different oil:ethanol ratios. A)S1E2; B)S2E1; C)H1E2; D)H2E1.**

**Table 5. Structural parameters evaluated by SAXS for dilution Line 9 of phase diagrams formulated with water/Tween80/ethanol/sunflower oil or HOSO with different oil:ethanol ratios.**

System	S1E2			H1E2			S2E1			H2E1		
	Structure	d (Å)	r <sub>0</sub> (Å)	Structure	d (Å)	r <sub>0</sub> (Å)	Structure	d (Å)	r <sub>0</sub> (Å)	Structure	d (Å)	r <sub>0</sub> (Å)
10	Isotropic	-	-									
20	Isotropic	-	-									
30	Lamellar	79.43	-	Lamellar	73.8	-	Lamellar	80.51	-	Lamellar	77.14	-
40	Lamellar	79.68	-	Lamellar	78.13	-	Hexagonal	86.9	32.14	Lamellar	83.25	-
50	Hexagonal	83.89	27.44	Hexagonal	82.99	27.05	Hexagonal	90.03	30.33	Lamellar	82.55	-
60	Hexagonal	88.33	25.70	Hexagonal	89.13	25.84	Hexagonal	94.37	28.38	Hexagonal	95.13	28.60
70	Isotropic	-		Isotropic	-		Isotropic	-		Hexagonal	97.88	25.43
>80	Isotropic	-										

#### **4. DISCUSSION**

The results showed that both oil unsaturation and cosurfactant content exerted influence on quaternary systems behavior. The extent of this influence varied with the water content, leading to formation of different types of structure. W/O microemulsion ( $L_2$  phase) occurred up to nearly 20% (w/w) of water, while O/W microemulsion ( $L_1$  phase) were formed after 60% (w/w) water. These systems were visually transparent and presented Newtonian behavior as a consequence of their small droplets diameters [15,22,23]. In addition, the low values of electrical conductivity observed for  $L_1$  and  $L_2$  phases (Figure 2) suggest that the droplets or swelling micelles were dispersed in the continuous medium as discrete structures [24]. However, the values for  $L_1$  phase were higher since the water was the continuous medium. Moreover, the distance  $d$  between the centers of micellar  $L_2$  structures was smaller (between 65 and 76 Å) in comparison to the  $L_1$  phase (bigger than 100 Å). The higher distance could be mainly attributed to a lower volume fraction of droplets in  $L_2$  phase due to the low oil content.

Increasing water content of  $L_2$  systems or decreasing for  $L_1$  systems resulted in higher viscosity due to formation of a greater amount of droplets and micelles, increasing the friction between them and consequently the viscosity of the systems. Systems formed with intermediate water content (between 30% and 60%, w/w) showed birefringence with different liquid crystalline structures formation. The water increment promoted swelling of the W/O micelles and the self-assembly of the surfactant moieties could form elongated micelles, reverse hexagonal phase ( $H_2$ ) or a lamellar phase ( $L\alpha$ ) and a hexagonal phase ( $H_1$ ) after  $L\alpha$  region (Figure 7). The parameters obtained by SAXS showed that the hexagonal systems were formed with the water outside the structure, characterizing a

$H_1$  phase. In addition, the radius was around 27 Å, which could be attributed to a combination of the surfactant tail length (around 24 Å for a single molecule) [25] and the low content of sunflower oil added. In this region electrical conductivity behavior (Figure 2) was in agreement with the model of ‘sticky droplet collisions,’ one of the commonly accepted mechanisms to explain the percolative conduction [24,26,27].

Higher cosurfactant content led to lower viscosity (Table 4) for  $L_2$  phase, because of its role in the oil–water interface [28]. The ethanol self-assembling directed their OH groups among the surfactant polar fraction and the surrounded water as well as the hydrocarbon fraction was located between the surfactant hydrophobic chain [29]. Thus, the ethanol increased the flexibility of the interface and the fluidity of this microemulsion [1,19]. This cosurfactant ability produced bigger area of micellar structure in the phase diagram (Figure 3), making possible to form W/O microemulsion with less surfactant content. Other studies about the microemulsion and micelles formation showed similar results [30,31]. An opposite rheological behavior was observed for  $L_1$  phase as higher viscosity was observed at higher cosurfactant concentration. Short-chain alcohols exert influence on the systems by their effect on the water structure as solvent and could explain the increase of the viscosity values [32], since not all cosurfactant moieties are onto the interface. The alcohol is susceptible to the partition phenomenon and depending on their relative solubility, they tend to migrate to one of the phases [29,33]. Thus, increasing ethanol content would favor its migration to aqueous continuous phase and led to higher viscosity. Increasing ethanol content decreased distance  $d$  between the planes of the  $\text{La}$  structures (Table 5), viscosity (Table 4), elasticity modulus (Figure 6) and eliminate shear time-dependence. These results were also observed for  $H_1$  systems and could indicate that at lower cosurfactant content the ethanol showed more affinity with water and at higher concentration such

alcohol interact with surfactant at the interface making the structure softer and more packed.

The oil unsaturation also exerted some influence on systems properties only at intermediate water content. Systems with sunflower oil presented higher distances between the crystalline structures, which could be related to its less packed or more crooked spatial arrangement caused by the higher unsaturation of this oil. Moreover, rheological measurements showed that the oil had no effect on viscoelastic behavior (Figure 6), but systems with HOSO presented lower behavior index and higher viscosity. However, this tendency inverted at 50% (w/w) of water content at higher cosurfactant concentration (Table 4). The more shear-thinning behavior observed for systems produced with HOSO could be attributed to the lower distance between the structures and the more organized structure of this oil, since the interaction energy between surfactant and oil decreases with the unsaturation increase [14]. In addition, increase in water content makes the ethanol less available to interact with the surfactant at interface, favoring the partition phenomenon due to higher affinity and miscibility of these polar compounds [29,34]. Consequently these structures became denser, which can be noted with the slight decrease in the structures radius (Table 5). Results showed that the LC region appeared earlier for the system S2E1 (40–60%, w/w of water) and later for H2E1 (60–70%, w/w of water). It means that H2E1 system was capable to extend the lamellar region, delaying the phase inversion from W/O to O/W. Moreover, this oil effect was masked by the ethanol addition, showing that both, cosurfactant and unsaturation effects exerted important influence on systems properties.

## 5. CONCLUSION

The utilization of sunflower oil and others biocompatible ingredients allowed to form microemulsions O/W and W/O. However, it was necessary a high amount of surfactant and/or cosurfactant to form these one single phase systems. In addition, water addition changed the surfactant self-assembly and its interaction with the compounds. At lower water content L<sub>2</sub> phase was produced with small particle size and distances between their structures, and presented Newtonian behavior. At intermediate water content (above 20%, w/w) complex structures were formed with the lamellar L<sub>a</sub> phase and further water addition led to the formation of the hexagonal region (H<sub>1</sub>). These structures deviated from Newtonian behavior showing viscoelasticity and thixotropy. At last O/W microemulsions (water content more than 60%, w/w) were formed with similar properties of L<sub>2</sub> phase. The different systems were affected for both ethanol and oil unsaturation. Higher ethanol content led to lower viscosity and elasticity, besides of lower distances between the crystalline structures. These results were related to the ability of the ethanol to increase interface flexibility and to make its conformation more packed. However, lower oil unsaturation formed systems with higher pseudoplasticity and viscosity, which is attributed to the smaller distances between the crystalline structures. The oil with less unsaturation was also capable to retard the system inversion from W/O to O/W. The influence of the oil could be attributed to the spatial arrangement caused by the double or single bounds of the oil chain, modifying the chain volume and its flexibility. At last, both cosurfactant and oil unsaturation exerted influence on microemulsion and liquid crystalline properties, besides of the higher concentration ethanol masked the influence of oil unsaturation.

## 6. ACKNOWLEDGEMENTS

The authors would like to thank Fapesp (EMU 09/54137-1), CNPq and Capes for their financial support. The authors also thank the Brazilian Synchrotron Light Laboratory (LNLS) for the opportunity to carry out SAXS measurements.

## 7. REFERENCES

- [1] J. Flanagan, H. Singh, Microemulsions: A potential delivery system for bioactives in food, *Crit. Rev. Food Sci. Nutr.* 46 (2006) 221–237.
- [2] H. Zhang, Y. Xu, L. Wu, X. Zheng, S. Zhu, F. Feng, L. Shen, Anti-yeast activity of a food-grade dilution-stable microemulsion, *Appl. Microbiol. Biot.* 87 (2010) 1101-1108.
- [3] F.-F. Lv, L.-Q. Zheng, C.-H. Tung, Phase behaviour of the microemulsions and the stability of the chloramphenicol in the microemulsion-based ocular drug delivery system, *Int. J. Pharm.* 301 (2005) 237-246.
- [4] B.P. Binks, P.D.I. Fletcher, L. Tian, Influence of nanoparticle addition to Winsor surfactant microemulsion system, *Colloid. Surface. A.* 363 (2010) 8-15.
- [5] S.P. Moulik, B.K. Pal, Structure, dynamics and transport properties of microemulsions, *Adv. Colloid. Interfac.* 78 (1998) 99-195.
- [6] A.K. Rakshit, S.P. Moulik, Physicochemistry of W/O Microemulsions: Formation, Stability, and Droplet Clustering, in: M. Fanun (Ed.), *Microemulsions: Properties and Applications*, CRC Press, New York, 2009, chapter 2.
- [7] J. Sjöblom, R. Lindberg, S.E. Friberg, Microemulsions – Phase equilibria characterization, structures, applications and chemical reactions, *Adv. Colloid. Interfac.*, 65 (1996) 125-287.
- [8] S. Engstrom, K. Larsson, Microemulsion in foods, in: P. Kumar, K.L. Mittal (Eds.), *Handbook of Microemulsion Science and Technology*, Dekker, New York, 1999, pp. 789-796.

- [9] L. De Campo, A. Yaghmur, N. Garti, M.E. Leser, B. Folmer, O. Glatter, Five-component food-grade microemulsions: Structural characterization by SANS, *J. Colloid. Interf. Sci.* 274 (2004) 251-267.
- [10] A. Yaghmur, L. De Campo, A. Aserin, N. Garti, O. Glatter, Structural characterization of five-component food grade oil-in-water nonionic microemulsions, *Phys. Chem. Chem. Phys.* 6 (2004) 1524-1533.
- [11] N. Patel, U. Schmid, M.J. Lawrence, Phospholipid-based microemulsions suitable for use in foods, *J. Agr. Food Chem.* 54 (2006) 7817–7824.
- [12] J.-L. Feng, Z.-W. Wang, J. Zhang, Z.-N. Wang, F. Liu, Study on food-grade vitamin E microemulsions based on nonionic emulsifier, *Colloid. Surface. A.* 339 (2009) 1–6.
- [13] K. Zielinska, K.A. Wilk, A. Jezierski, T. Jesionowski, Microstructure and structural transition in microemulsions stabilized by aldonamide-type surfactants, *J. Colloid. Interf. Sci.* 321 (2008) 408-417.
- [14] T.T. Phan, J.H. Harwell, D.A. Sabatini, Effects of triglyceride molecular structure on optimum formulation of surfactant-oil-water systems, *J. Surfactants Deterg.* 13 (2010) 189-194.
- [15] C.R.B. Mendonça, Y.P. Silva, W.J. Böckel, E.F. Simó-Alfonso, G. Ramis-Ramos, C.M.S. Piatnicki, C.I.D. Bica, Role of the co-surfactant nature in soybean W/O microemulsions, *J. Colloid. Interf. Sci.* 337 (2009) 579-585.
- [16] D. Skoric, S. Jocis, Z. Sakac, N. Lecic, Genetic possibilities for altering sunflower oil quality to obtain novel oils, *Can. J. Physiol. Pharm.* 86 (2008) 215-221.
- [17] B. Delplanque, The nutritional value of sunflower oils: linoleic sunflower seeds and seeds with high oleic content, *OCL-Ol. Corps Gras Li.* 7 (2000) 467–472.
- [18] J. Cui, B. Yu, Y. Zhao, W. Zhu, H. Li, H. Lou, G. Zhai, Enhancement of oral absorption of curcumim by self-microemulsifying drug delivery systems, *Int. J. Pharm.* 371 (2009) 148–155.

- [19] A. Yaghmur, A. Aserin, N. Garti, Phase behaviour of microemulsions based on food-grade nonionic surfactants: Effect of polyols and short-chain alcohols, *Colloid. Surface. A.* 209 (2002) 71–81.
- [20] N. Garti, A. Aserin, S. Ezrahi, E. Wachtel, Water solubilization and chain-length compatibility in nonionic microemulsions, *J. Colloid Interf. Sci.* 169 (1995) 428–436.
- [21] A.M. Percebom, L. Piculell, W. Loh, Polyion-surfactant ion complex salts formed by a random anionic copolyacid at different molar ratios of cationic surfactant: phase behavior with water and n-alcohols, *J Phys. Chem. B.* 116 (2012) 2376-2384.
- [22] F. Cordobés, J.M. Franco, C. Gallegos, Rheology of the lamellar liquid-crystalline phase in polyethoxylated alcohol/water/heptane systems, *Grasas Aceites.* 56 (2005) 96-105.
- [23] M.A. Polizelli, V.R.N Telis, L.Q. Amaral, E. Feitosa, Formation and characterization of soy bean oil/surfactant/water microemulsions, *Colloid. Surface. A.* 281 (2006) 230-236.
- [24] S.K. Mehta, G. Kaur, K.K. Bhasin., Analysis of Tween based microemulsion in the presence of TB drug rifampicin, *Colloid. Surface. B.* 60 (2007) 95-104.
- [25] A. Amani, P. York, H. de Waard, J. Anwar, Molecular dynamics simulation of a polysorbate 80 micelle in water, *Soft Matter.* 7 (2011) 2900-2908.
- [26] S.K. Mehta, K. Bala, Tween-based microemulsions: a percolation view, *Fluid Phase Equilibr.* 172 (2000) 197-209.
- [27] P.D.I. Fletcher, B.H. Robinson, Dynamic Process in water-in-oil microemulsions, *Ber. Bunsen Phys. Chem.*, 85 (1981) 863-867.
- [28] C.A. Miller, P. Neogi. Interfacial phenomena: equilibrium and dynamic effects. New York: M. Dekker, 2 ed. 494 p., (Surfactant science series; v.17). (2008).
- [29] K.X. Resende, M.A. Corrêa, A.G. de Oliveira, M.V. Scarpa, Effect of cosurfactant on the supramolecular structure and physicochemical properties of non-ionic biocompatible microemulsions. *Braz. J. Pharm. Sci.* 44 (2008) 35-42.

- [30] J. Flanagan, K. Kortegaard, D. Neil Pinder, T. Rades, H. Singh, Solubilisation of soybean oil in microemulsions using various surfactants, *Food Hydrocolloid.* 20 (2006) 253–260.
- [31] R.C. Santana, L.H. Fasolin, R.L Cunha, Effects of a cosurfactant on the shear-dependent structures of systems composed of biocompatible ingredients. *Colloids Surf. A.* 20 (2012) 54-60.
- [32] M. Tomsic, A. Jamnik, Simple alcohols and their role in the structure and interactions of microemulsion systems, in: M. Fanun (Ed), *Microemulsions, properties and applications*, CRC Press, Boca Raton, 2008, chapter 6.
- [33] R. Nagarajan, E. Ruckenstein, Molecular theory of microemulsions. *Langmuir.* 16 (2000) 6400-6415.
- [34] R. Leung, D. Shah, Solubilization and phase equilibria of water-in-oil microemulsions. II. Effect of alcohols, oil, and salinity on single-chain surfactant systems. *J. Colloid. Interf. Sci.* 120 (1987) 330-344.

**– CAPÍTULO 4 –**

***Organic acids as cosurfactant in self-assembly systems***



**ORGANIC ACIDS PARTITION ON PRODUCTION OF MICROEMULSIONS AND LIQUID  
CRYSTALLINE FORMULATED WITH TRYACYLGLICEROLS**

L.H. Fasolin, R.C. Santana, R.L. Cunha\*

***Submitted to Journal of Colloids and Interface Science***

Department of Food Engineering, Faculty of Food Engineering, University of Campinas – UNICAMP, CEP: 13083-862, Campinas, SP, Brazil

\*Corresponding author. TEL: +551935214047; FAX: +551935214027; EMAIL:  
[rosiane@fea.unicamp.br](mailto:rosiane@fea.unicamp.br)

**ABSTRACT**

The effect of short-chain organic acids as cosurfactant in microemulsions and liquid crystalline systems and their behavior in relation to the oil prevailing unsaturation (High oleic sunflower oil - HOSO or commercial sunflower oil) was evaluated through SAXS and rheological measurements. Results showed that the self-assembly of the compounds and the rheological behavior depended on the cosurfactant and the oil properties. In general, HOSO solubilized larger content of acetic acid due its lower hydrophobicity, while the sunflower oil could entrap more propionic acid. This affinity differences between oil and cosurfactant changed the diffusion mechanism of the acid through the surfactant and oil tails as well as its susceptibility to the partition phenomenon. This phenomenon was also influenced by water content that affected the partition and dissociation of the cosurfactant. Systems with acetic acid formed more rigid structures with higher viscosity, shear-thinning behavior and bigger distances between the crystalline structures due its tendency to

migrate to water phase. On the other hand, propionic acid was less susceptible to dissociation being able to solubilize higher oil content. As a result, their structures were softer with lower viscosity and slightly smaller distances. The surfactant self-assembly was dependent on the hydrophilicity of the systems. HOSO+acetic acid system allowed the higher organization of the surfactant, led to more complex structures. Thus, the edible oils can be used to prepare different liquid crystalline and microemulsion systems, but their properties depend on the combination of the components.

*Keywords:* *organic acid, microemulsion, liquid crystalline, tryacylglycerol, SAXS, rheology*

## **1. INTRODUCTION**

Surfactant molecules can self-assemble into a large variety of morphologies, including micelles, microemulsions and liquid-crystalline (LC) phases, such as lamellar, hexagonal, or cubic phases [1]. All these systems are formed spontaneously and they are composed by oil and water stabilized by an interfacial film of surfactant [2]. As these systems provide both organic and aqueous environment, they can simultaneously solubilize large amount of hydrophilic and hydrophobic compounds [3, 4], including food additives, nutraceuticals, aromatic compounds, cosmetic compounds, active ingredients, and drugs [5]. In addition, these systems could be typically associated with a cosurfactant in order to make the interface more flexible, contributing to the formation of microemulsions [6]. However, the properties of these spontaneous systems are dependent on various factors such as the rigidity of the amphiphilic surfactant, type of oil, cosurfactant and temperature [7-9].

Many recent studies have been performed with the aim of preparing microemulsions using ingredients accepted by the industry, but most of the reported works have used at least one non-biocompatible ingredient or cyclic oils (which are highly susceptible to oxidation) [10-12]. Tryacylglycerols (vegetable oils) are an alternative to the use of cyclic oils, but the possibility of using vegetable oils as the oil phase has been scarcely investigated despite of their economical importance. Sunflower (*Helianthus annuus* L.) oil is one of the most commonly used vegetable oil, consisting of about 90% of unsaturated fatty acids, which are mainly oleic (C18:1, 16-19%) and linoleic (C18:2, 68-72%) [13]. In order to upgrade the use of sunflower oil, new varieties have been selected, such as high oleic sunflower oil (HOSO), in which the main fatty acid is represented by oleic acid [14]. Among the amphiphilic compounds, polyoxyethylene sorbitan esters (Tweens) are probably the most widely used surfactants, showing the polyoxyethylene head groups attached to a sorbitan ring, which increases the hydrophilicity of the sorbitan fatty esters (Yaghmuir et al., 2004). Regarding the cosurfactants, alcohols are the most used in microemulsion formulations and, among the alcohols, ethanol has the lowest toxicity [15, 16]. However, the use of alcohol restricts the use of those systems to specific consumer groups or applications. In this respect, the use of organic acids as cosurfactants have been recently reported as an alternative to the use of alcoholic compounds [8, 17-20]. These acids increase the transparent single region in the phase diagram, acting as cosurfactant and cosolvent. Behavior of different organic acids in microemulsions depends of their chain length in the same way as alcohols [17, 19, 20]. The n-alkyls acids with longer chain are capable to solubilize higher water content in w/o region. However, to obtain fully dilutable systems, e.g., W/O microemulsions that are able to invert into an O/W microemulsion, the chain length should not exceed three carbons [19]. Thus, the aim of

this work was to construct phase diagrams using sunflower oil or HOSO, water, Tween 80 as surfactant and short-chain organic acids as cosurfactant in order to form a fully-dilutable systems, evaluating the effect of the prevailing oil unsaturation in association with the cosurfactant effect on microemulsion and liquid crystalline production.

## **2. MATERIAL AND METHODS**

### ***2.1. Material***

Sunflower oil and HOSO were kindly donated by Cargill (Mairinque, Brazil) and surfactant polyoxyethylene sorbitan monoleate (Tween 80) was purchased from Sigma-Aldrich Co. (EUA). The cosurfactant propionic acid 99.5% (Vetec, Brazil) and acetic acid 99 % (Synth, Brazil) were of analytical grade.

### ***2.2. Phase behavior and diagrams construction***

The four-component systems (Table 1) were described using pseudo-ternary diagrams produced by spontaneous emulsification method at room temperature (25 °C). The influence of the prevailing oil unsaturation was performed using sunflower oil or HOSO with different cosurfactants. An initial mixture of surfactant, cosurfactant and oil was prepared under magnetic stirring at different ratios of surfactant:oil+cosurfactant (10:90; 20:80; 30:70; 40:60; 50:50; 60:40; 70:30; 80:20 and 90:10) [21]. The 1:2 oil:cosurfactant ratio was used in order to obtain a higher single phase area and make the microemulsion formation easier [22]. Then, deionized water was titrated to the initial mixture under constant stirring with volume increments of 10% (w/w) forming water dilution lines 1 up to 9. Line 1 corresponds to 10% initial mixture of surfactant and 90% oil+cosurfactant, and so

on, up to the line 9, which represents the system with 90% surfactant and 10% oil+cosurfactant. Each system was named according to its formulation: first, in accordance to the initial surfactant concentration and then, with the water content. For example, a system on the line 8 (80% initial surfactant concentration), diluted with 40% water was denominated as 8040. Each formulation was stirred for 15 min and then stored at 25°C for at least one week before to construction of the phase diagrams.

**Table 1. Composition of the formulations used to construct phase diagrams**

<b>System nomenclature</b>	<b>Surfactant</b>	<b>Oil</b>	<b>Cosurfactant</b>	<b>Oil:cosurfactant ratio</b>
SP	Tween80	Sunflower	Propionic Acid	1:2
HP	Tween80	HOSO	Propionic Acid	1:2
SA	Tween80	Sunflower	Acetic Acid	1:2
HA	Tween80	HOSO	Acetic Acid	1:2

### **2.3. Phase diagrams characterization**

After the phase diagrams construction, they were delimitated in different regions. The formulations that presented turbidity and/or phase separation with one milk-like phase were classified as macroemulsions or emulsions (EM). Translucid systems with phase separation were named as two transparent phases (2TP) and represented Winsor I or Winsor II systems. At last, the translucent one phase region was characterized as microemulsion O/W ( $L_1$ ), W/O ( $L_2$ ) or liquid crystalline (LC) based on polarized light microscopy, electrical conductivity. Firstly, the polarized light microscopy was performed to identify the liquid crystalline zone and conductivity measurements were carried out in order to identify the continuous phase of the microemulsions ( $L_1$  or  $L_2$ ). The conductivity of the samples was determined at 25°C using a bench top conductivimeter Orion 3 Star (Thermo

Electron Co., USA) coupled to a conductivity cell (Orion 013016MD). For light polarized microscopy, a drop of sample was placed between a cover slip and a glass slide to be examined under polarized light. An optical microscope Olympus BX51TF (Olympus, Japan) equipped with a digital camera was used to analyze the samples at room temperature. The isotropic or anisotropic behavior of the samples could be observed and pictures were taken at a magnification of 20×. In addition, characteristic parameters of the systems were calculated, including the total LC region ( $A_{LC}$ ), the microemulsion area ( $A_{OW}$  and  $A_{W/O}$ ), the maximal amount of aqueous phase dispersed in the W/O microemulsion (Wm) and the minimum surfactant concentration at this corresponding condition (Sm) [12, 23]. At last, systems corresponding to the dilution lines 8 and 9 (single phase), were subjected to small angle X-ray scattering (SAXS) and rheological measurements in order to better define and characterize the microemulsions and liquid crystalline structures.

## **2.4. Microemulsions and liquid crystalline characterization**

### **2.4.1. Small angle X-Ray Scattering (SAXS)**

Quantitative information of the LC and microemulsions structures was obtained by means of small angle X-ray scattering (SAXS) measurements performed at room temperature using the beamline of the National Synchrotron Light Laboratory (LNLS, Campinas, Brazil). The beamline is equipped with an asymmetrically cut and bent silicon (1 1 1) monochromator that yields a monochromatic ( $\lambda = 1.54 \text{ \AA}$ ) and horizontally focused beam. A position-sensitive X-ray detector and a multichannel analyzer were used to record the SAXS intensity,  $I(q)$ , as a function of modulus of scattering vector  $q$ :  $q = (4\pi/\lambda) \sin(\theta/2)$ ,  $\theta$  being the scattering angle. Each SAXS pattern corresponds to a data collection time of

100 s. Microemulsion patterns are formed by one peak, which can be related to the distance between the micellar structures according Equation 1.

$$d = \frac{2\pi}{q} \quad (1)$$

where  $d$  is the structure distance and  $q$  the scattering vector.

For liotropic mesophases (liquid crystal), the position and relative intensity of scattering vector allow the determination of crystallographic similarities, by analyzing the relative distances between the peaks, which are dictated by the reflection laws [2, 24, 25]. For lamellar structures, the distances in relation to the first peak is 1:2:3:4:... and the distance is characterized by the distance  $d$  between their planes, which is determined according Equation 1. On another hand, the relation is given by 1: $\sqrt{3}$ : $\sqrt{4}$ : $\sqrt{7}$ :... for hexagonal structures consisting of infinitely long cylinder-like aggregates packed in a hexagonal array and separated by the continuous phase. The lattice parameter ( $a$ ) is calculated according Equation 2 and represents the distance from the centre of one cylinder to another including the total diameter of the cylinder and the thickness of the water layer.

$$a = \left[ \frac{4\pi}{q_{100}\sqrt{3}} \right] \quad (2)$$

where  $a$  is the lattice parameter and  $q_{100}$  the first peak position.

Moreover, the cubic phase could present five different symmetry groups depending on the relation between the positions of the peaks [2, 24]. In this case, the lattice parameter,  $a$  (the cubic unit cell size), of a cubic structure is obtained according Equation 3.

$$a = \frac{2\pi\sqrt{h^2 + k^2 + l^2}}{q_{hkl}} \quad (3)$$

where  $a$  is the lattice parameter,  $h$ ,  $k$  and  $l$  are the corresponding Miller indexes and  $q_{hkl}$  the scattering vector of the  $[hkl]$  reflection. After plotting  $1/d_{hkl} = (q_{hkl}/2\pi)$  vs  $m = (h^2 + k^2 + l^2)$ , the lattice parameter is obtained from the slope of the curve [24].

#### 2.4.2. *Rheological measurements*

The rheological measurements were performed using a rheometer Physica MCR301 (Anton Paar, Austria) at 25°C. Measurements were performed using cone-plate geometry (50 mm, 2° angle, truncation 208 µm). All measurements were done in triplicate.

Flow curves were obtained by an up-down-up steps program with shear rate ranging from 0 to 100 s<sup>-1</sup>. Newtonian viscosity  $\mu$  (Pa.s) or the apparent viscosity at low shear rate (apparent viscosity at 3 s<sup>-1</sup> -  $\eta_3$ ) (Pa.s) was also evaluated.

## 3. RESULTS

### 3.1. *Phase diagrams*

The systems with different composition and ingredients concentration were visually observed to construct the pseudo-ternary phase diagrams (Figure 1). Similar behavior was

observed for all diagrams. When the surfactant was in excess (upper corner), a single phase (translucid or not) was formed as observed along the dilutions Lines 8 and 9 for both organic acids and oils, and Line 7 for HA systems. For these lines the L<sub>1</sub> and L<sub>2</sub> (O/W and W/O microemulsions) regions were separated by a liquid crystalline (LC) phase, which exhibited an opaque appearance with high viscosity or gel formation. Phase separation occurred as the systems composition moved away from the Tween80-water line (higher oil:cosurfactant content) with the observation of different characteristics. Systems formed a milk-like emulsion (EM) with water in excess (left corner), but in the right corner (oil:cosurfactant in excess) systems tended to show two transparent phases, characterizing Winsor I systems (microemulsion + oil phase). However, the regions boundaries of the phase diagrams and some parameters associated to them varied depending on the diagram composition, as shown in Table 2.

The different oils did not result in significant changes in the parameters of the systems with the addition of propionic acid, but they showed differences when acetic acid was used. The single phase area was higher in HA systems due to the presence of microemulsion and liquid crystalline in the Line 7, that did not appear in other diagrams (Figure 1). Moreover, the acetic acid addition allowed solubilizing higher water content for both oil but, with sunflower oil, less surfactant was necessary. The higher water solubilization of acetic acid systems is reflected in the microemulsion area, which was larger for this acid, mainly the L<sub>2</sub> region. Phase diagrams with organic acid presented lower liquid crystalline phase for both oils in comparison to the use of ethanol as cosurfactant in systems with same surfactant and oil composition [22]. However, the differences in the microemulsion and LC areas could not be considered significant among

these systems, except for HA that presented bigger areas due to the presence of single phase systems in dilution Line 7.

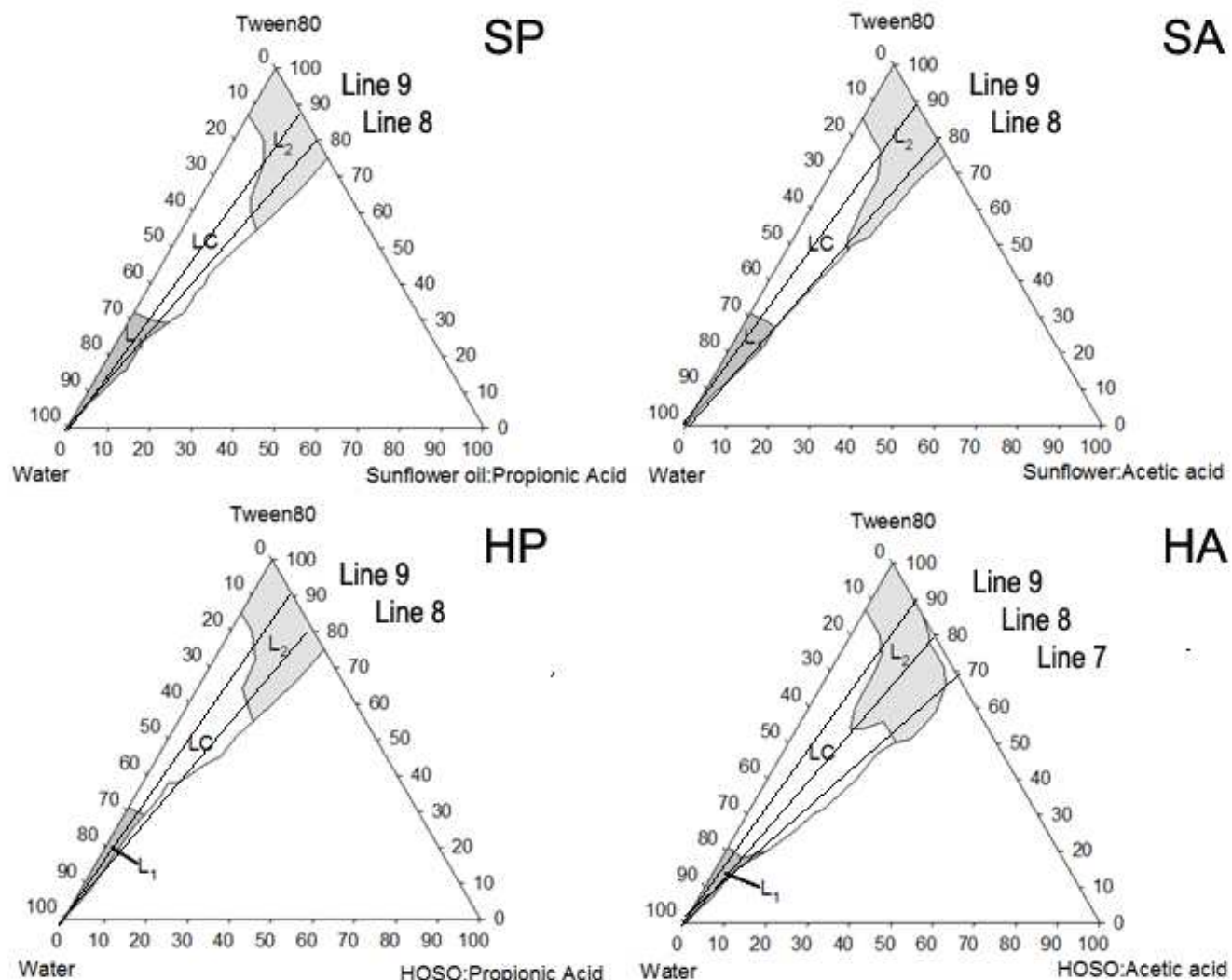


**Figure 1. Phase diagrams formulated with water/Tween80/cosurfactant/sunflower oil or HOSO using propionic or acetic acid as cosurfactant. (LC) Liquid crystalline, (L<sub>2</sub>) W/O microemulsion and (L<sub>1</sub>) O/W microemulsion.**

Regarding the phase inversion, the production of W/O system that could be changed into O/W without phase separation is difficult, but could be attained by the use of cosurfactant with small number of carbons. This behavior was reported for alcohols, the most commonly used cosurfactant [26, 27], and similarly to systems with organic acids (Sternath et al., 2006, Zhang et al., 2009). This behavior could be more difficult in the system composed of triacylglycerol because of its chain length. In the phase diagrams (Figure 1) fully dilutable systems were obtained however, in general, high surfactant concentration was necessary to promote the inversion from W/O to O/W without phase separation.

**Table 2. Characteristic parameters for phase diagrams formulated with water/Tween80/cosurfactant/sunflower oil or HOSO using propionic or acetic acid as cosurfactant**

Parameter	Systems			
	SP	SA	HP	HA
Maximal solubilized water (Wm) (%w/w)	26.7	37	26.8	35
Minimal surfactant (Sm) (%w/w)	55	48	55	54
Microemulsion area (Ame) (%)	11	12.9	10.6	13.7
Crystalline liquid area (Alc) (%)	12.8	11.3	11.4	19.2

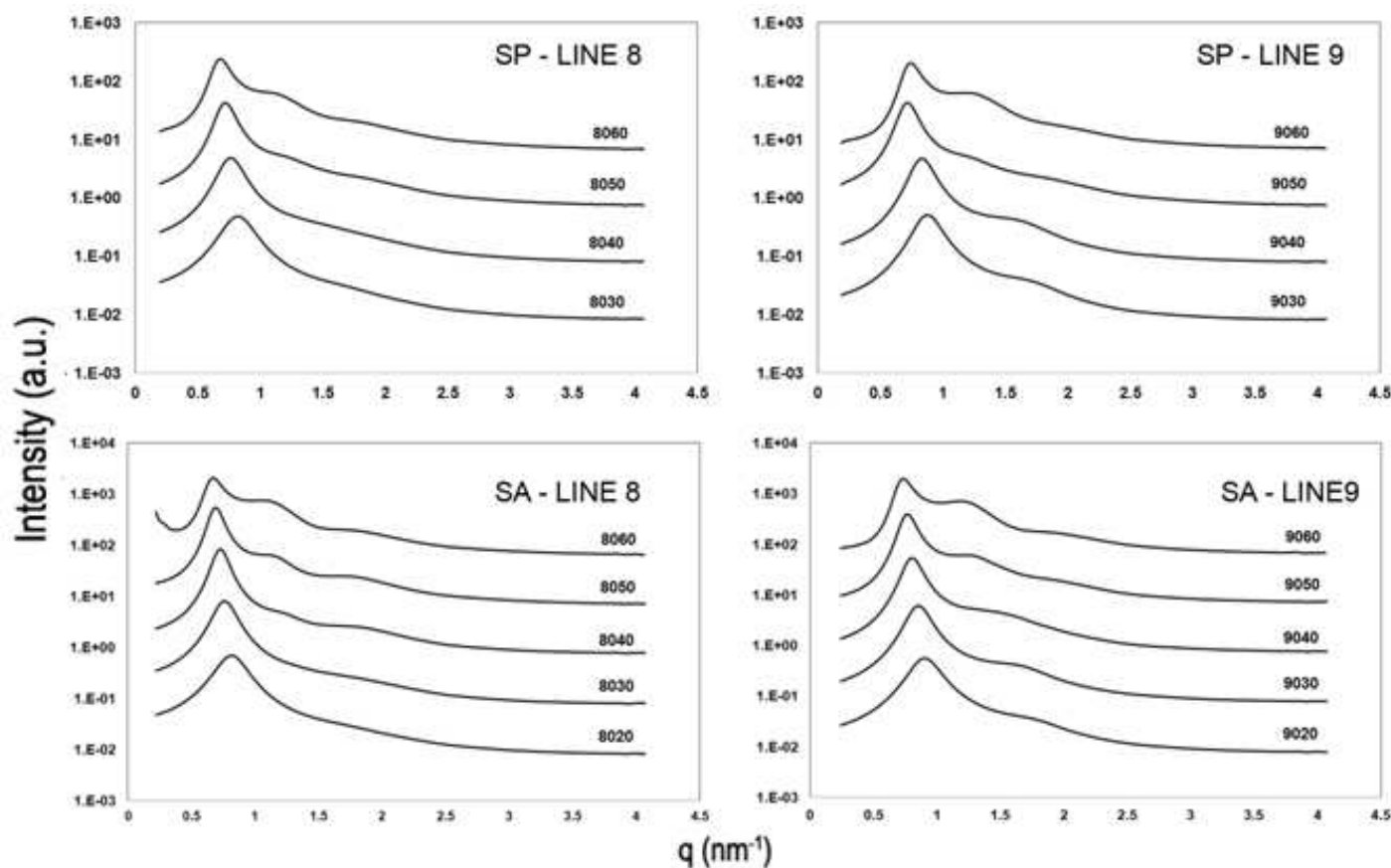
### **3.2. Small-angle scattering (SAXS) measurements**

Figure 2 and 3 shows SAXS scattering curves of systems obtained with different cosurfactants and oils. The results showed that the cosurfactant type and oil unsaturation exerted influence on the structures formed. When sunflower oil was used similar structures were observed comparing systems with the same water concentration (Table 3 and Figure 2). A L<sub>2</sub> phase was observed in the beginning of the titration, changing to a lamellar phase

with 30% (w/w) of water. A normal hexagonal phase was formed with addition of 40 -50% (w/w) of water. However, all systems formed O/W microemulsion after 70% (w/w) of water. The presence of more than one peak in SAXS patterns indicates higher organization of the systems and the displacement of the peaks to smaller values of the scattering vector  $q$  indicates bigger distances between the structures (Figure 2). The distance  $d$  or the lattice parameter  $a$  increased with the water content and decreased at higher surfactant concentration (Line 9). In addition, the higher values of  $d$  and  $a$  were observed in the systems formulated with acetic acid.

**Table 3. Structural parameters evaluated by SAXS for systems formulated with water/Tween80/sunflower oil using propionic or acetic acid as cosurfactant**

Water fraction (%w/w)	SP – Line 8			SP – Line 9			SA – Line 8			SA – Line 9			
	Phase	d (Å)	a (Å)										
55	10	L <sub>2</sub>	67.22	-	L <sub>2</sub>	65.76	-	L <sub>2</sub>	69.87	-	L <sub>2</sub>	66.54	-
	20	L <sub>2</sub>	73.21	-	L <sub>2</sub>	70.56	-	L <sub>2</sub>	77.02	-	L <sub>2</sub>	72.91	-
	30	L <sub>α</sub>	76.31	-	L <sub>α</sub>	71.	-	L <sub>α</sub>	83.16	-	L <sub>α</sub>	74.27	-
	40	H <sub>1</sub>	-	95.08	H <sub>1</sub>	-	86.53	H <sub>1</sub>	-	98.99	L <sub>α</sub>	78.47	-
	50	H <sub>1</sub>	-	101.07	H <sub>1</sub>	-	92.96	H <sub>1</sub>	-	105.50	H <sub>1</sub>	-	95.08
	60	H <sub>1</sub>	-	106.67	H <sub>1</sub>	-	97.00	H <sub>1</sub>	-	107.86	H <sub>1</sub>	-	98.99
	>70	L <sub>1</sub>	80.15	-	L <sub>1</sub>	74.23	-	L <sub>1</sub>	82.23	-	L <sub>1</sub>	77.98	-



**Figure 2. SAXS patterns for systems formulated with water/Tween80/sunflower oil/cosurfactant using propionic or acetic acid as cosurfactant**

On the other hand, greater differences in the structures were observed in systems formulated with HOSO (Table 4 and Figure 3), which depended on the organic acid used as cosurfactant. The propionic acid delayed the onset of the lamellar phase to 40% (w/w) water in systems with lower surfactant concentration (Line 8). However, the behavior was the same as that observed for sunflower oil systems with the surfactant increase (Line 9). The use of acetic acid in systems containing HOSO led to the larger differences in the structures, particularly at the intermediate water content, which was very dependent on the surfactant content. In the Line 9 (higher cosurfactant content), the organization behavior

was quite similar to SA system, but the LC phase appeared only with 40% (w/w) of water content. However, at lower surfactant content (Line 8), the lamellar phase was replaced by a more complex cubic phase, which extended to a larger water content range in the Line 7 (30 – 70% w/w of water) (data not shown). The higher complexity of these systems organization can be observed in Figure 3, due to the higher quantity of peaks. The sequence of these peaks was  $1:\sqrt{2}:\sqrt{3}:\sqrt{4}:\sqrt{6}:\sqrt{8}$ , respectively, classifying this structure as Pn3m, a diamond type.

**Table 4. Structural parameters evaluated by SAXS for systems formulated with water/Tween80/HOSO/cosurfactant using propionic or acetic acid as cosurfactant**

Water fraction (%w/w)	HP – Line 8			HP – Line 9			HA – Line 8			HA – Line 9			
	Phase	d (Å)	a (Å)										
86	10	L <sub>2</sub>	71.54	-	L <sub>2</sub>	65.43	-	L <sub>2</sub>	67.64	-	L <sub>2</sub>	63.51	-
	20	L <sub>2</sub>	72.97	-	L <sub>2</sub>	67.64	-	L <sub>2</sub>	72.97	-	L <sub>2</sub>	68.76	-
	30	L <sub>2</sub>	77.53	-	Lα	72.34	-	L <sub>2</sub>	77.70	-	L <sub>2</sub>	72.97	-
	40	Lα	83.16	-	H <sub>1</sub>	-	88.12	Pn3m	-	79.37	Lα	73.93	-
	50	H <sub>1</sub>	-	102.14	H <sub>1</sub>	-	93.23	Pn3m	-	81.97	Lα	76.70	-
	60	H <sub>1</sub>	-	103.23	H <sub>1</sub>	-	7.98	H <sub>1</sub>	-	78.75	H <sub>1</sub>	-	100
	70	L <sub>1</sub>	70.15		L <sub>1</sub>	63.66	-	H <sub>1</sub>	-	108	H <sub>1</sub>	-	107
	<80	L <sub>1</sub>	76.34	-	L <sub>1</sub>	70.27	-	L <sub>1</sub>	68.20	-	L <sub>1</sub>	59.87	-

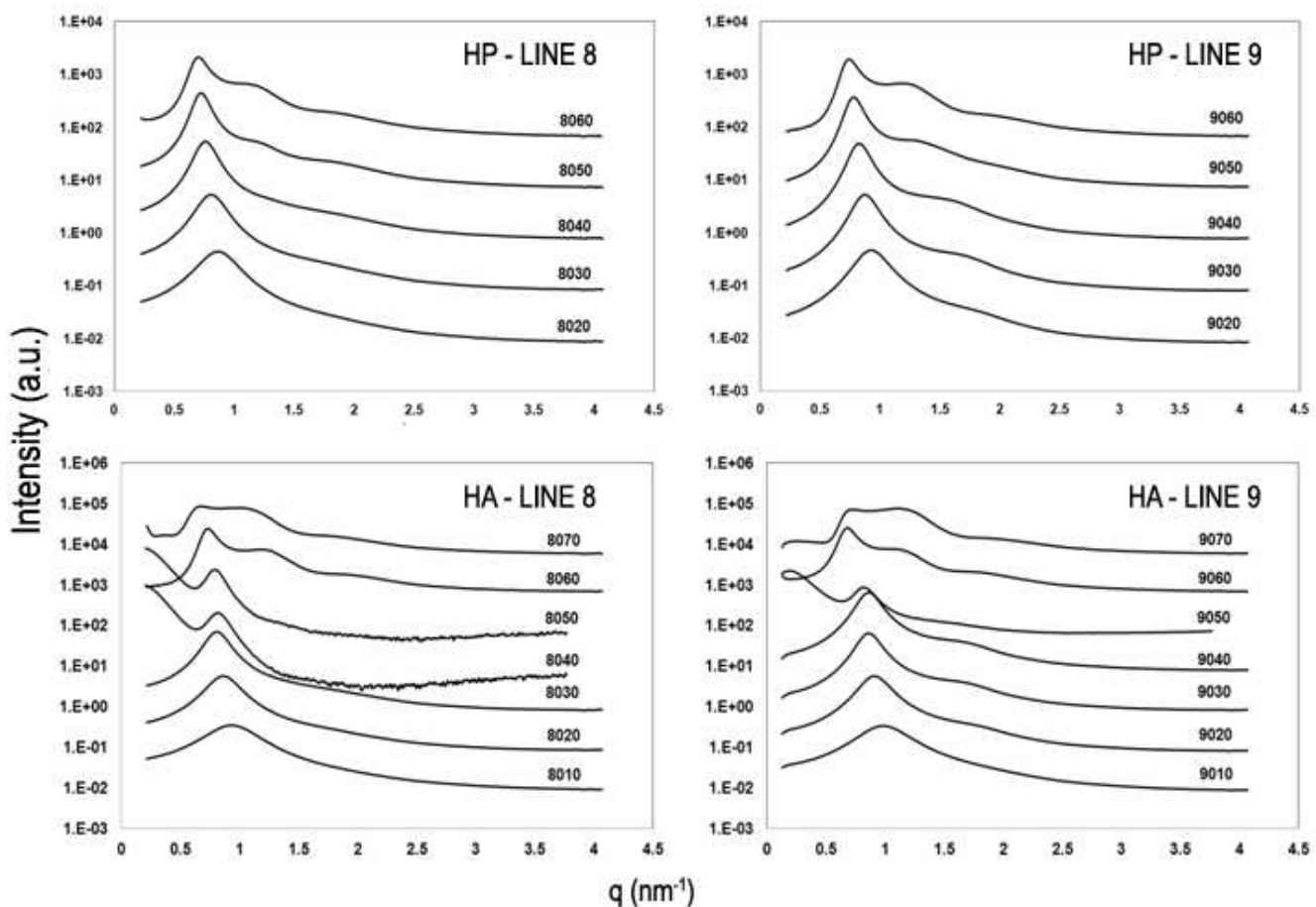


**Figure 3.** SAXS patterns for systems formulated with water/Tween80/HOSO/cosurfactant using propionic or acetic acid as cosurfactant.

### 3.3. Rheological measurements

The cosurfactant type exerted large influence on the rheological behavior. Systems produced with propionic acid presented Newtonian behavior throughout the dilution Line 8 (Table 5). However, the increase of the surfactant content (Line 9) led to a slight shear-thinning behavior at the intermediate water content (40-50% w/w). Besides, the viscosity values were very similar and showed the same tendency for both oil with this acid (system with HOSO presented slightly higher viscosity than those with sunflower oil).

Systems produced with acetic acid showed shear-thinning behavior in a large range of water content and higher viscosity values than propionic acid systems, with lower values of flow index (*n*) ranging from 0.85 up to 0.96 for dilution lines 8 and 9. These systems showed very high viscosities, reaching values up to 32,000 mPa.s. Some samples presented gel-like structures, so a rheological behavior could not be fit to the data (Table 5). In relation to the oil type used, sunflower oil presented higher viscosity than HOSO, when acetic acid was used.

**Table 5. Rheological properties of different systems formulated with water/Tween80/cosurfactant/sunflower oil or HOSO using propionic or acetic acid as cosurfactant**

System	SP				SA				HP				HA			
	$\eta$ or $\eta_3$ (mPa.s)	k (Pa.s <sup>n</sup> )	n	R <sup>2</sup>	$\eta$ or $\eta_3$ (mPa.s)	k (Pa.s <sup>n</sup> )	n	R <sup>2</sup>	$\eta$ or $\eta_3$ (mPa.s)	k (Pa.s <sup>n</sup> )	n	R <sup>2</sup>	$\eta$ or $\eta_3$ (mPa.s)	k (Pa.s <sup>n</sup> )	n	R <sup>2</sup>
8000	243	-	1	0.99	422	-	1	0.99	251	-	1	0.99	305	-	1	0.99
8010	334	-	1	0.99	603	-	1	0.99	364	-	1	0.99	477	-	1	0.99
8020	419	-	1	0.99	1183	-	1	0.99	470	-	1	0.99	816	-	1	0.99
8030	651	-	1	0.99	4417	5.88	0.95	0.99	812	-	1	0.99	2071	-	1	0.99
8040	1488	-	1	0.99	32100	NM	NM	-	1995	-	1	0.99	6926	12.07	0.90	0.99
8050	1754	-	1	0.99	6150	13.57	0.79	.99	2317	-	1	0.99	3965	6.43	0.91	0.99
8060	212	-	1	0.99	284	0.66	0.79	0.99	207	-	1	0.99	537	-	1	0.99
8070	18	-	1	0.99	13.5	-	1	0.99	18	-	1	0.99	17	-	1	0.99
8080	4	-	1	0.99	3	-	1	0.99	4	-	1	0.99	3	-	1	0.99
8090	1	-	1	0.99	1	-	1	0.99	1	-	1	0.99	1	-	1	0.99
9000	350	-	1	0.99	498	-	1	0.99	367	-	1	0.99	425	-	1	0.99
9010	521	-	1	0.99	730	-	1	0.99	537	-	1	0.99	639	-	1	0.99
9020	704	-	1	0.99	1217	-	1	0.99	733	-	1	0.99	1040	-	1	0.99
9030	1439	-	1	0.99	4090	5.12	0.96	0.99	1532	-	1	0.99	2593	-	1	0.99
9040	4519	6.17	0.93	0.99	12860	NM	NM	-	4452	5.63	0.96	0.99	14880	NM	NM	-
9050	5042	8.44	0.90	0.99	6570	12.88	0.85	0.99	4726	9.21	0.88	0.99	8855	26.75	0.75	0.99
9060	573	-	1	0.99	408	0.58	0.93	0.99	495	-	1	0.99	197	0.32	0.91	0.99
9070	29	-	1	0.99	23	0.03	0.97	0.99	30	-	1	0.99	25	0.03	0.97	0.99
9080	5	-	1	0.99	4	-	1	0.99	4	-	1	0.99	4	-	1	0.99
9090	1	-	1	0.99	1	-	1	0.99	1	-	1	0.99	1	-	1	0.99

\*NM– non measurable system

#### **4. DISCUSSION**

The use of organic acids with different number of carbons led to different behavior of the surfactant self-assembly depending on the oil used. The small difference between cosurfactants structure led to different physical properties that could change the diffusion mechanism between the oil, water and surfactant tails. Moreover, depending on its concentration, the cosurfactant is susceptible to the partition phenomenon, which was observed in other works using additives and cosurfactants as amines, ethanol and n-alkyl compounds [22, 28-32]. These mechanisms exerted influence on the structure formation and behavior of the fully dilutable systems and were closely related to the physicochemical characteristics of the oil. HOSO is composed mainly by oleic acid that presents only one unsaturation, showing lower hydrophobicity in comparison to sunflower oil (composed mainly by two double bounds). In addition, the higher unsaturation degree of the sunflower oil lead to more bulky and crooked spatial arrangement, increasing the interfacial tension and decreasing its interaction with the surfactant moieties [33]. Given these differences it is possible to consider that the self-assembly of the components could be a result of the affinity between oil and cosurfactant. The oil with lower hydrophobicity (HOSO) would be able to solubilize larger amount of acetic acid (the organic acid with lower carbon chain, or lower “hydrophobicity”). On the other hand, the combination of this oil with propionic acid could make the cosurfactant more susceptible to the partition phenomenon. Moreover, the same analogy could be made to sunflower oil, which would have more affinity with propionic acid. However, this behavior also depended on the water fraction content.

In the initial mixture (absence of water), the cosurfactant (propionic or acetic acid) was dispersed in the surfactant tails, helping to solubilize the oil content. With the water

addition, acids started to modulate the interface, forming L<sub>2</sub> systems. However, small chain organic acids have high solubility in water, tending to diffuse into the water phase of the microemulsion. In addition, these acids can dissociate in water, decreasing the pH of the system. The pH of the systems varied from 3.2 - 4.5, depending on the water content. However, the pKa of these acids is 4.7 and 4.9 for acetic and propionic acid, respectively, i.e. the ionization degree is very low (1-2% of the content added), which means that the major fraction of these acids were present in the neutral form. The neutral form of these acids would be dispersed into the surfactant film [17], while the protonated moieties would be in the core of the W/O microemulsion water droplets. The propionic acid has lower ionization degree in comparison to the acetic acid, which means that there were more molecules of propionic acid at the surfactant tails and in the interface in comparison with acetic acid. This high concentration of cosurfactant at the interfacial film exerted influence on the rheological behavior. Although all systems have shown the same rheological behavior in low water concentration (0-20% w/w), propionic acid could module the interface making it softer with lower viscosity than systems with acetic acid. Moreover, the water also played an important role in the rheological behavior. The water increment promoted swelling of the W/O micelles and the self-assembly of the surfactant moieties could form elongated micelles affecting the rheology of the system and increasing its viscosity [34].

When 30-40% (w/w) of water was added, the type of oil also started to influence the surfactant self-assembly and lamellar structures were formed. Sunflower oil entangled easily with surfactant tails because of its bulky and crooked conformational arrangement, leading to liquid crystalline structures with less water even at lower surfactant content (Line 8). Systems with HOSO also produced LC phase, but only at higher surfactant

concentration or with more water content. As observed before, the oil unsaturation (hydrophobicity) influenced the cosurfactant partition and consequently the distance between the lamellae. On the other hand, the more hydrophobic oil (sunflower oil) facilitated the partition of the acetic acid to the water, giving to this structure (SA) greater distance between the lamellae (40% w/w of water), as compared to HA. Moreover, with higher amount of cosurfactant partitioned, there were less moieties available at the interface, making it more organized and rigid. However, the interaction between oil and cosurfactant had more effect on the physical properties in colloidal domain. The rheological behavior takes in account the bulky properties so, in this case, only the cosurfactant partition affected this property, independently on the oil unsaturation. Acetic acid partition to water phase produced more rigid structures in comparison to the propionic acid, reflecting on the higher shear-thinning behavior and viscosity values.

At intermediate water content (40-60% w/w), similar influence of components on the structure formation and phase inversion to O/W structures was observed. However, it is interesting to notice the behavior of the surfactant in these systems. Tween80 presents HLB value around 15, which means that this surfactant present higher affinity for hydrophilic compounds. Thus, the surfactant self-assembly and interactions with other components in HA systems could occur more easily, due to the highr hydrophilicity of the system. In addition, the ability of the acetic acid to diffuse into HOSO and surfactant tails improve this organization, promoting the formation of more complex structures, as bicontinuous cubic phase and retarding the phase inversion. The opposite behavior was observed for SP systems, composed by more hydrophobic ingredients. This system presented phase inversion to O/W structures in Line 8 at 40% (w/w) originating normal hexagonal structures.

At 60% (w/w) water content, even the more favorable combination to form reverse structures with positive curvature (HA) changed to normal hexagonal phase, becoming water the continuous medium. At this water concentration it is possible to observe the higher tendency of the acetic acid to migrate to the aqueous phase as compared to propionic acid. This strong partition of the cosurfactant can be observed in SAXS measurements through the larger distances between the hexagonal cylinders in systems with acetic acid. At higher water concentration (70% w/w) systems showed the formation of O/W microemulsions. The deprotonated moieties of cosurfactant could be solubilized into the surfactant film in a manner in which two molecules of surfactant formed a group together with one molecule of these organic acids, increasing the tendency to form negative curves, i.e., oil-in-water microemulsions ( $L_1$  phase) [17]. This behavior was observed for all systems, except for HA formulation that presented a delayed conversion to isotropic O/W microemulsion, since the higher affinity between oil+cosurfactant and surfactant favored the LC structures. The lower viscosity value of aqueous continuous medium combined with the presence of distant structures or discrete droplets (depending on the water content), which led to the Newtonian behavior.

## 5. CONCLUSION

The organic acids acted as cosurfactant and cosolvent in systems with biocompatible ingredients and were able to form microemulsion and liquid crystalline systems. The self-assembly of the systems led to different structures (micellar, lamellar, hexagonal and cubic) depending on the components concentration and their interactions. However, the interaction between oil and cosurfactant was dependent of the chain length

of the acid and unsaturation of the oil. The oil with lower hydrophobicity (HOSO) would be able to solubilize larger amount of acetic acid (acid with lower carbon chain). On the other hand, the combination of this oil with propionic acid could make the cosurfactant more susceptible to the partition phenomenon. However, the diffusion and partition phenomenon were dependent on the water content. In general, acetic acid was more susceptible to dissociation and partition due to higher affinity with water. The migration of this acid to aqueous phase decreased its availability at the interface. As a consequence, systems with acetic acid presented more rigid structures with higher viscosity, shear-thinning behavior and bigger distance between their micellar structures. On the other hand, propionic acid was less susceptible to ionic dissociation and tended to migrate between the surfactant tails, being able to solubilize the oil content. Their structures were softer with lower viscosity and generally with smaller distances between the micellar structures. The surfactant also played an important role, which was dependent on the hydrophilicity of the systems. More hydrophilic components allowed the higher organization of the surfactant, leading to more complex structures. Thus, this study showed that edible oils could be used to prepare different liquid crystalline structures and microemulsion systems, depending on the cosurfactant and surfactant used and this compositions.

## **6. ACKNOWLEDGEMENTS**

The authors would like to thank Fapesp (EMU 09/54137-1), CNPq and Capes for their financial support. The authors also thank the Brazilian Synchrotron Light Laboratory (LNLS) for the opportunity to carry out SAXS measurements.

## 7. REFERENCES

- [1] B.P. Binks, P.D.I. Fletcher, L. Tian, Colloid Surface A 363 (2010) 8.
- [2] A. Yaghmur, L. de Campo, S. Salentinig, L. Sagalowicz, M.E. Leser, O. Glatter, Langmuir 22 (2006) 517.
- [3] L. de Campo, A. Yaghmur, N. Garti, M.E. Leser, B. Folmer, O. Glatter, Journal of Colloid and Interface Science 274 (2004) 251.
- [4] S. Engstrom, K. Larsson, in: P. Kumar, K.L. Mittal, (Ed.)^(Eds.)Handbook of microemulsion science and technology; Dekker, New York, 1999, p 789.
- [5] A. Sernath, A. Aserin, Adv Colloid Interfac 128 (2006) 47.
- [6] F.F. Lv, L.Q. Zheng, C.H. Tung, International journal of pharmaceutics 301 (2005) 237.
- [7] B.K. Paul, R.K. Mitra, J Colloid Interf Sci 288 (2005) 261.
- [8] H. Zhang, Y.Q. Xu, L.J. Wu, X.D. Zheng, S.M. Zhu, F.Q. Feng, L.R. Shen, Appl Microbiol Biot 87 (2010) 1101.
- [9] X.G. Zhang, J.F. Dong, G.Y. Zhang, X.L. Hong, X.F. Li, J Colloid Interf Sci 285 (2005) 336.
- [10] M. Fanun, Colloid Surface A 369 (2010) 246.
- [11] C.C. Lin, H.Y. Lin, H.C. Chen, M.W. Yu, M.H. Lee, Food Chem 116 (2009) 923.
- [12] A. Yaghmur, A. Aserin, N. Garti, Colloids and Surfaces A: Physicochemical and Engineering Aspects 209 (2002) 71.
- [13] D. Skoric, S. Jocic, Z. Sakac, N. Lecic, Can J Physiol Pharm 86 (2008) 215.
- [14] B. Delplanque, Ocl-Ol Corps Gras Li 7 (2000) 467.
- [15] J.L. Feng, Z.W. Wang, J. Zhang, Z.N. Wang, F. Liu, Colloid Surface A 339 (2009) 1.
- [16] N. Patel, U. Schmid, M.J. Lawrence, J Agr Food Chem 54 (2006) 7817.

- [17] A. Cid-Samamed, L. Garcia-Rio, D. Fernandez-Gandara, J.C. Mejuto, J. Morales, M. Perez-Lorenzo, *Journal of Colloid and Interface Science* 318 (2008) 525.
- [18] X.Q. Li, J.L. Chai, S.C. Shang, H.L. Li, J.J. Lu, B. Yang, Y.T. Wu, *J Chem Eng Data* 55 (2010) 3224.
- [19] A. Spernath, A. Aserin, N. Garti, *Journal of Colloid and Interface Science* 299 (2006) 900.
- [20] H. Zhang, Y. Shen, P.F. Weng, G.Q. Zhao, F.Q. Feng, X.D. Zheng, *Int J Food Microbiol* 135 (2009) 211.
- [21] J. Cui, B. Yu, Y. Zhao, W. Zhu, H. Li, H. Lou, G. Zhai, *International journal of pharmaceutics* 371 (2009) 148.
- [22] L.H. Fasolin, R.C. Santana, R.L. Cunha, *Colloid Surface A* 415 (2012) 31.
- [23] N. Garti, A. Aserin, S. Ezrahi, E. Wachtel, *J Colloid Interf Sci* 169 (1995) 428.
- [24] P. Alexandridis, U. Olsson, B. Lindman, *Langmuir* 14 (1998) 2627.
- [25] Z.N. Wang, Z.Y. Diao, F. Liu, G.Z. Li, G.Y. Zhang, *J Colloid Interf Sci* 297 (2006) 813.
- [26] N. Garti, M. Avrahami, A. Aserin, *J Colloid Interf Sci* 299 (2006) 352.
- [27] S.K. Mehta, G. Kaur, R. Mutneja, K.K. Bhasin, *J Colloid Interf Sci* 338 (2009) 542.
- [28] E. Caponetti, A. Lizzio, R. Triolo, W.L. Griffith, J.S. Johnson, *Langmuir* 8 (1992) 1554.
- [29] J.G. del Rio, D.G. Hayes, V.S. Urban, *J Colloid Interf Sci* 352 (2010) 424.
- [30] Y. Mrestani, R.H.H. Neubert, A. Krause, *Pharmaceut Res* 15 (1998) 799.
- [31] H.N. Singh, C.D. Prasad, S. Kumar, *J Am Oil Chem Soc* 70 (1993) 69.
- [32] M.F. Zhou, R.D. Rhue, *J Colloid Interf Sci* 241 (2001) 199.
- [33] T.T. Phan, J.H. Harwell, D.A. Sabatini, *J Surfactants Deterg* 13 (2010) 189.

- [34] R.D. Santana, L.H. Fasolin, R.L. da Cunha, Colloid Surface A 398 (2012) 54.



**– CAPÍTULO 5 –**

***Polysaccharide interaction in self-assembly systems***



## GELLAN- POLYSORBATE INTERACTION IN CONCENTRATED POLYSACCHARIDE SYSTEMS

FASOLIN, L.H., PICONE, C.S.F., SANTANA, R.C., CUNHA, R.L.\*

*Submitted to Food Research International*

Department of Food Engineering, Faculty of Food Engineering, University of Campinas – UNICAMP, CEP: 13083-862, Campinas, SP, Brazil

\*Corresponding author. TEL: +551935214047; FAX: +551935214027; EMAIL: rosiane@fea.unicamp.br

### **ABSTRACT**

The association of gellan gum and a nonionic surfactant in the gel formation was explored in systems with high biopolymer concentration (3% w/w). Gels formed at different concentrations of polysorbate 80 (0-60% w/w) and pH (3.0 and 5.0) were evaluated regarding to microstructure, mechanical and rheological properties. The high concentration of polysaccharide in water at more acidic pH (3.0) favored the molecules aggregation, producing harder gels even at high temperatures. The thermal rheological measurements showed two distinct behaviors which depended on the predominance of polysaccharide or surfactant in the systems. The gellan gum properties were predominant at lower surfactant concentrations. However, the surfactant micelles could enhance the linkage between the macromolecules through the few remaining hydrophobic sites of the biopolymer and consequently increase the gel strength that presented strain-hardening behavior. As the surfactant concentration was increased to 30% (w/w), different slopes in the rheological

curves were observed which were attributed to the structuration of the polysorbate. At higher concentration of polysorbate, the prevailing surfactant prevented the gellan gum aggregation and the influence of the gum in the rheological behavior was not observed anymore. The surfactant self-assembly produced gel-like structures weaker than the gellan network, presenting a strain-weakening behavior. Thus, results suggest that depending on the medium conditions, gellan-polysorbate80 interaction could produce gels with different technological properties.

*Keywords:* *surfactant, biopolymer, surfactant based gels, self-assembly, mechanical properties*

## **1. INTRODUCTION**

Surfactant molecules have the ability to self-assemble into a large variety of morphologies, including different kinds of micelles, vesicles and flexible bilayers. At high concentrations they can spontaneously form a large variety of highly organized mesophases, as cubic, hexagonal and lamellar structures (Binks et al., 2010; Trickett & Eastoe, 2008). Moreover, these surfactant-based systems could act as delivery vehicles of hydrophobic and hydrophilic bioactive compounds, due to the amphiphilic character of surfactant moieties (Qian et al., 2012; Rees & Robinson, 1993; Testard & Zemb, 2002). Surfactants can be classified as cationic, anionic, zwitterionic or nonionic, depending on the hydrophilic head. Aiming their application in pharmaceutical and food systems, the use of nonionic surfactants is more appropriate due to the higher toxicity of ionic surfactants. Polysorbates are nonionic surfactants derived from PEG-ylated sorbitan (hydrophilic group) esterified with fatty acids (hydrophobic group), with a total of 20 ethylene oxide

subunits per molecule. The hydrocarbon chains provide the hydrophobic character of the polysorbates, while their hydrophilic nature is provided by the ethylene oxide (Jiao, 2008; Kerwin, 2008; Picone & Cunha, 2013; Yaghmur et al., 2002). The structure of the polysorbates can vary according to the length of the polyoxyethylene chain, type of fatty acid and degree of esterification, which exert influence on the self-assembly mechanisms (Petersen & Ulrich, 2011).

Besides the influence of different structural arrangement among the polysorbates, external factors can affect the surfactant behavior in solution as temperature, pH, pressure and the presence of additives, as biopolymers (Fan et al., 2011; Lawrence, 1994; Picone & Cunha, 2013; Tomasic et al., 2005). However, the interaction between surfactant and biopolymers is dependent on the bulk variables (e.g. concentration, molar ratio, ionic strength, temperature, etc) (Barreiro-Iglesias et al., 2003; Tomasic et al., 2005). Moreover, the intrinsic characteristic of surfactant and polyelectrolyte also influence this ability of self-assembly and/or interaction (Barreiro-Iglesias et al., 2003; Goddard, 2002; Pepic et al., 2009).

Gellan gum is an linear extracellular polysaccharide produced by the bacterium *Sphingomonas elodea*, and composed of repeating tetrasaccharide (1,3- $\beta$ -D-glucose, 1,4- $\beta$ -D-glucuronic acid, 1,4- $\beta$ -D-glucose, 1,4- $\alpha$ -L-rhamnose) units containing one carboxyl side group. Gellan gum presents gelling properties, forming firm, hard and translucent gels, which are resistant at low pH values. These properties are dependent on the ionic strength, presence and type of cations, pH, temperature and polymer concentration during its gelation (Moritaka et al., 1995; Picone & Cunha, 2011; Yamamoto & Cunha, 2007). To our knowledge the gellan gum interaction with surfactants has not been reported yet, but there are works reporting the interaction of surfactants with other

biopolymers as chitosan, glucomannan and carrageenan (Evmenenko et al., 2000; Grant et al., 2006; Pepic et al., 2009; Yin et al., 2008). However, most of these works use ionic surfactants that generally present a toxicity degree in comparison to nonionic (Guo & Guo, 2010). Moreover, a small range of surfactant and/or polysaccharide concentration was studied; focusing on the chemical interaction between the components. Thus, the aim of this work was evaluate the gellan-surfactant physical interactions using concentrated polysaccharide solution (3.0% w/w). The influence of surfactant concentration and pH in the systems arrangement was evaluated regarding to the microstructure, mechanical properties and thermal rheological behavior of the gels.

## **2. MATERIAL AND METHODS**

### ***2.1. Material***

Deacylated gellan gum powder (Kelcogel® F) was kindly donated by Kelco Biopolymers (San Diego, CA). The surfactant polyoxyethylene sorbitan monooleate (Tween 80) was purchased from Sigma-Aldrich Co. (EUA). The acetic acid 99 % (Synth, Brazil) and other reagents were of analytical grade.

### ***2.2. Gel preparation***

Gelled systems with different Tween80 concentrations (0-50% w/w) were produced with deionized water (natural pH) or with 0.1M acetate buffer pH 3.0 in order to evaluate the effect of pH in surfactant-polysaccharide interactions. Firstly, Tween80 at different concentrations (0-60% w/w) was added to 100 ml deionized water. The solutions were heated at 80°C in a jacketed vessel, then 3.0% (w/w) of gellan powder was added. The

solution was maintained at 80°C during 30 min under constant stirring to solubilize the gum. The rheological measurements were carried out just after the heat treatment. For the analyses of the mechanical properties and microstructure, the mixtures were poured into cylindrical plastic tubes (21 mm inner diameter x 21 mm height) and Petri dishes, respectively, before being cooled to 10°C. The gels were maintained at 10°C for 48 h in order to ensure complete gel formation.

### ***2.3. Zeta potential***

Zeta potential of gellan gum was measured in a Zetasizer Nano-ZS (Malvern Instruments, Worcestershire, UK) with a detection angle of 173°, equipped with a MPT-2 Autotitrator (Malvern Instruments, Worcestershire, UK). The zeta potential of 0.1% (w/w) gellan gum solutions at different pH was determined using titration curves from pH 3.0 to 7.0 by adding 0.25 M NaOH or 0.25 M HCl. The measurements were carried out at 25°C in triplicate.

### ***2.4. Electrical conductivity measurements***

The electrical conductivity ( $\kappa$ ) was determined at 80°C before gellan addition in order to characterize the surfactant arrangement. The measurements were carried out at different pH (3.0 and 5.0) using a bench top conductivimeter Orion 3 Star (Thermo Electron Co., USA) coupled to a conductivity cell (Orion 013016MD).

### ***2.5. Mechanical properties***

Mechanical properties were determinated by uniaxial compression measurements using a TA-XT Plus Texture Analyzer (Stable Micro Systems, Godalming, UK) with a

cylindrical acrylic plate (60 mm diameter) lubricated with silicon oil to minimize friction between the sample and the probe. Compression was carried out at sample temperature (10 °C) with a crosshead speed of 1 mm/s up to 80% of the original sample height. Hencky stress ( $\sigma_H$ ) and strain ( $\varepsilon_H$ ) were calculated from the force-deformation data according to the Equations 1 and 2 (Steffe, 1996), respectively

$$\sigma_H = F(t) \left[ \frac{H(t)}{H_0 A_0} \right] \quad (1)$$

$$\varepsilon_H = -\ln \left[ \frac{H(t)}{H_0} \right] \quad (2)$$

where  $F(t)$  is the force (N) at time  $t$ ,  $A_0$  ( $m^2$ ) and  $H_0$  (m) are the initial area and height of the sample, respectively, and  $H(t)$  is the height (m) at time  $t$ . The stress ( $\sigma_R$ ) and strain ( $\varepsilon_R$ ) at rupture were calculated considering the rupture point as the maximum point of the stress-strain curve. The stress-strain data before the rupture point was fitted to the Blatz, Sharda and Tschoegl (BST) equation (Blatz et al., 1974), which assumes a relationship between deformation energy and radial deformation under compression that deviates from the ideal Hookean behavior (Equations 3 and 4).

$$\sigma = \frac{2E_{BST}}{3\eta} (\lambda^\eta - \lambda^{-2\eta}) \quad (3)$$

$$\lambda = \frac{R_t}{R_0} \quad (4)$$

where  $\lambda$  is the radial deformation (dimensionless),  $R_0$  is the initial sample radius (m),  $R_t$  is the radial deformation (m) at t (s) and  $E_{BS7}$  is the elasticity modulus (Pa) predicted by the model. The parameter  $\eta$  (dimensionless) is an empirical measure of deviation from the ideal behavior where  $\eta = 2$  corresponds to an ideal rubber elasticity sample,  $\eta$  values higher than two characterize the so-called strain-hardening behavior and  $\eta$  values lower than two corresponding to strain-weakening samples. Five gels of each system were analyzed.

## ***2.6. Rheological measurements***

The thermal behaviour of the samples was evaluated by oscillatory shear measurements in a strain-controlled rheometer Physica MCR301 (Anton Paar, Austria) equipped with a stainless steel cone-plate geometry (50 mm, 2° angle, truncation 208µm). The samples were transferred onto the rheometer plate (which was preheated at 80°C) immediately after the heat treatment. A solvent trap accessory was coupled around the geometry in order to avoid sample evaporation. Cooling sweeps were carried out from 70°C to 5°C at 1 °C/min, setting 0.1 Hz frequency and 1% strain. The contribution of the elastic and viscous characteristics was evaluated from storage ( $G'$ ) and loss ( $G''$ ) moduli, respectively. Changes in the slope of complex viscosity vs. temperature curves were maximized from the derivation of the data using the Savitzky & Golay filter (Savitzky & Golay, 1964). The transition temperature or gel point was considered significant when the slope of  $\log(\eta^*)$  was higher than 0.1.

### **2.7. Scanning electron microscopy (SEM)**

Pieces of gel (approximately 10 mm x 2 mm x 2 mm) were fixed overnight in 2.5% glutaraldehyde in cacodylate buffer (0.1 M) at pH 7.2. After rinsing in cacodylate buffer (0.1 M), the samples were fractured in liquid nitrogen, followed by another rinse with cacodylate buffer. The fractured samples were post fixed overnight in 1% buffered osmium tetroxide and then dehydrated in a graded ethanolic series (30, 50, 70, 90 and 100% v/v). In order to avoid structural damage, the samples were dried at CO<sub>2</sub> critical point (Balzers Critical Point Dryer CPD03, Tokyo, Japan) and then mounted on aluminum stubs and coated with gold in a SCD 050-Balzer Sputter Coater (Tokyo, Japan). At least three images of typical structures were recorded at a magnification of 1000 $\times$  using JEOL JSM 5800 LV (Tokyo, Japan) microscope operating at 10 kV.

### **2.8. Statistical analysis**

The results were evaluated using the analysis of variance (ANOVA) with the software STATISTICA 5.5 (Statsoft Inc., Tulsa, USA, 2000) and the significant differences ( $p < 0.05$ ) between the mean values evaluated by the Tukey procedure.

## **3. RESULTS AND DISCUSSION**

### **3.1. Zeta potential**

Figure 1 shows that gellan gum was negatively charged in the entire range of pH studied, from pH 3.0 to 7.0. The value was nearly constant around -40 mV between pH 4.0 and 7.0, but at pH 3.5 the charge density showed a pronounced increase. This result is in

agreement with de Jong and van de Velde (2007) that showed that the pKa of this polysaccharide is around 3.5. At pH 3.0 the zeta potential value was close to -25 mV.

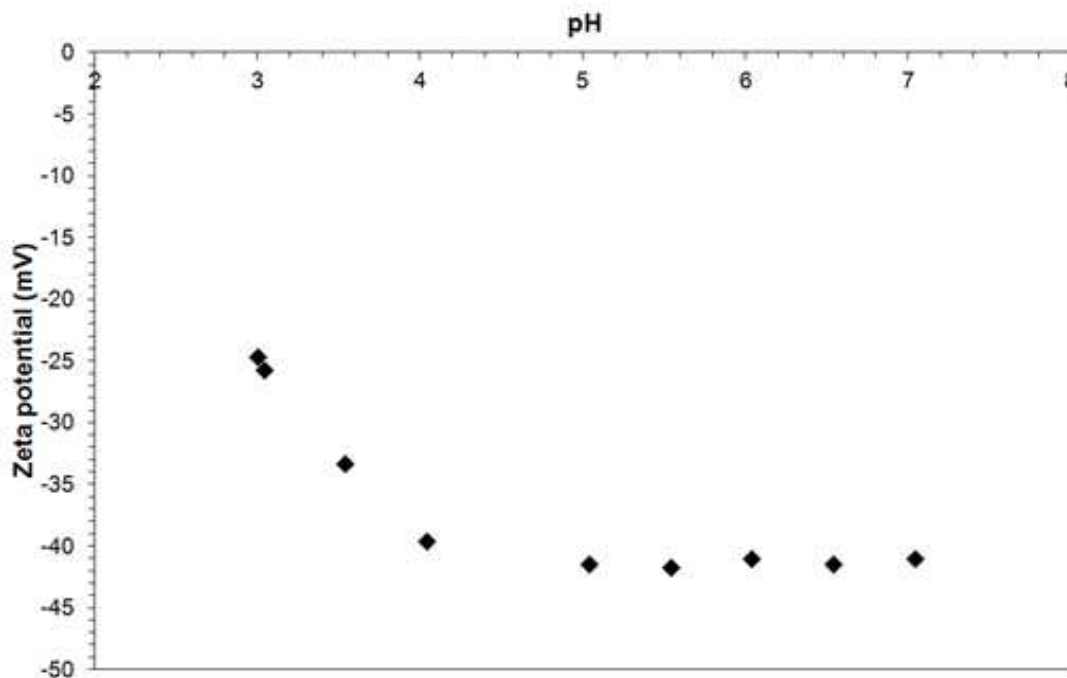


**Figure 1. Zeta potential profile of gellan gum at different pH values.**

### **3.2. Conductivity measurements**

The electrical conductivity of systems containing surfactant + water is showed in Figure 2. At lower water content the systems are formed by discrete reverse micelles that did not interact between themselves, not contributing to the electrical conductivity. Structural changes can occur and liquid crystalline systems may be formed with the surfactant concentration decrease, increasing the values of  $\kappa$  up to a maximum point. At lower surfactant content, conductivity values decrease, characterizing normal micellar systems (Mehta et al., 2007).

Despite the nonionic character of Tween80, the electrical conductivity results showed that acidification with acetate buffer at pH 3.0 affected the self-assembly of the

systems. The acid acetic pKa is around 4.8, which means that only a small fraction of this acid is ionized at pH 3.0. The neutral form of the acid may be dispersed into the surfactant phase, increasing the flexibility of the surfactant on the water interface and changing the ability of entrapping water to the structure (Cid-Samamed et al., 2008). Figure 2 shows that at pH 5.0 the maximum value of  $\kappa$  occurred around 30-40% (w/w) of Tween80, while at more acidic pH the inversion to “normal systems” (water as continuous medium) happened at 10-20% (w/w) of surfactant.

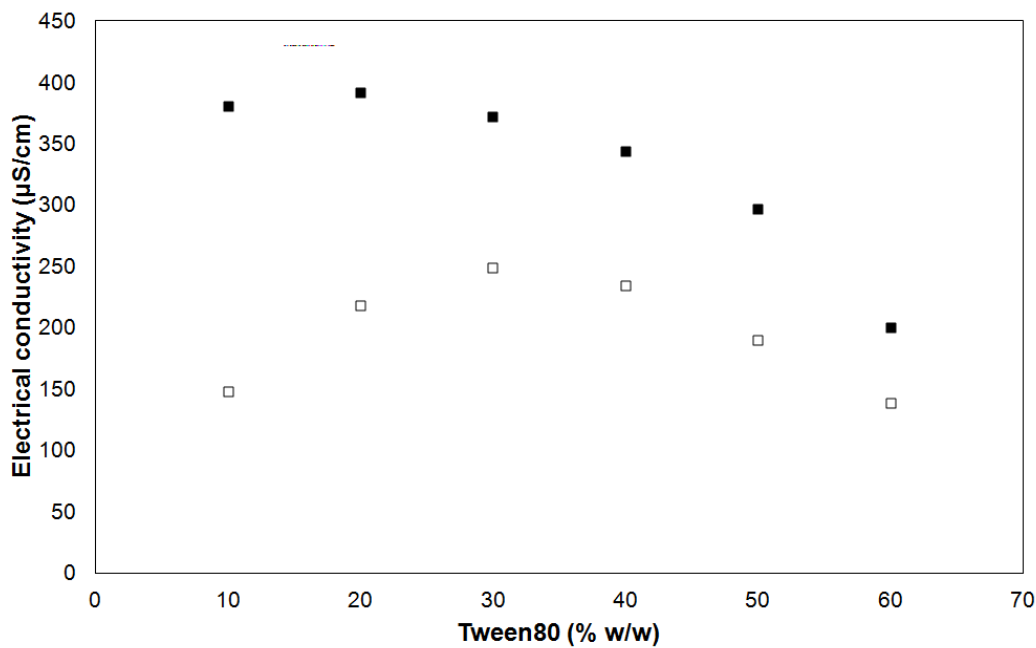


**Figure 2. Electrical conductivity ( $\kappa$ ) of Tween80/water systems at 80°C. (■) pH 3.0, and (□) pH 5.0.**

### **3.3. Scanning electron microscopy**

Micrographs of typical gellan gel structures (Figure 3A), showed a porous network as previously observed by other authors (de Jong & van de Velde, 2007; Picone & Cunha, 2011). The surfactant addition apparently did not change the gel network (Figure 3B). However at pH 3.0 the network presented a more compact structure with smaller pores

(Figure 3C). Systems with high Tween80 concentration (>20% w/w) could not be subjected to SEM, since the gel dissolved in the buffers during preparation of the samples.

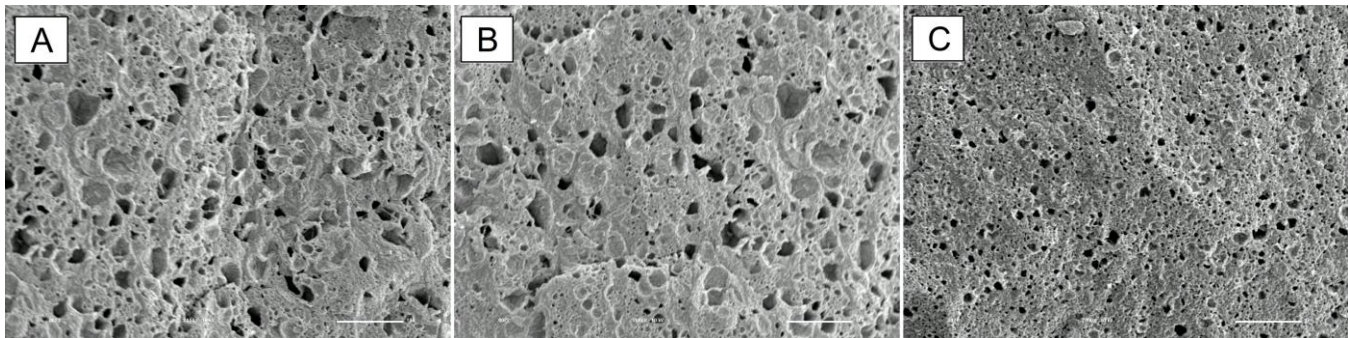


**Figure 3. SEM micrographs of 3.0% (w/w) gellan gum gels. (A) Natural pH (5.0) and no addition of Tween80; (B) Natural pH and 10% of Tween80 and (C) pH 3.0 and 10% of Tween80. Magnification 1,000 ×.**

#### **3.4. Oscillatory measurements**

The thermal rheological behavior of the systems during cooling is shown in Figure 4. Gelation of gellan solutions (3.0% w/w) at natural pH and in the absence of Tween80 (Figure 4A), shows that the system was predominantly viscous in the beginning of cooling, showing higher values of loss modulus ( $G''$ ) than storage modulus ( $G'$ ). However, the  $G'$  became higher than  $G''$  with temperature decrease, which is characteristic of gel formation. Table 1 shows the crossover temperature or gelling point for gellan gum at natural pH, which was around 56°C. However Miyoshi et al. (1996), reported a transition temperature around 40°C for 3.0% gellan gum solution. Such difference could be attributed to the different degree of acylation and mineral composition of the gellan gum used, which could change the ionic strength of the gum and consequently its conformational transition. On the other hand, crossover was not observed and  $G'$  was higher than  $G''$  within the

temperature range evaluated in more acidic condition (pH 3.0), showing that this systems presented an elastic character with gel behavior in all temperature range studied.

With the surfactant addition, two different transitions were observed, which could be related to gellan or polysorbate effect depending on the concentration of these components. At lower concentrations (10 – 30 % w/w) of Tween 80, the predominant behavior was attributed to the polysaccharide, with one or none gel point, depending on the pH. The storage and loss moduli became closer with the surfactant addition, but the difference between G' and G" was bigger for system at pH 3. The moduli values did not show strong differences at 10°C for all surfactant concentrations, but at 70 °C these values tended to decrease with Tween 80 concentration higher than 30% (w/w) (Figure 4D). At these surfactant concentration, the rheological profile of both pH studied did not show a significant change in the complex viscosity that could characterize a specific gel point (Table 1). At 30% (w/w) of surfactant a transitional behavior and a different slope could be observed between 53 and 56°C for both pH values (Figure 4D and Table 1). This slope (around 40-50 °C) could be attributed to the surfactant self-assembly (Picone & Cunha, 2013), which forms more complex structures at lower temperatures (Venugopal et al., 2011; Wadsten-Hindrichsen et al., 2007). The rheological behavior clearly changed at 50% (w/w) Tween 80 could be attributing to the polysorbate structuration (Figure 4F). Moreover, the pH did not exerted influence, since this surfactant used was nonionic. The rheograms showed a change in the slope close to 45°C at both pH conditions (Table 1) and such temperature decreased with higher surfactant concentration, as previously reported (Picone & Cunha, 2013). Moreover, at these concentrations the surfactant was able to form complex gel-like structures, but these they were weaker in comparison to those formed in systems with only gellan.

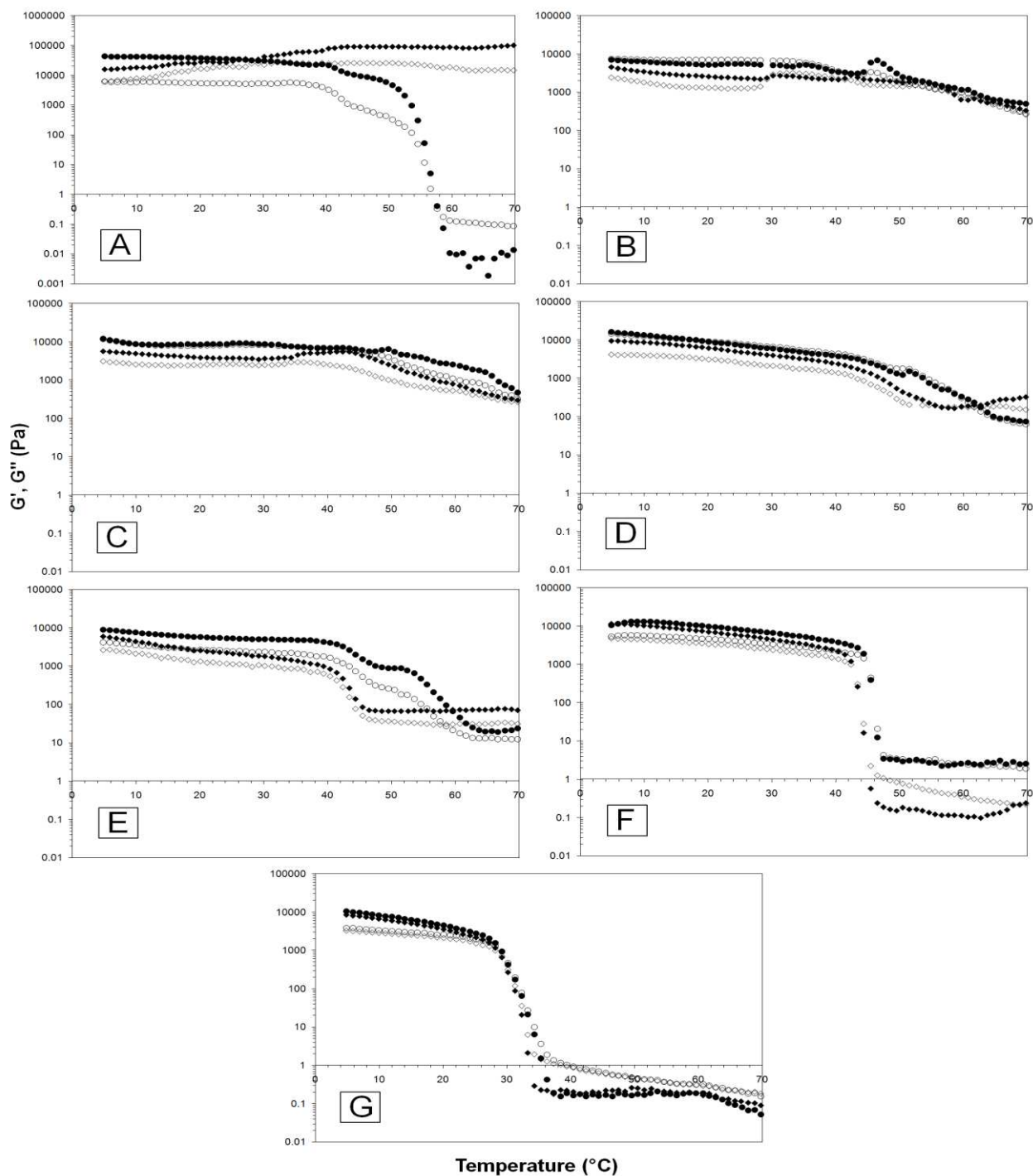


**Figure 4. Thermal scanning rheograms of gels with 3.0% (w/w) gellan gum at natural pH (5.0) and pH 3.0 containing different concentrations of Tween80. (A) 0%; (B) 10%; (C) 20%; (D), 30%; (E), 40%, (F) 50% and (G) 60%. ( $\blacklozenge, \diamond$ ) pH 3.0 and ( $\bullet, \circ$ ) natural. Full and empty symbols refers to  $G'$  and  $G''$ , respectively.**

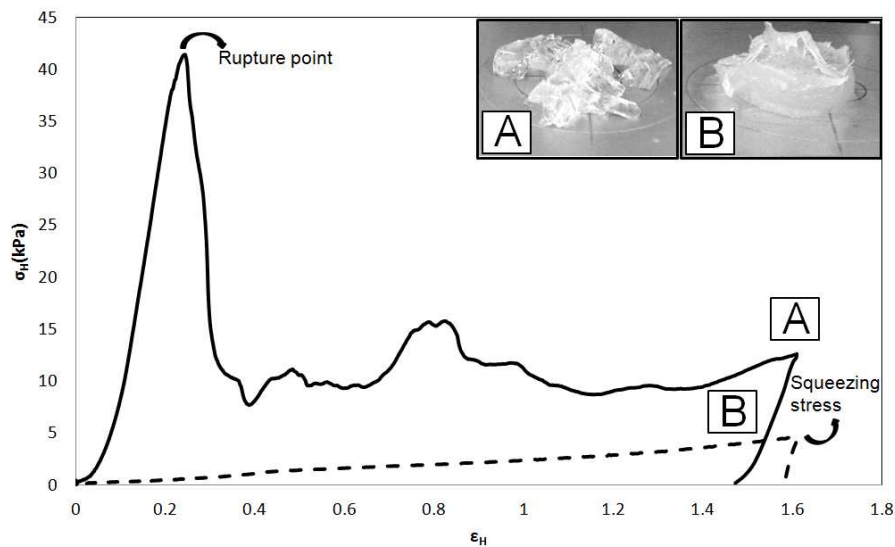
**Table 1.** Gel or transition temperatures for systems with 3.0% (w/w) gellan gum at natural pH (5.0) or pH 3.0 with different Tween80 concentration.

pH	Tween80 (%)	Transition temperatures (°C)	
		Surfactant structuration	Polysaccharide gelling
3.0	0	-	>70
	10	-	>70
	20	-	>70
	30	53 ± 2.3	>70
	40	47 ± 0.5	>70
	50	44 ± 0.7	-
	60	35 ± 2.1	-
	0	-	56 ± 2.5
5.0	10	-	64 ± 0.7
	20	-	66 ± 1.8
	30	57 ± 1.0	66 ± 0.2
	40	48 ± 1.1	59 ± 0.7
	50	47 ± 3.1	-
	60	36 ± 0.5	-

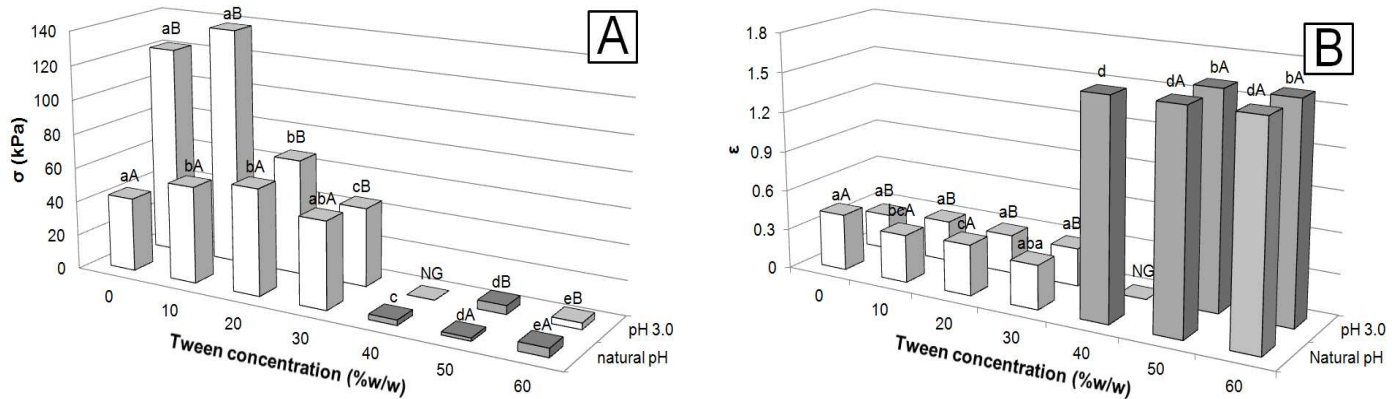
### **3.5. Mechanical properties**

Figure 5 shows typical stress-strain curves obtained from the uniaxial compression measurements. Overall, two different tendencies were observed. The curve (A) represents a hard gel that presented a clear rupture point. Curve (B) shows the behavior of a squeezing gel, which means that such gel did not show a rupture point but it flowed with the force application presenting a maximum or squeezing stress. It was observed that the surfactant exerted influence on the mechanical properties, which were dependent on its concentration and the system pH. From 40% (w/w) of Tween80 the gels were smashed,

showing no rupture point (Figure 6). Harder (maximum stress at rupture –  $\sigma_{\max}$ ) or less deformable (lower strain at rupture –  $\varepsilon_{\max}$ ) gels were obtained in absence or low concentration (<30% w/w) of Tween80 and at lower pH (Figure 6). On the other hand, the values of the maximum stress ( $\sigma_{\max}$ ) decreased with the surfactant concentration increase, followed by an increase in the deformability ( $\varepsilon_{\max}$ ) of the gels.



**Figure 5. Typical uniaxial compression curves for 3.0% (w/w) gellan gum gels. (A) Gel with rupture point and (B) squeezing gel.**



**Figure 6. Mechanical properties of gels of 3.0% (w/w) gellan gum at natural pH and pH 3.0 at different Tween80 concentrations. (A) Maximum stress ( $\sigma$ ) and (B) Strain ( $\epsilon$ ). White bars refer to gels with rupture point and gray bars to squeeze gels. Means with different letters show statistically significant differences ( $p<0.05$ ): Capital letters (between pH) and small letter (Tween 80 concentration). NG – non-self supporting gels.**

The linear region is limited to the range where the applied stress causes no damage to the gel structure and the strain is totally reversible. Such behavior can be evaluated from the elastic modulus ( $E_{BST}$ ). Moreover, the BST fitting ( $\eta$  values) can characterize the nonlinear region of the stress-strain curves besides the maximum stress and strain. The BST parameters (Table 2) showed that the formed gels behaved as strain-hardening ( $\eta>2$ ) or strain weakening ( $\eta<2$ ) depending on the Tween 80 concentration. Strain-hardening behavior was observed until 30% e 40% (w/w) surfactant content at pH 3.0 and 5.0, respectively. The addition of surfactant increased this parameter up to 20% (w/w) of surfactant, decreasing from 30%. Moreover, the system became softer with 50% (w/w) surfactant and a squeezing gel was formed with strain-weakening behavior. In relation to the elastic modulus ( $E_{BST}$ ) no tendency was clearly observed and other authors

observed that the BST model was not a good predictor of the elasticity modulus parameters for harder gels (Picone et al., 2011; Valim et al., 2009).

**Table 2. BST parameters of gels of 3.0% (w/w) gellan gum at natural pH and pH 3.0 with different Tween80 concentrations.**

pH	Tween80 (%)	BST parameters		
		$E_{\text{BST}}$ (kPa)	$\eta$	$R^2$
3.0	0	3.1 ± 0.32	12.2 ± 0.7	0.98
	10	1.2 ± 0.1	16.6 ± 0.6	0.97
	20	92.4 ± 23.2	39.2 ± 4.3	0.99
	30	33.3 ± 1.0	30.3 ± 3.8	0.99
	40	NG	NG	-
	50	6.8 ± 0.5	0.8 ± 0.01	0.90
	60	6.7 ± 0.34	1.4 ± 0.1	0.91
	0	85.1 ± 3.6	18.9 ± 0.4	0.90
5.0	10	139 ± 38.4	20.1 ± 1.7	0.91
	20	63.2 ± 6.2	32.4 ± 4.8	0.99
	30	44.2 ± 7.3	31.8 ± 1.7	0.99
	40	11.2 ± 1.5	8.1 ± 0.6	0.99
	50	2.7 ± 0.06	1.2 ± 0.03	0.92
	60	4.2 ± 0.41	0.8 ± 0.02	0.96

\*NG – non-self supporting gels

#### 4. DISCUSSION

The gelation mechanism of gellan gum is related to its conformational coil-helix transition. At high temperatures this polysaccharide is in coil conformation, and with cooling the transition occurs followed by the association between the helices, resulting in

the network formation (Milas & Rinaudo, 1996). Coil-helix transition is independent of the solution pH, but the helix-coil transition was observed only at 5.0 (Figure 4A), as previously reported (Picone & Cunha, 2011). This behavior could be related to the lower electrostatic repulsion at acid pH (Figure 1) that could improve the aggregation of the biopolymer (Yamamoto & Cunha, 2007) with a strong network formation even at high temperatures. Such network can be observed in the micrographs (Figure 3) with more compact structure with smaller porous and its strength could be evaluated from the mechanical properties. The denser network was able to distribute more homogeneously the force applied, showing gels with higher stress at rupture or hardness. In addition, gels at low pH presented low deformability (Figure 6) and a strain-hardening behavior ( $\eta>2$ ) (Table 2). However, with polysorbate addition the gelation behavior changed and the interaction surfactant-polysaccharide was dependent on the pH and Tween80 concentration, resulting in different physical gel properties.

At lower surfactant concentration (10% w/w) the SEM results (Figure 3) showed that Tween 80 addition did not change visually the gel microstructure, which means that its properties were more dependent on gellan-gellan interactions. However, the rheological behavior was quite similar at both pH, which means that the surfactant presence strongly modified the gelation properties at gellan natural pH, led to a behavior similar to the obtained at pH 3.0 (Figure 4B and Table 1). The surfactant concentration used in these systems was much greater than the critical micelle concentration (CMC). Therefore, the surfactant moieties could be aggregated in the micellar form, which could occupy the pores formed by the gellan gum network. According to the electrical conductivity measurements (Figure 2), at this concentration, the surfactant was self-assembled in “normal structures” with the hydrophobic tails in the core of the structure and the

hydrophilic head driven to the water medium. Since the deacylated gellan gum was used, few hydrophobic groups remained linked to its hydrophilic backbone. However, these groups could have linked to the hydrophobic tails of the polysorbate creating a crosslink effect. This arrangement was previously reported as necklace with surfactant pearls (Grant et al., 2006; Tsianou & Alexandridis, 2004). However, such arrangement changed the rheological behavior of gellan pure systems (Figure 4) preventing the strong aggregation of the polysaccharide macromolecule that showed a decrease in the storage modulus ( $G'$ ) at low temperatures for both pH. Moreover, the decrease in the water content led to a more concentrated gellan solution. The network formed by this concentrated solution offered more resistance to the normal forces applied, which could explain the increase in the stress at rupture (Figure 6). Such arrangement (necklace with surfactant pearls), was also observed with addition of 20% (w/w) Tween 80 and natural pH, but at more acidic pH softer gels with lower stress at rupture were produced. Electrical conductivity measurements (Figure 2) indicated that at pH 3.0 the surfactant could be more organized or starting to form reverse structures. The surfactant molecules present high mobility and its self-assembly in structured systems is more dynamic occurring in different time scale (1μs) compared to the kinetics of polymerization or gelling process (1ms) (Magno et al., 2009). Thus, this surfactant self-assembly in reverse structures could have caused a steric effect, preventing the polysaccharide aggregation and consequently hindering the formation of harder gels like the obtained with lower surfactant concentrations.

At 30% (w/w) Tween 80 concentration systems at both pH reached the maximal electrical conductivity values (Figure 2) and the mechanical properties between gels at natural and more acidic pH were similar. Two slopes were observed in the thermal rheological behavior (Figure 4C and Table 1), one associated to gellan gelation and the

other could be related to the surfactant structuration. Depending on the concentration of the surfactant and its physical characteristics, the molecular self-assembly can occur, assuming a large variety of morphologies denominated as liquid crystalline phase (Binks et al., 2010). The liquid crystalline systems present high viscosity or even gel-like structures depending on the moieties organization (Lawrence, 1994; Rehage, 2005).

Above this concentration, the surfactant properties were predominant at both pH, but with some influence of gellan network. At 40% (w/w) Tween 80 two distinct behaviors were observed during gel formation. At natural pH the interaction mechanism was the same as observed at 30% (w/w) surfactant. The surfactant was still not able to form gel-like structure; however there were some linkages between gellan gum macromolecules, conferring the strain-hardening behavior ( $\eta>2$ ) (Table 2) even for the squeezing gel formed at pH 5.0. On the other hand, at pH 3.0 non-self-supporting gel was obtained. The reverse surfactant structure and the higher aggregation degree of the gellan gum at this pH prevented the formation of a network, leading to separated aggregates, which resulted in a granulated (particulate) appearance. At 50% and 60% (w/w) Tween 80, only the slope related to the surfactant structuration was observed in the rheological curves (Figure 4F-G). Such Tween 80 temperature dependence structuration was previously reported (Picone & Cunha, 2013), showing that between 50-70% (w/w) this surfactant presented a gel-point. In that study, the crossover temperature decreased from 45°C to 37°C with surfactant concentration increase from 50 to 60% (w/w). Such result was closer to the observed in the present study in the presence of gellan (Table 1) for both pH. Moreover, the high surfactant concentration prevented the interactions between gellan gum molecules (Holmberg et al., 2002; Tsianou & Alexandridis, 2004) and decreased the storage moduli. At last, the surfactant based gels with predominance of surfactant

properties did not present rupture point (Figure 6), showing a strain-weakening behavior (Table 2).

## 5. CONCLUSION

The conformational arrangement of gellan gum and the self-assembly of polysorbate 80 led to gelled structures with different behaviors, which were dependent on the surfactant concentration and pH. The high concentration of gellan gum formed gels dependent on the pH. At natural pH the gel point temperature of pure gellan gels was high, while at acidic pH the system showed harder gels with elastic behavior independent of the temperature. The gellan gum properties prevailed in systems with up to 20% of surfactant. However, at this concentration, the surfactant micelles prevented the gellan-gellan interactions changing the sample rheological behavior. With surfactant increase transition systems were observed with two temperature transitions that could be related to the polysaccharide gelation and surfactant structuration. At higher Tween80 concentrations (50-60% w/w) the surfactant self-assembled in gel-like liquid crystalline structures with prevailing behavior of the polysorbate80. Thus, depending on the conditions of the systems, the physical properties of the gelled systems could present predominant behavior related to gellan or surfactant. Moreover, gellan-polysorbate 80 interactions could produce harder or softer gels with different technological characteristics. These differences could allow the application of these gels in products with different aims, as texture modifiers or vehicle for bioactives in food, pharmaceutical or cosmetic industries.

## 6. ACKNOWLEDGEMENTS

The authors would like to thank Fapesp (EMU 09/54137-1), CNPq (Universal 479459/2012-6) and Capes for their financial support.

## 7. REFERENCES

- Barreiro-Iglesias, R., Alvarez-Lorenzo, C., & Concheiro, A. (2003). Poly(acrylic acid) microgels (carbopol (R) 934)/surfactant interactions in aqueous media Part I: Nonionic surfactants. *International Journal of Pharmaceutics*, 258 (1-2), 165-177.
- Binks, B. P., Fletcher, P. D. I., & Tian, L. (2010). Influence of nanoparticle addition to Winsor surfactant microemulsion systems. *Colloids and Surfaces a-Physicochemical and Engineering Aspects*, 363 (1-3), 8-15.
- Blatz, P. J., Sharda, S. C., & Tschoegl, N. W. (1974). Strain Energy Function for Rubber-Like Materials Based on a Generalized Measure of Strain. *Transactions of the Society of Rheology*, 18 (1), 145-161.
- Cid-Samamed, A., Garcia-Rio, L., Fernandez-Gandara, D., Mejuto, J. C., Morales, J., & Perez-Lorenzo, M. (2008). Influence of n-alkyl acids on the percolative phenomena in AOT-based microemulsions. *Journal of Colloid and Interface Science*, 318 (2), 525-529.
- de Jong, S., & van de Velde, F. (2007). Charge density of polysaccharide controls microstructure and large deformation properties of mixed gels. *Food Hydrocolloids*, 21 (7), 1172-1187.
- Evmenenko, G., Theunissen, E., & Reynaers, H. (2000). Structural investigations of carrageenan-surfactant systems by synchrotron X-ray scattering. *Journal of Polymer Science Part B-Polymer Physics*, 38 (21), 2851-2859.
- Fan, Y. X., Liu, Y., Xi, J. G., & Guo, R. (2011). Vesicle formation with amphiphilic chitosan derivatives and a conventional cationic surfactant in mixed systems. *Journal of Colloid and Interface Science*, 360 (1), 148-153.

Goddard, E. D. (2002). Polymer/surfactant interaction: Interfacial aspects. *Journal of Colloid and Interface Science*, 256 (1), 228-235.

Grant, J., Cho, J., & Allen, C. (2006). Self-assembly and physicochemical and rheological properties of a polysaccharide-surfactant system formed from the cationic biopolymer chitosan and nonionic sorbitan esters. *Langmuir*, 22 (9), 4327-4335.

Guo, P., & Guo, R. (2010). Ionic Liquid Induced Transition from Wormlike to Rod or Spherical Micelles in Mixed Nonionic Surfactant Systems. *Journal of Chemical and Engineering Data*, 55 (9), 3590-3597.

Holmberg, K., Jönsson, B., Kronberg, B., & Lindman, B. (2002). *Surfactants and Polymers in Aqueous Solution*. Chichester: John Wiley & Sons.

Jiao, J. (2008). Polyoxyethylated nonionic surfactants and their applications in topical ocular drug delivery. *Advanced Drug Delivery Reviews*, 60 (15), 1663-1673.

Kerwin, B. A. (2008). Polysorbates 20 and 80 used in the formulation of protein biotherapeutics: Structure and degradation pathways. *Journal of Pharmaceutical Sciences*, 97 (8), 2924-2935.

Lawrence, M. J. (1994). Surfactant Systems - Their Use in Drug-Delivery. *Chemical Society Reviews*, 23 (6), 417-424.

Magno, M., Tessendorf, R., Medronho, B., Miguel, M. G., & Stubenrauch, C. (2009). Gelled polymerizable microemulsions. Part 3 Rheology. *Soft Matter*, 5 (23), 4763-4772.

Mehta, S. K., Kaur, G., & Bhasin, K. K. (2007). Analysis of Tween based microemulsion in the presence of TB drug rifampicin. *Colloids and Surfaces B-Biointerfaces*, 60 (1), 95-104.

Milas, M., & Rinaudo, M. (1996). The gellan sol-gel transition. *Carbohydrate Polymers*, 30 (2-3), 177-184.

Miyoshi, E., Takaya, T., & Nishinari, K. (1996). Rheological and thermal studies of gel-sol transition in gellan gum aqueous solutions. *Carbohydrate Polymers*, 30 (2-3), 109-119.

- Moritaka, H., Nishinari, K., Taki, M., & Fukuba, H. (1995). Effects of Ph, Potassium-Chloride, and Sodium-Chloride on the Thermal and Rheological Properties of Gellan Gum Gels. *Journal of Agricultural and Food Chemistry*, 43 (6), 1685-1689.
- Pepic, I., Filipovic-Grcic, J., & Jalsenjak, I. (2009). Bulk properties of nonionic surfactant and chitosan mixtures. *Colloids and Surfaces a-Physicochemical and Engineering Aspects*, 336 (1-3), 135-141.
- Petersen, S., & Ulrich, J. (2011). Effectiveness of Polyoxyethylene Nonionic Emulsifiers in Emulsification Processes Using Disc Systems. *Chemical Engineering & Technology*, 34 (11), 1869-1875.
- Picone, C. S. F., & Cunha, R. L. (2011). Influence of pH on formation and properties of gellan gels. *Carbohydrate Polymers*, 84 (1), 662-668.
- Picone, C. S. F., & Cunha, R. L. (2013). Formation of nano and microstructures by polysorbate–chitosan association. *Colloids and Surfaces A: Physicochemical and Engineering Aspects*, 418 (0), 29-38.
- Picone, C. S. F., Maximo, G. J., Kuhn, K. R., Ros-Polski, V., & Cunha, R. L. (2011). An assessment of the texture of acidified sodium caseinate gels with added inulin using response surface methodology. *International Journal of Dairy Technology*, 64 (3), 353-359.
- Qian, C., Decker, E. A., Xiao, H., & McClements, D. J. (2012). Nanoemulsion delivery systems: Influence of carrier oil on beta-carotene bioaccessibility. *Food Chemistry*, 135 (3), 1440-1447.
- Rees, G. D., & Robinson, B. H. (1993). Microemulsions and Organogels - Properties and Novel Applications. *Advanced Materials*, 5 (9), 608-619.
- Rehage, H. (2005). Rheological Properties of Viscoelastic Surfactant Solutions. In R. Zana (Ed.), *Dynamics of Surfactant Self-Assemblies: Micelles, Microemulsions, Vesicles and Lyotropic Phases* (pp. 419-473): CRC Press.
- Savitzky, A., & Golay, M. J. E. (1964). Smoothing + Differentiation of Data by Simplified Least Squares Procedures. *Analytical Chemistry*, 36 (8), 1627-&.
- Steffe, J. F. (1996). *Rheological Methods in Food Process Engineering*: Freeman Press.

Testard, F., & Zemb, T. (2002). Understanding solubilisation using principles of surfactant self-assembly as geometrical constraints. *Comptes Rendus Geoscience*, 334 (9), 649-663.

Tomasic, V., Tomasic, A., Smit, I., & Filipovic-Vincekovic, N. (2005). Interactions in mixed cationic surfactants and dextran sulfate aqueous solutions. *Journal of Colloid and Interface Science*, 285 (1), 342-350.

Trickett, K., & Eastoe, J. (2008). Surfactant-based gels. *Advances in Colloid and Interface Science*, 144 (1-2), 66-74.

Tsianou, M., & Alexandridis, P. (2004). Surfactant–Polymer Interactions. In M. Abe & J. F. Scamehorn (Eds.), *Mixed Surfactant Systems* (2nd ed.). New York: Marcel Dekker.

Valim, M. D., Cavallieri, A. L. F., & Cunha, R. L. (2009). Whey Protein/Arabic Gum Gels Formed by Chemical or Physical Gelation Process. *Food Biophysics*, 4 (1), 23-31.

Venugopal, E., Bhat, S. K., Vallooran, J. J., & Mezzenga, R. (2011). Phase Behavior of Lipid-Based Lyotropic Liquid Crystals in Presence of Colloidal Nanoparticles. *Langmuir*, 27 (16), 9792-9800.

Wadsten-Hindrichsen, P., Bender, J., Unga, J., & Engstrom, S. (2007). Aqueous self-assembly of phytantriol in ternary systems: Effect of monoolein, distearoylphosphatidylglycerol and three water-miscible solvents. *Journal of Colloid and Interface Science*, 315 (2), 701-713.

Yaghmur, A., Aserin, A., & Garti, N. (2002). Phase behavior of microemulsions based on food-grade nonionic surfactants: effect of polyols and short-chains alcohols. *Colloids and Surfaces a-Physicochemical and Engineering Aspects*, 209 (1), 71-81.

Yamamoto, F., & Cunha, R. L. (2007). Acid gelation of gellan: Effect of final pH and heat treatment conditions. *Carbohydrate Polymers*, 68 (3), 517-527.

Yin, W. C., Zhang, H. B., Huang, L., & Nishinari, K. (2008). Effects of SDS on the sol-gel transition of konjac glucomannan in SDS aqueous solutions. *Colloid and Polymer Science*, 286 (6-7), 663-672.



**– CAPÍTULO 6 –**

***Microemulsion-based gels***



**MICROEMULSION-BASED GELS USING GELLAN AS GELLING AGENT**

FASOLIN, L.H., PICONE, C.S.F., SANTANA, R.C., CUNHA, R.L.\*

***To be submitted to Food Hydrocolloids***

Department of Food Engineering, Faculty of Food Engineering, University of Campinas – UNICAMP, CEP: 13083-862, Campinas, SP, Brazil

\*Corresponding author. TEL: +551935214047; FAX: +551935214027; EMAIL: rosiane@fea.unicamp.br

**ABSTRACT**

Gelation of microemulsions could be useful in developing different types of textures/structures microgels or bulky gels. The use of gellan gum as gelator in systems formed by water+Tween80+High oleic sunflower oil (HOSO) was studied. In addition, the use of acetic acid as cosurfactant in these systems was also investigated. Microstructure, mechanical and rheological properties of these systems with varied composition were evaluated. Gel properties without cosurfactant showed dependence on the aqueous phase/surfactant concentration ratio. Systems with high water concentration showed dense gellan gum network with elastic behavior independent on the temperature. Besides the gellan aggregation, in these systems surfactant micelles could promote the linkage between the macromolecules through the few hydrophobic sites of the biopolymer and consequently increase the gel strength. On the other hand, at gellan/surfactant ratio lower than 2.3 the polysorbate association predominated, with formation of softer gel-like structures. The use of cosurfactant promoted the formation of microgels instead of bulky

gels. Self-supporting gels were formed only at high water content, since the concentration of microparticles was not sufficient to produce a compact particulate gel. Moreover, the use of acetic acid destabilized the liquid crystal in simpler structures and gel-like structures were not formed. Thus, depending on the systems composition microgels or bulky gels could be formed with different technological properties, allowing their use in different industries and products.

*Keywords: polysorbate, biopolymer, cosurfactant, mechanical properties, rheology, gellan gum*

## **1. INTRODUCTION**

Recently, a great variety of gelled systems have been developed according to cosmetic, pharmaceutical and food industries demand, in special intelligent (stimuli-responsive) hydrogels and organogels (Hou, et al., 2012; Kawano, Kobayashi, Taguchi, Kunitake, & Nishimi, 2010; Lu, Shao, Zhang, Wang, & Wang, 2012; Minkenberg, et al., 2012), since they show potential application in topological formulations, bioactives delivery and texture modification. Gelation of microemulsion systems could be useful in developing these different types of gels. Such process was firstly reported using gelatin (Haering & Luisi, 1986). Depending on the gelled phase these systems are classified as microemulsion-based hydrogels (MBH) or microemulsion-based gels (MBG) for organogels. Microemulsions are spontaneously formed and they are macroscopically homogeneous due to the droplets size, which are in colloidal domain. Therefore, microemulsions are isotropic, transparent and thermodynamically stable mixtures usually composed by oil, water and surfactant (Hoar & Schulman, 1943; Yaghmur, et al., 2006).

These systems are typically associated with a cosurfactant in order to make the interface more flexible, contributing to the formation of microemulsions (Lv, Zheng, & Tung, 2005). The characteristics of microemulsions have attracted considerable attention, mainly because of their ability to solubilize large amount of lipophilic or hydrophilic additives, enhancing reactions efficiency and allowing chemical reactions as preparation of inorganic particles or enzymes immobilization (de Campo, et al., 2004; Sjoblom, Lindberg, & Friberg, 1996). In addition, the gelation of the microemulsion could improve the protection and delivery properties as well as favor the use of these systems as textures modifiers (Chen, et al., 2007; Kantaria, Rees, & Lawrence, 1999; Zhu, et al., 2009). These microemulsion-based gels (MGH and MBG) have been widely studied in the last decade and most studies used gelatin as gelling agent (Kantaria, et al., 1999; Lopez, et al., 2004; Zhao, Cao, Zheng, & Zhang, 2006), but other biopolymers have been reported as alginate, xanthan gum, gellan gum and carrageenan in the production of bulky and microspheres of MBG and MBH (Josef, Zilberman, & Bianco-Peled, 2010; Koop, et al., 2012; Spiclin, Homar, Zupancic-Valant, & Gasperlin, 2003; Valenta & Schultz, 2004; Wang, Gong, Lin, Shen, & Wang, 2008).

Gellan gum is a linear extracellular polysaccharide produced by the bacterium *Sphingomonas elodea*. This polysaccharide is composed of repeating tetrasaccharide (1,3- $\beta$ -D-glucose, 1,4- $\beta$ -D-glucuronic acid, 1,4- $\beta$ -D-glucose, 1,4- $\alpha$ -L-rhamnose) units containing one carboxyl side group. Gellan gum forms firm, hard and brittle gels, but these properties are dependent on the ionic strength, presence and type of cations, pH, temperature and polymer concentration (Moritaka, Nishinari, Taki, & Fukuba, 1995; Picone & Cunha, 2011; Yamamoto & Cunha, 2007). The gelation mechanism of this gum is a two-step process involving the formation of double helices during cooling of the

random coil chains. After this coil–helix transition, the gellan double helix can aggregate to form junction zones. Hydrogen bonds between the junction zones are induced by lowering pH or adding salts, resulting in macroscopic gel formation (Yamamoto, et al., 2007). The use of gellan as gelling agent in microemulsions was scarcely investigated and it was reported only microspheres formation (Gan, Gan, Zhu, Zhang, & Zhu, 2009; Wang, et al., 2008). Thus, the aim of this work was to evaluate the effect of the microemulsion composition and presence of cosurfactant in the microstructure, rheological and mechanical properties of microemulsion-based gels of gellan.

## **2. MATERIAL AND METHODS**

### ***2.1. Material***

High oleic sunflower oil (HOSO) was kindly donated by Cargill (Mairinque, Brazil) and deacylated gellan gum powder (Kelcogel® F) by Kelco Biopolymers (San Diego, CA). The surfactant polyoxyethylene sorbitan monooleate (Tween 80) was purchased from Sigma-Aldrich Co. (EUA). The cosurfactant acetic acid 99 % (Synth, Brazil) and other reagents were of analytical grade.

### ***2.2. Gel preparation***

The systems chosen for gellan gum addition were derived from the phase diagram previously obtained (Chapter 4). Besides the formulations using cosurfactant, systems with absence of this component were also studied (Figure 1B). An initial mixture of surfactant and HOSO with or without cosurfactant (1:2 HOSO:acetic acid) was prepared under magnetic stirring. Then, deionized water was titrated to the initial mixture under constant

stirring up to the desired concentration. The systems were heated at 80°C in a jacketed vessel and 3.0% (w/w) of gellan powder was added. The solution was maintained at 80°C during 30 min under constant stirring to solubilize the gum.

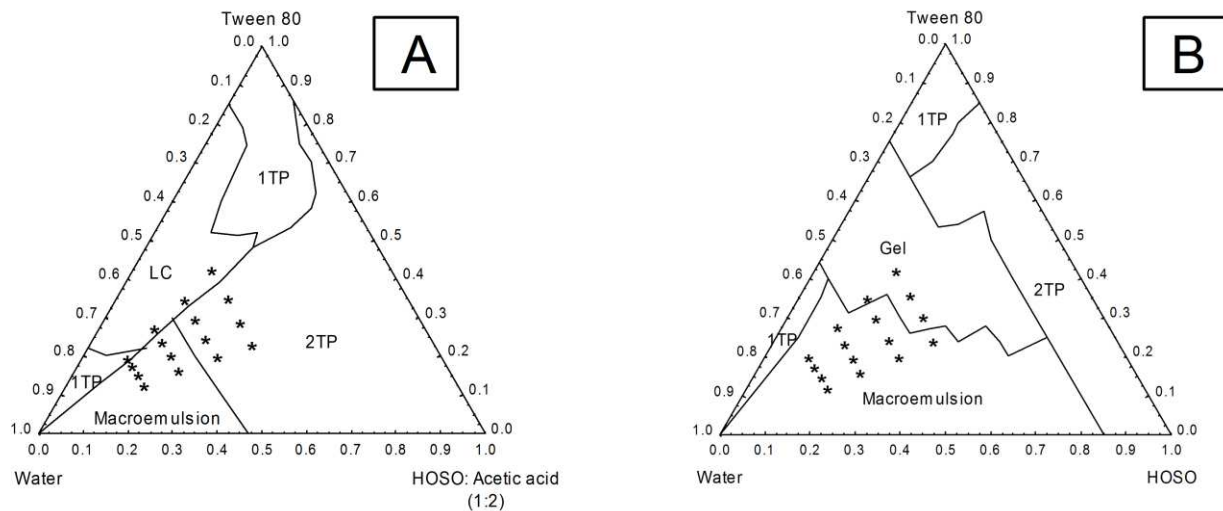


**Figure 1. Phase diagrams composed by water + Tween80 + HOSO. (A) With acid acetic addition and (B) without acid acetid. \*Formulations with gellan addition. 1TP = one transparent phase, 2TP = two transparent phase and LC = liquid crystalline phase.**

The composition of the systems is showed in Table 1. Each system was named according to its formulation: firstly, in accordance to the initial surfactant concentration and then, to the water content. For example, a system on the line 6 (initial surfactant concentration 60% w/w), diluted with 40% (w/w) water was denominated as 6040. For the rheological measurements, the solutions were analyzed just after the preparation at 80°C. For the analyses of the mechanical properties and microstructure, the systems were poured into cylindrical plastic tubes (21 mm inner diameter x 21 mm height) and Petri dishes, respectively, which were cooled to 10°C. The gels were maintained at 10°C for 48 h in order to assure complete gel formation.

**Table 1. Composition of the systems.**

System	Without cosurfactant			With cosurfactant			
	Water (%w/w)	HOSO (%w/w)	Tween80 (% w/w)	Water (%w/w)	HOSO (% w/w)	Acetic acid (% w/w)	Tween80 (% w/w)
4040	40	36	24	40	12	24	24
5040	40	30	30	40	10	20	30
6040	40	24	36	40	8	16	36
7040	40	18	42	40	6	12	42
4050	50	30	20	50	10	20	20
5050	50	25	25	50	8.3	16.7	25
6050	50	20	30	50	6.7	13.3	30
7050	50	15	35	50	5	10	35
4060	60	24	16	60	8	16	16
5060	60	20	20	60	6.7	13.3	20
6060	60	16	24	60	5.3	10.7	24
7060	60	12	28	60	4	8	28
4070	70	18	12	70	6	12	12
5070	70	15	15	70	5	10	15
6070	70	12	18	70	4	8	18
7070	70	9	21	70	3	6	21

### **2.3. Mechanical properties**

Mechanical properties were measured by uniaxial compression measurements using a TA-XT Plus Texture Analyzer (Stable Micro Systems, Godalming, UK) with a cylindrical acrylic plate (60 mm diameter) lubricated with silicon oil to minimize friction between the sample and the probe. Compression was carried out at sample temperature (10 °C) with a crosshead speed of 1 mm/s up to 80% of the original sample height. Hencky stress ( $\sigma_H$ ) and strain ( $\epsilon_H$ ) were calculated from the force-deformation data according to the equations 1 and 2 (Steffe, 1996), respectively

$$\sigma_H = F(t) \left[ \frac{H(t)}{H_0 A_0} \right] \quad (1)$$

$$\varepsilon_H = -\ln \left[ \frac{H(t)}{H_0} \right] \quad (2)$$

where  $F(t)$  is the force (N) at time t,  $A_0$  ( $\text{m}^2$ ) and  $H_0$  (m) are the initial area and height of the sample, respectively, and  $H(t)$  is the height (m) at time t.

The maximum stress ( $\sigma_{max}$ ) and strain ( $\varepsilon_{max}$ ) values were obtained from the maximum point of the stress-strain curve. Five gels of each system were analyzed.

#### **2.4. Rheological measurements**

The thermal stability of the samples was evaluated by oscillatory shear measurements in a strain-controlled rheometer Physica MCR301 (Anton Paar, Austria) equipped with a stainless steel cone-plate geometry (50 mm, 2° angle, truncation 208 $\mu\text{m}$ ). Immediately after the heat treatment the samples were transferred onto the rheometer plate, which was preheated at 80°C. To avoid sample evaporation, a solvent trap accessory was used around the geometry. A cooling sweep was carried out between 80°C and 5°C at 1 °C/min, 0.1 Hz and 1% strain. The contribution of the storage ( $G'$ ) and loss ( $G''$ ) moduli were evaluated and changes in the slope of complex viscosity vs. temperature curves were maximized from the derivation of the data using the Savitzky & Golay filter (Savitzky & Golay, 1964). The transition temperature or gel point was considered significant when the slope of  $\log(\eta^*)$  was higher than 0.1.

### **2.5. Scanning electron microscopy (SEM)**

Pieces of gel (approximately 10 mm x 2 mm x 2 mm) were fixed overnight in 2.5% glutaraldehyde in cacodylate buffer (0.1 M) at pH 7.2. After rinsing in cacodylate buffer (0.1 M), the samples were fractured in liquid nitrogen, followed by another rinse with cacodylate buffer. The fractured samples were post fixed overnight in 1% buffered osmium tetroxide and then dehydrated in a graded ethanolic series (30, 50, 70, 90 and 100% v/v). In order to avoid structural damage, the samples were dried at CO<sub>2</sub> critical point (Balzers Critical Point Dryer CPD03, Tokyo, Japan) and then mounted on aluminum stubs and coated with gold in a SCD 050-Balzer Sputter Coater (Tokyo, Japan). At least three images of typical structures were recorded at a magnification of 1,000× using JEOL JSM 5800 LV (Tokyo, Japan) microscope operating at 10 kV.

### **2.6. Statistical analysis**

The results were evaluated using the analysis of variance (ANOVA) with the software STATISTICA 5.5 (Statsoft Inc., Tulsa, USA, 2000) and the significant differences ( $p < 0.05$ ) between the mean values evaluated by the Tukey procedure.

## **3. RESULTS AND DISCUSSION**

### **3.1. Microemulsion-based gels**

MBG and MBH were produced based on the pseudo-ternary phase diagrams without cosurfactant addition (Figure 1B). Before the gellan addition, all the systems were macroemulsions, gel-like structures or presented phase separation (at 25°C), but with the temperature increase, single-phase or systems with simpler structures were formed

(Venugopal, Bhat, Vallooran, & Mezzenga, 2011; Wadsten-Hindrichsen, Bender, Unga, & Engstrom, 2007). After gum addition, a macroscopically uniform gel was formed with no phase separation during cooling process. Gellan aqueous solutions shows a system predominantly viscous at temperature higher than sol-gel transition with higher values of  $G''$  than  $G'$  (Moritaka, et al., 1995; Picone, et al., 2011) . Such gel point temperature at natural pH of gellan aqueous solution is dependent on the gum concentration (Miyoshi, Takaya, & Nishinari, 1996). At 3.0% (w/w) polysaccharide, the gel point temperature was 56 °C (Chapter 5). However, it should be observed that the biopolymer concentration is relative to the total volume of solution, which means that, in relation to the aqueous phase, its concentration was higher, ranging from 4.3 up to 7.5% (w/w).

The thermal scanning rheology showed different behavior depending on the systems composition (Figure 2). The interaction between gellan gum and Tween80 was mostly physical and depended on the ratio of these components (Chapter 5). Aqueous phase/surfactant ratio lower than 2.3 showed a prevailing surfactant influence on the rheological behavior of these systems (Chapter 5). At lower water content (40% w/w) (Figure 2A) all systems were below this aqueous phase/surfactant ratio value and the rheological curves showed a great difference between  $G'-G''$  values at the highest and lowest temperature as well as a defined crossover temperature (Table 2). Similar behavior was obtained for systems containing Tween80 and water with (Chapter 5) or without gellan gum (Picone & Cunha, 2013), showing that such behavior was predominantly related to the Tween80 self-assembly. Depending on the concentration of the surfactant and its physical characteristics, the molecular self-assembly can occur assuming a large variety of morphologies denominated as liquid crystalline phase, including lamellar, hexagonal and cubic structures (Binks, Fletcher, & Tian, 2010; Lawrence, 1994; Rehage, 2005). However,

with the increase of aqueous phase/surfactant ratio, the G'/G" plateau became closer (Figure 2 B-D), showing the influence of gellan gum on systems structuration and network formation. In addition, these systems showed storage moduli (G') at lower temperature higher than systems in absence of oil (Chapter 5).

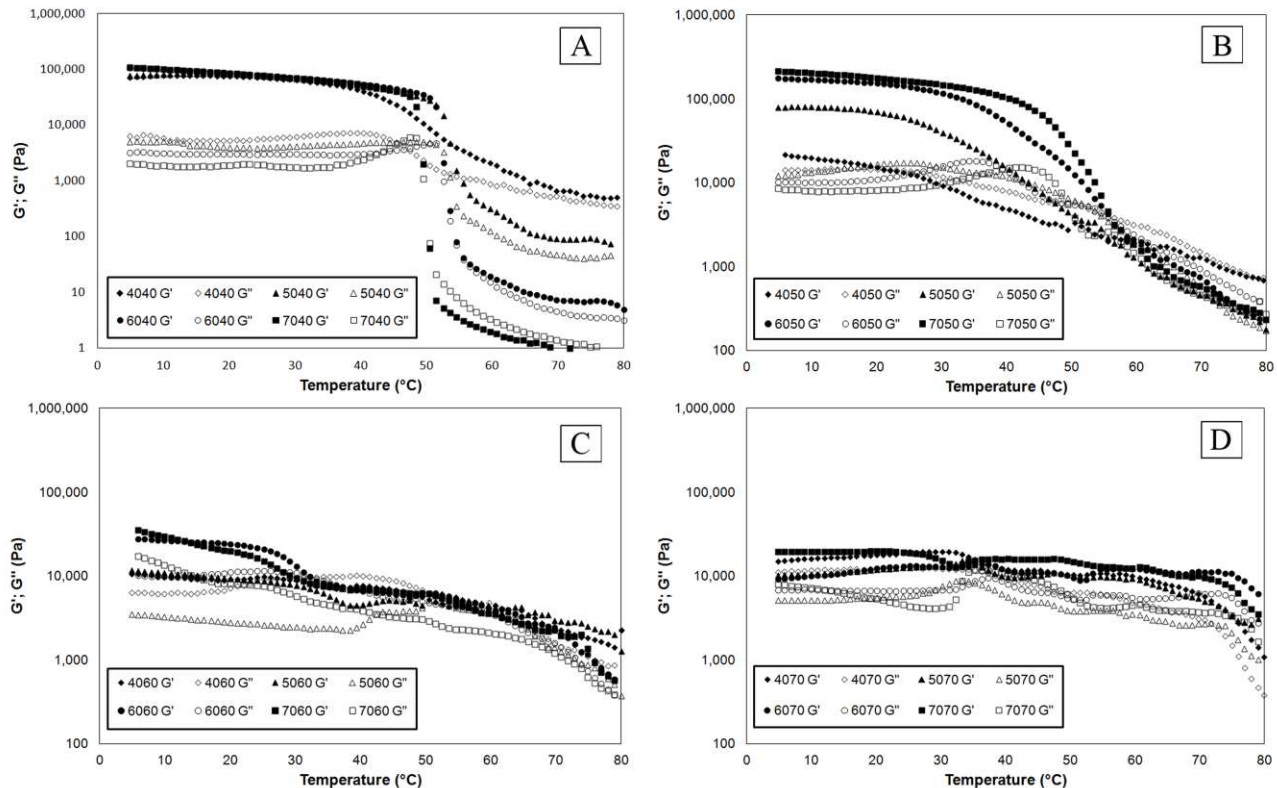


**Figure 2. Thermal scanning rheograms of gels with 3.0% (w/w) gellan gum in systems formulated with water + HOSO + Tween80. (A) 40% water; (B) 50% water; (C) 60% water and (D) 70% water. Full symbols ( $G'$ ), empty symbols ( $G''$ ).**

The presence of oil increased the polarity difference within the system, showing that the structuration dynamics of the surfactant was more complex, promoting the formation of more rigid gels, with higher values of  $G'$ . Systems with aqueous phase/surfactant ratios higher than 2.3 (higher than 60% w/w water) showed lower variation of  $G'$  and  $G''$  against temperature. Besides, the values of  $G'$  were lower and

decreased at low temperatures in a similar way to gels without oil (Chapter 5). These results showed that gellan network exerted more influence than Tween80 at higher water concentration. Therefore, all systems at 60% and 70% (w/w) of water G' around 10,000 Pa (Figures 2C-D) and lower temperature dependence, in a similar way to rheograms obtained for systems formulated with water + Tween80 + gellan, at lower surfactant concentrations (Chapter 5).

**Table 2. Temperature transition of some systems with 3.0% (w/w) gellan gum in systems formulated with water + HOSO + Tween80 without acetic acid.**

System	Temperature transition
4040	52
5040	53
6040	52
7040	50
4050	-
5050	55
6050	56
7050	55

The micrographs of microemulsion-based gels can be observed in Figure 3. Their structures were similar to pure gellan solution, which was composed by a porous network (de Jong & van de Velde, 2007). However, Figure 3 shows some spherical structures were entrapped in the gellan network, which could be related to oil droplets. The SEM micrographs also showed that the structures were dependent on the system composition. Smaller and apparently less polydisperse oil droplets were obtained with oil/surfactant ratio decrease (Figure 3C-D), showing that the lower surfactant concentration (18% w/w real composition) was sufficient to cover the interfacial area of smaller droplets. On the other

hand, with water addition, the gellan network became denser due to the more available water to the gum dispersion and gel network formation (Figure 3E-F). These differences in the microstructure are related to different gel strength and consequently its behavior under compression.

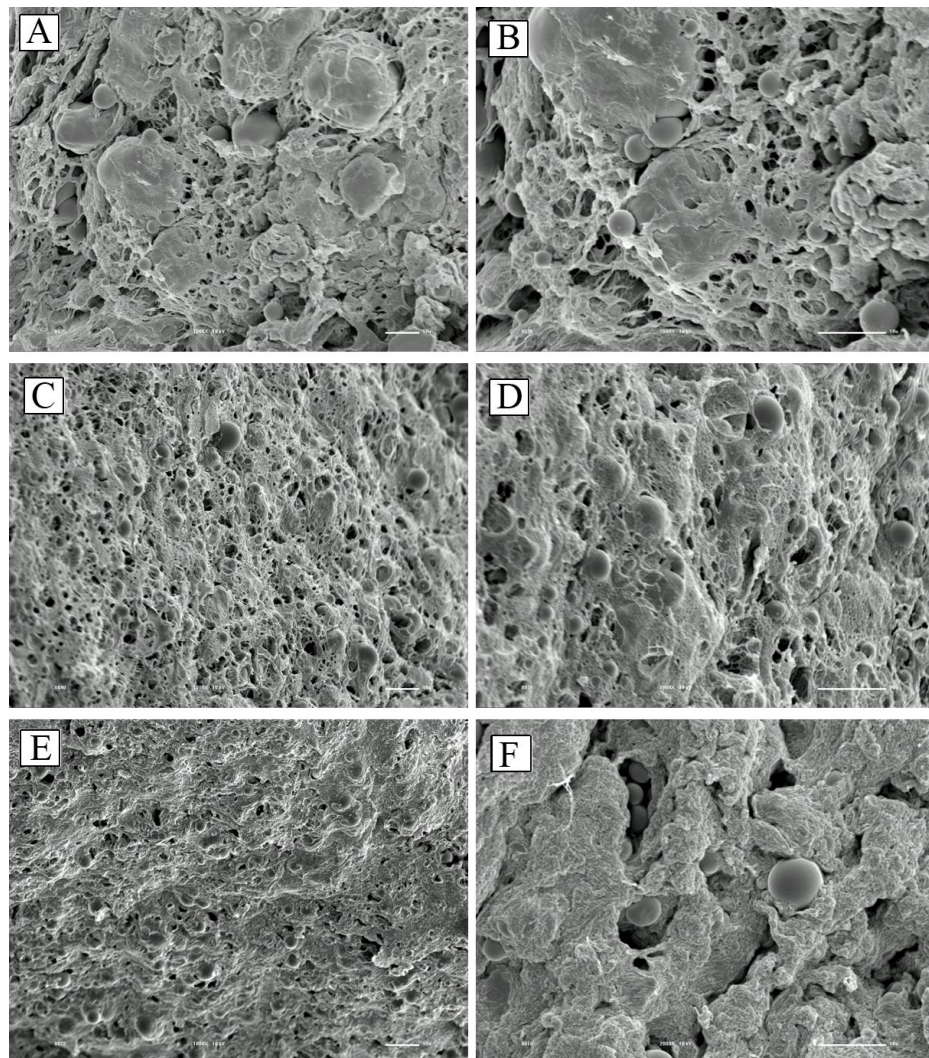


**Figure 3. SEM micrographs of 3.0% (w/w) gellan gum gels formulated with water + HOSO + Tween80. (A and B) 4040, (C and D) 5040 and (E and F) 6070. (A, C and E) 1000 $\times$  magnification and (B, D and F) 2000 $\times$  magnification.**

All gels were self-supported showing rupture point that varied with their microstructure and consequently composition (Figure 4). The oil/surfactant ratio and water

content were the most important factors. The “necklace with surfactant pearls” arrangement could be attributed for systems with prevailing gellan network (Grant, Cho, & Allen, 2006; Tsianou & Alexandridis, 2004). Since the deacylated gellan gum was used, few hydrophobic groups may have remained linked to the hydrophilic backbone. However, these groups could have linked to the hydrophobic tails of the polysorbate creating a crosslink effect. This crosslink could explain the increase of gel strength with the addition of Tween 80. Moreover, the greater amount of water allowed the formation of a denser gellan network, which enabled a better distribution of the applied force during the uniaxial compression measurements, increasing the maximum stress (Picone, et al., 2011). At last, these gels were harder in comparison to the gels formed in absence of oil (Chapter 5), showing the higher organization and structuration of surfactant moieties due to the increase of the difference in the systems polarity. In relation to the deformability of the gels, systems did not present a clear tendency with significant differences ( $p<0.05$ ). However, some increase in this parameter could be observed with surfactant and oil addition mainly of lower water concentrations.

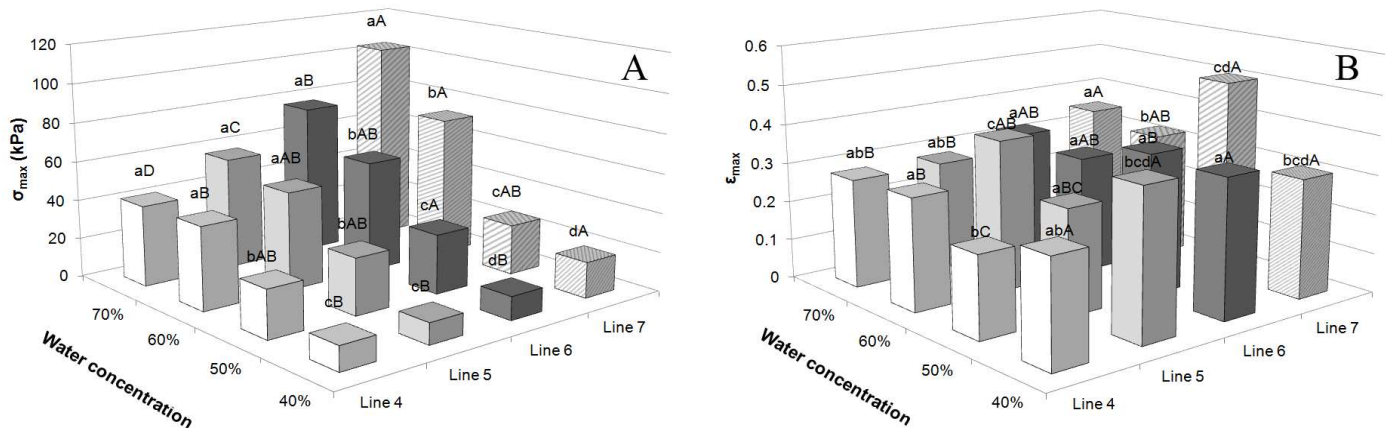


**Figure 4. Mechanical properties of gels with 3.0% (w/w) gellan gum in systems composed by water + HOSO + Tween80 without acetic acid addition. (A) Maximum stress ( $\sigma_{\max}$ ) and (B) strain ( $\epsilon_{\max}$ ). Means with different letters show statistically**

**significant differences ( $p<0.05$ ): Capital letters on the z axis (surfactant concentration) and small letter on the x axis (water concentration).**

### ***3.2. Effect of cosurfactant***

The effect of the cosurfactant on the gelation of systems composed by Tween80, HOSO, water and gellan (Figure 1A) is discussed in this section. Different from the systems without acetic acid addition, a cubic bicontinuous phase was present in the dilution Line 7 of the phase diagram, while the other lines showed two transparent phases or macroemulsion characteristics. The cosurfactant addition made the surfactant film more ductile (Binks, et al., 2010; Lv, et al., 2005; Santana, Fasolin, & Cunha, 2012), since the cosurfactant led to liquid crystalline destabilization, promoting the production of a higher microemulsion region. Organic acids in neutral form could be dispersed into the surfactant phase, increasing the flexibility of the surfactant film at interface, leading to different structural arrangements (Cid-Samamed, et al., 2008). The thermal rheological behaviors of these systems are shown in Figure 5. The loss moduli increased with surfactant addition and prevailed over  $G''$  at lower water content (40% w/w) (Figure 5A). Some systems presented higher storage modulus at high temperatures. Such behavior was observed for systems with no oil addition (Chapter 5). However, a temperature transition around 41°C was observed, which could be referent to the surfactant structuration (Table 3). With the water increment (Figure 5B, C and D) systems with higher surfactant content showed a structuration at low temperatures, attributed to the surfactant self-assembly. On the other hand, lower surfactant content systems showed that at high temperatures the system still presented a higher elastic behavior than viscous (Figure 5). The microstructure (Figure 6) showed that these systems did not form bulk gels, but microstructures attributed to the conformational self-assembly of the surfactant systems. Thus, this behavior could be

attributed to the gelling of the aqueous phase and a consequent separation of the other compounds.

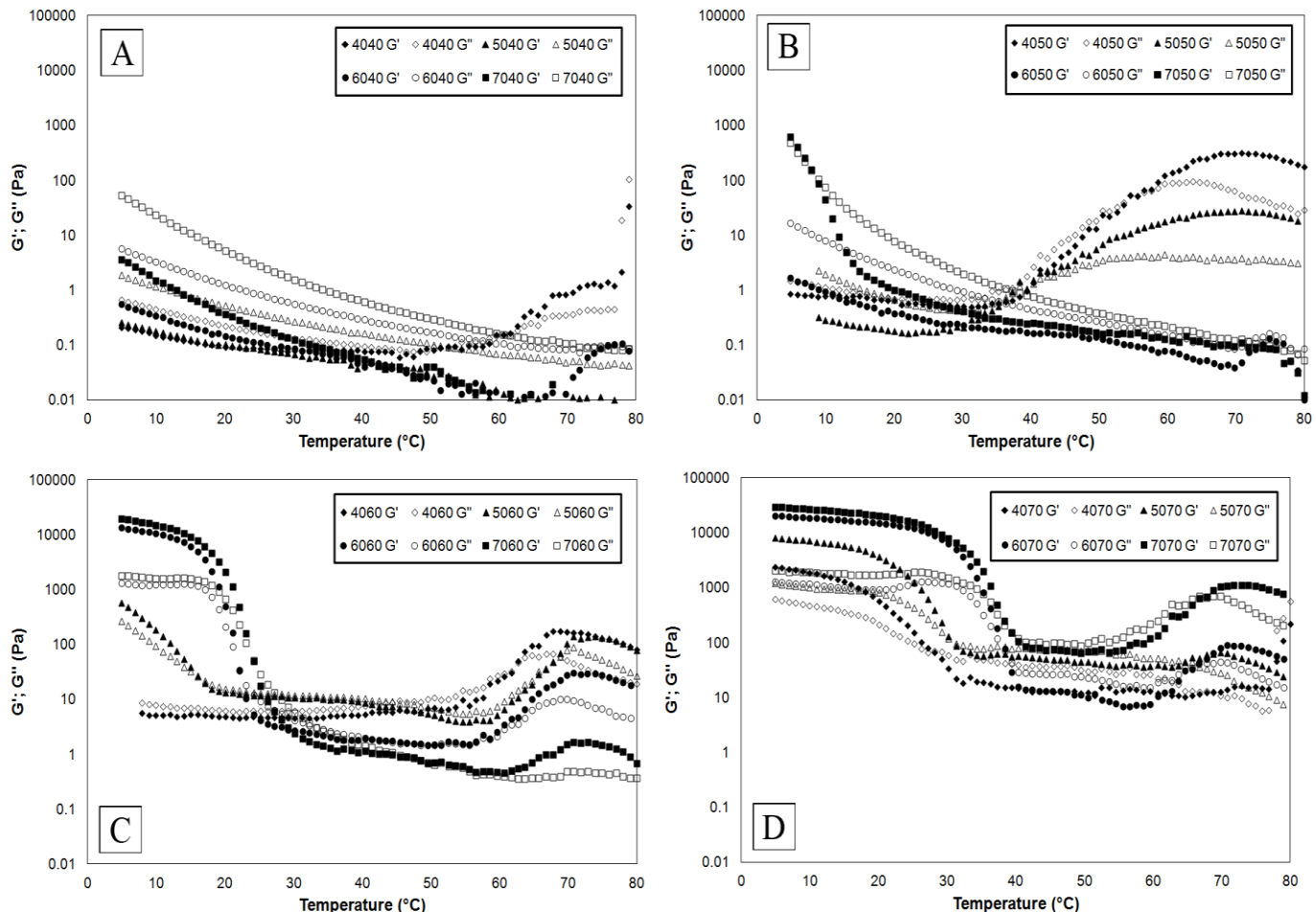


**Figure 5. Thermal scanning rheograms of gels with 3.0% (w/w) gellan gum in systems formulated with water + HOSO + Tween80 + acetic acid. (A) 40% of water; (B) 50% of water; (C) 60% of water and (D) 70% of water. Full symbols ( $G'$ ), empty symbols ( $G''$ ).**

**Table 3. Temperature transition for systems with 3.0% (w/w) gellan gum in systems formulated with water + HOSO + Tween80 +acetic acid.**

System	Temperature transition
4040	40
5040	-
6040	-
7040	-
4050	40
5050	40
6050	-
7050	-
4060	21
5060	20
6060	23
7060	25
7040	24
7050	25
7060	39
7070	39

Microgels or particulate gels (Figure 6) were formed by interconnected channels that could be a result from the bicontinuous or worm-like structures, since the self-assembly of the systems at 25°C could change with the heat treatment (Venugopal, et al., 2011; Wadsten-Hindrichsen, et al., 2007). The space between these channels was occupied by the Tween80+oil+acetic acid mixture, which was removed with the buffer used in the SEM analyzes. The phase separation that resulted in this kind of structure was increased by the use of acid acetic. The pH of the systems ranged from 3.2 up to 3.7, close to pKa of gellan gum (3.5) (de Jong, et al., 2007), which means that this polysaccharide presents lower charge density in these systems compared to the obtained

without cosurfactant. As a result, the macromolecules aggregated disorderly at lower pH and gellan gels were stronger and denser (Picone, et al., 2011; Yamamoto, et al., 2007).

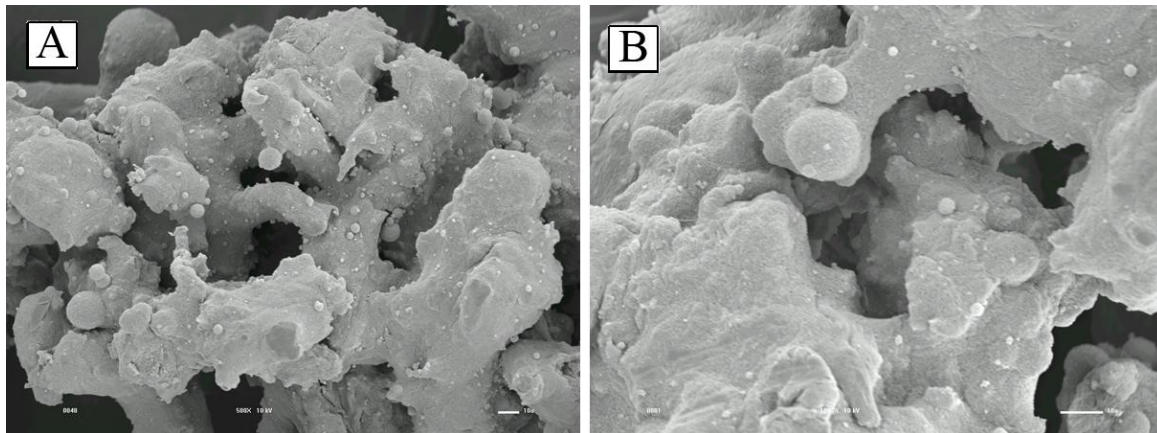


**Figure 6. SEM micrographs of 3.0% (w/w) gellan gum gels formulated with water + HOSO + Tween80 + acetic acid (System 7070). (A) 1000 $\times$  magnification and (B) 2000 $\times$  magnification.**

The mechanical properties were a consequence of the structure of these systems and the composition exerted important influence on such properties (Figure 7). Surfactant aggregation or surfactant gels were not obtained, unlike the gels without cosurfactant addition (section 3.1) or formulated with only gellan gum and Tween80 (Chapter 5). Non-self supporting gels were obtained in systems with 40% and 50% (w/w) water. The use of cosurfactant destabilized the gel-like structure of the polysorbate and self-assembly probably presented more simple organization with high viscosity but without self supporting structures. Microgels were formed, but the concentration or interaction between these particles was not sufficient to form self-supporting gels. However, particulate self-supporting gels were formed with the water increase, showing different mechanical properties depending on the surfactant content. In dilution Lines 4 and 5, squeezing gels were formed, which means that they did not present a rupture point but flowed with the

force application presenting a maximum or squeezing stress. However, systems 6070 and 7070 showed hard gels with a clear rupture point. Probably, the higher surfactant content could form channels or fill voids within the gellan network leading to stronger gels.

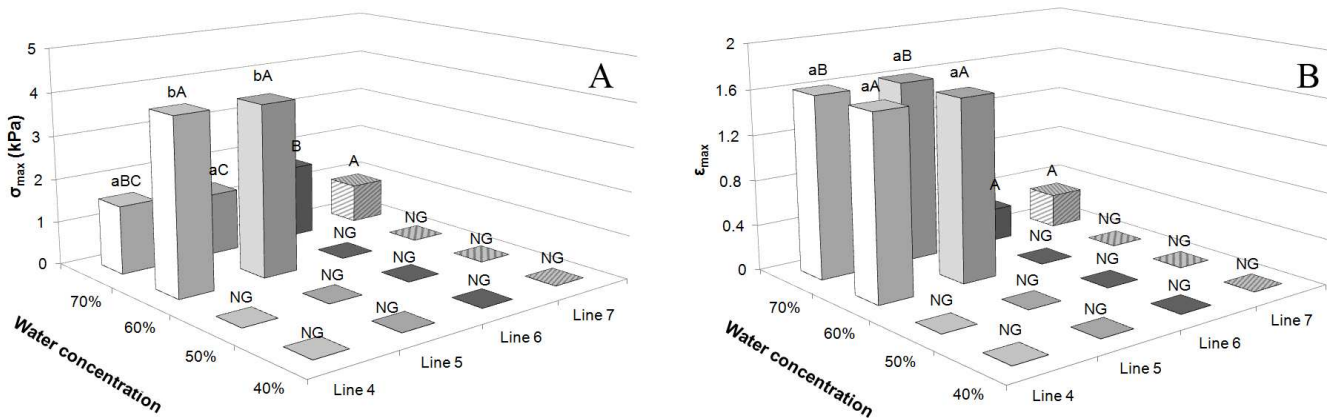


**Figure 7. Mechanical properties of gels with 3.0% (w/w) gellan gum in systems composed by water + HOSO + Tween80 + acetic acid. (A) Maximum ( $\sigma_{\text{Max}}$ ) and (B) Strain ( $\epsilon_{\text{Max}}$ ). Means with different letters show statistically significant differences ( $p<0.05$ ): Capital letters on the z axis (surfactant concentration) and small letter on the x axis (water concentration). NG means non-self supporting gels.**

#### 4. CONCLUSIONS

Bulky or microgels were obtained from microemulsions with the addition of gellan gum in systems formed by water, Tween80 and HOSO. The properties and type of gel were dependent on the systems composition, as well as on the presence of the cosurfactant. Bulky gels were formed when the acetic acid was not used leading to the prevailing of gellan gum or polysorbate characteristics, depending on the aqueous/surfactant ratio. Gellan network prevailed in systems with biopolymer/surfactant ratio over 2.3 and gel point temperature was not observed during cooling. Moreover, the

greater amount of water led to denser gellan network with some oil droplets entrapped. The increase of the surfactant content also led to harder gels, since the surfactant micelles promoted the crosslink between the polysaccharide macromolecules, reinforcing the gellan network. However when the polysorbate concentration was sufficiently high (ratio lower than 2.3), the excess of surfactant prevented these connections and decreased the rupture stress. In addition, the presence of oil led to large differences in the systems polarity, which resulted in a high organization of the Tween 80 structure and bulky gels harder than obtained in absence of oil. The use of acetic acid as cosurfactant produced different gelled structures. Microgels with worm-like or bicontinuous structures were formed only in high water concentration. The presence of cosurfactant prevented the formation of surfactant self-assembled structures with formation of softer gels. However, the particulate gels presented two different behaviors, depending on the surfactant concentration. At higher surfactant concentration harder gels were obtained, while at lower content squeezing gel behavior was observed. Thus, different structures with technological potential were obtained, which can be modulated depending on the concentration of ingredients. These bulky or microgels could be useful in cosmetic, pharmaceutical and food industries as vehicles for bioactives, promoting a controlled delivery and texture modification.

## **5. ACKNOWLEDGEMENTS**

The authors would like to thank Fapesp (EMU 09/54137-1), CNPq and Capes for their financial support.

## 6. REFERENCES

- Binks, B. P., Fletcher, P. D. I., & Tian, L. (2010). Influence of nanoparticle addition to Winsor surfactant microemulsion systems. *Colloids and Surfaces a-Physicochemical and Engineering Aspects*, 363(1-3), 8-15.
- Chen, H. B., Mou, D. S., Du, D. R., Chang, X. L., Zhu, D. D., Liu, J., Xu, H. B., & Yang, X. L. (2007). Hydrogel-thickened microemulsion for topical administration of drug molecule at an extremely low concentration. *International Journal of Pharmaceutics*, 341(1-2), 78-84.
- Cid-Samamed, A., Garcia-Rio, L., Fernandez-Gandara, D., Mejuto, J. C., Morales, J., & Perez-Lorenzo, M. (2008). Influence of n-alkyl acids on the percolative phenomena in AOT-based microemulsions. *Journal of Colloid and Interface Science*, 318(2), 525-529.
- de Campo, L., Yaghmur, A., Garti, N., Leser, M. E., Folmer, B., & Glatter, O. (2004). Five-component food-grade microemulsions: structural characterization by SANS. *Journal of Colloid and Interface Science*, 274(1), 251-267.
- de Jong, S., & van de Velde, F. (2007). Charge density of polysaccharide controls microstructure and large deformation properties of mixed gels. *Food Hydrocolloids*, 21(7), 1172-1187.
- Gan, L., Gan, Y., Zhu, C. L., Zhang, X. X., & Zhu, J. B. (2009). Novel microemulsion in situ electrolyte-triggered gelling system for ophthalmic delivery of lipophilic cyclosporine A: In vitro and in vivo results. *International Journal of Pharmaceutics*, 365(1-2), 143-149.
- Grant, J., Cho, J., & Allen, C. (2006). Self-assembly and physicochemical and rheological properties of a polysaccharide-surfactant system formed from the cationic biopolymer chitosan and nonionic sorbitan esters. *Langmuir*, 22(9), 4327-4335.
- Haering, G., & Luisi, P. L. (1986). Hydrocarbon Gels from Water-in-Oil Microemulsions. *Journal of Physical Chemistry*, 90(22), 5892-5895.
- Hoar, T. P., & Schulman, J. H. (1943). Transparent water-in-oil dispersions the oleopathic hydro-micelle. *Nature*, 152, 102-103.

Hou, Y., Xin, F., Yin, M., Kong, L., Zhang, H., Sun, T., Xing, P., & Hao, A. (2012). Stimuli-responsive supramolecular organogels that exhibit a succession of micro-morphologies. *Colloids and Surfaces A: Physicochemical and Engineering Aspects*, 414(0), 160-167.

Josef, E., Zilberman, M., & Bianco-Peled, H. (2010). Composite alginate hydrogels: An innovative approach for the controlled release of hydrophobic drugs. *Acta Biomaterialia*, 6(12), 4642-4649.

Kantaria, S., Rees, G. D., & Lawrence, M. J. (1999). Gelatin-stabilised microemulsion-based organogels: rheology and application in iontophoretic transdermal drug delivery. *Journal of Controlled Release*, 60(2-3), 355-365.

Kawano, S., Kobayashi, D., Taguchi, S., Kunitake, M., & Nishimi, T. (2010). Construction of Continuous Porous Organogels, Hydrogels, and Bicontinuous Organo/Hydro Hybrid Gels from Bicontinuous Microemulsions. *Macromolecules*, 43(1), 473-479.

Koop, H. S., Da-Lozzo, E. J., de Freitas, R. A., Franco, C. R. C., Mitchell, D. A., & Silveira, J. L. M. (2012). Rheological Characterization of a Xanthan-Galactomannan Hydrogel Loaded with Lipophilic Substances. *Journal of Pharmaceutical Sciences*, 101(7), 2457-2467.

Lawrence, M. J. (1994). Surfactant Systems - Their Use in Drug-Delivery. *Chemical Society Reviews*, 23(6), 417-424.

Lopez, F., Venditti, F., Ambrosone, L., Colafemmina, G., Ceglie, A., & Palazzo, G. (2004). Gelatin microemulsion-based gels with the cationic surfactant cetyltrimethylammonium bromide: A self-diffusion and conductivity study. *Langmuir*, 20(22), 9449-9452.

Lu, S. Y., Shao, Z. Q., Zhang, Z. L., Wang, F. J., & Wang, W. J. (2012). Rheological Properties of New Stimuli-responsive Energetic Gels. *Chemical Journal of Chinese Universities-Chinese*, 33(2), 409-415.

Lv, F. F., Zheng, L. Q., & Tung, C. H. (2005). Phase behavior of the microemulsions and the stability of the chloramphenicol in the microemulsion-based ocular drug delivery system. *International Journal of Pharmaceutics*, 301(1-2), 237-246.

Minkenberg, C. B., Hendriksen, W. E., Li, F., Mendes, E., Eelkema, R., & van Esch, J. H. (2012). Dynamic covalent assembly of stimuli responsive vesicle gels. *Chemical Communications*, 48(79), 9837-9839.

Miyoshi, E., Takaya, T., & Nishinari, K. (1996). Rheological and thermal studies of gel-sol transition in gellan gum aqueous solutions. *Carbohydrate Polymers*, 30(2-3), 109-119.

Moritaka, H., Nishinari, K., Taki, M., & Fukuba, H. (1995). Effects of Ph, Potassium-Chloride, and Sodium-Chloride on the Thermal and Rheological Properties of Gellan Gum Gels. *Journal of Agricultural and Food Chemistry*, 43(6), 1685-1689.

Picone, C. S. F., & Cunha, R. L. (2011). Influence of pH on formation and properties of gellan gels. *Carbohydrate Polymers*, 84(1), 662-668.

Picone, C. S. F., & Cunha, R. L. (2013). Formation of nano and microstructures by polysorbate–chitosan association. *Colloids and Surfaces A: Physicochemical and Engineering Aspects*, 418(0), 29-38.

Rehage, H. (2005). Rheological Properties of Viscoelastic Surfactant Solutions. In R. Zana (Ed.), *Dynamics of Surfactant Self-Assemblies: Micelles, Microemulsions, Vesicles and Lyotropic Phases* (pp. 419-473): CRC Press.

Santana, R. C., Fasolin, L. H., & da Cunha, R. L. (2012). Effects of a cosurfactant on the shear-dependent structures of systems composed of biocompatible ingredients. *Colloids and Surfaces a-Physicochemical and Engineering Aspects*, 398, 54-63.

Savitzky, A., & Golay, M. J. E. (1964). Smoothing + Differentiation of Data by Simplified Least Squares Procedures. *Analytical Chemistry*, 36(8), 1627-&.

Sjoblom, J., Lindberg, R., & Friberg, S. E. (1996). Microemulsions - Phase equilibria characterization, structures, applications and chemical reactions. *Advances in Colloid and Interface Science*, 65, 125-287.

Spiclin, P., Homar, M., Zupancic-Valant, A., & Gasperlin, M. (2003). Sodium ascorbyl phosphate in topical microemulsions. *International Journal of Pharmaceutics*, 256(1-2), 65-73.

- Tsianou, M., & Alexandridis, P. (2004). Surfactant–Polymer Interactions. In M. Abe & J. F. Scamehorn (Eds.), *Mixed Surfactant Systems* (2nd ed.). New York: Marcel Dekker.
- Valenta, C., & Schultz, K. (2004). Influence of carrageenan on the rheology and skin permeation of microemulsion formulations. *Journal of Controlled Release*, 95(2), 257-265.
- Venugopal, E., Bhat, S. K., Vallooran, J. J., & Mezzenga, R. (2011). Phase Behavior of Lipid-Based Lyotropic Liquid Crystals in Presence of Colloidal Nanoparticles. *Langmuir*, 27(16), 9792-9800.
- Wadsten-Hindrichsen, P., Bender, J., Unga, J., & Engstrom, S. (2007). Aqueous self-assembly of phytantriol in ternary systems: Effect of monoolein, distearoylphosphatidylglycerol and three water-miscible solvents. *Journal of Colloid and Interface Science*, 315(2), 701-713.
- Wang, C. M., Gong, Y. H., Lin, Y. M., Shen, J. B., & Wang, D. A. (2008). A novel gellan gel-based microcarrier for anchorage-dependent cell delivery. *Acta Biomaterialia*, 4(5), 1226-1234.
- Yaghmur, A., de Campo, L., Salentinig, S., Sagalowicz, L., Leser, M. E., & Glatter, O. (2006). Oil-loaded monolinolein-based particles with confined inverse discontinuous cubic structure (Fd3m). *Langmuir*, 22(2), 517-521.
- Yamamoto, F., & Cunha, R. L. (2007). Acid gelation of gellan: Effect of final pH and heat treatment conditions. *Carbohydrate Polymers*, 68(3), 517-527.
- Zhao, X. Y., Cao, Q., Zheng, L. Q., & Zhang, G. Y. (2006). Rheological properties and microstructures of gelatin-containing microemulsion-based organogels. *Colloids and Surfaces a-Physicochemical and Engineering Aspects*, 281(1-3), 67-73.
- Zhu, W. W., Guo, C. Y., Yu, A. H., Gao, Y., Cao, F. L., & Zhai, G. X. (2009). Microemulsion-based hydrogel formulation of penciclovir for topical delivery. *International Journal of Pharmaceutics*, 378(1-2), 152-158.



**– CAPÍTULO 7–**  
***Conclusões gerais***



Sistemas com diferentes características físico-químicas e mecânico/estruturais foram obtidos a partir de sistemas auto-organizáveis. O estudo do diagrama de fases, formulado com etanol como co-surfactante mostrou que foram necessárias altas concentrações de surfactante e/ou co-surfactante para formar sistemas monofásicos. Além disso, a estrutura e comportamento desses sistemas foi dependente da composição do sistema, principalmente em relação à quantidade de água. Essas estruturas foram desde microemulsões A/O até O/A, passando por sistemas de organização complexa, chamados líquidos cristalinos, em concentrações intermediárias de água. Esses sistemas foram afetados pela concentração de etanol e insaturação do óleo. Baixas concentrações de etanol e maior hidrofobicidade do óleo levaram à formação de maior região líquido-cristalina. Por outro lado, a alta concentração de co-surfactante diminuiu a formação dessas estruturas, que foi consequência da habilidade do etanol em aumentar a flexibilidade da interface.

A substituição do etanol por ácido orgânico também permitiu a formação de região monofásica apenas em altas concentrações de surfactante. Todavia dependendo da combinação ácido-óleo, diferentes sistemas foram obtidos. O óleo com menor hidrofilicidade permitiu a solubilização de maiores quantidades de ácido propiônico enquanto o óleo mais hidrofílico interagiu com maiores quantidades de ácido acético. Por outro lado, essas diferenças de afinidade levaram a mudanças no mecanismo de estruturação do surfactante, bem como na difusão do co-surfactante e sensibilidade ao fenômeno de partição. Além disso, esses fenômenos também foram influenciados pela concentração de água, devido à susceptibilidade dos ácidos à dissociação em meio aquoso. A intensidade da partição dos ácidos para fora da interface influenciou na rigidez e comportamento reológico das estruturas. O ácido acético foi mais suscetível a esse

fenômeno, facilitando a formação de estruturas mais rígidas com comportamento pseudoplástico.

O diagrama com maior região monofásica (óleo de girassol alto oleico e ácido acético) foi escolhido para a última etapa do trabalho, relacionada à formação de géis a partir das microemulsões, devido à formação de estruturas bicontínuas. A fim de estudar a viabilidade da adição da goma gelana nesses sistemas para obtenção de sistemas gelificados, foi realizada uma etapa intermediária com o intuito de avaliar a interação desse polissacarídeo com o polissorbato 80 em diferentes valores de pH. Dois comportamentos principais foram observados, dependendo da razão entre água e surfactante. As propriedades da solução de gelana prevaleceram em baixas concentrações de surfactante (até 20% m/m) com a formação de géis fortes. Todavia, as micelas de surfactante impediram a interação gelana-gelana, mudando o comportamento reológico. Com o aumento de surfactante, foram observadas duas temperaturas de transição de fases. A primeira transição seria relacionada à gelificação da gelana e a segunda temperatura foi relacionada à estruturação do surfactante. Acima de 50% (m/m) o surfactante formou estruturas mais complexas do tipo gel e este comportamento foi predominante. Contudo, esses géis foram mais fracos e não apresentaram ponto de ruptura quando comparados aos géis com comportamento predominante da gelana.

A adição de gelana no diagrama de fases formulado com óleo de girassol alto oleico e ácido acético levou à formação de géis particulados ou microgéis. Esses géis foram obtidos apenas em altas concentrações de água e apresentaram dois tipos de comportamento. Em altas concentrações de surfactante, géis fortes foram observados, enquanto em baixas concentrações géis fracos e sem ponto de ruptura foram obtidos. Contudo, em sistemas sem co-surfactante, foram produzidos géis homogêneos

dependentes da composição do sistema. As características do polissacarídeo foram predominantes em maiores concentrações de água com a formação de uma densa rede de gelana com algumas gotas de óleo presas a essa rede. Contudo, em excesso de surfactante não houve interação entre as moléculas de gelana, diminuindo a força do gel. Além disso, a presença de óleo nesses sistemas levou a grandes diferenças de polaridade, que resultou em maior organização do surfactante e na produção de géis mais fortes que os obtidos na ausência de óleo.

Assim, os resultados obtidos nesse trabalho sugerem que os sistemas auto-organizáveis podem servir de base para obtenção de produtos com diferentes propriedades tecnológicas, úteis para diversos segmentos industriais. Além de envolver baixa energia de formação, a interação entre os ingredientes biocompatíveis permitiu a formação de sistemas com diferentes propriedades físico-químicas e estruturais. As microemulsões podem ser utilizadas como veículos de bioativos em sistemas líquidos sem a alteração das características do sistema original. Por outro lado, os géis de cristais líquidos podem ser utilizados pela indústria cosmética ou farmacêutica também como uso tópico. Por sua vez, os sistemas gelificados (géis e microgéis) poderiam ser empregados tanto como veiculadores de bioativos, sistemas de liberação controlada ou modificadores de textura.